

The Effect of Ethanol-Water Fumigation on the  
Performance and Emissions from a Direct-Injection  
Diesel Engine

A THESIS

SUBMITTED TO THE FACULTY OF THE GRADUATE SCHOOL  
OF THE UNIVERSITY OF MINNESOTA

BY

André Louis Olson

IN PARTIAL FULFILLMENT OF THE REQUIREMENTS  
FOR THE DEGREE OF  
Master of Science

David B. Kittelson  
(Faculty Adviser)

September 2010

Copyright © 2010 by André Louis Olson

**ALL RIGHTS RESERVED**

# Acknowledgments

My tenure as a graduate student at the University of Minnesota was marked by particularly trying periods of my life, and the support I received from others during the course of the program was a very important factor in the achievement of my M.S. degree. Therefore, the completion of this work would probably not had been possible without the help and support I had received from several people throughout my stay in graduate school.

First of all, I thank my adviser, Prof. David B. Kittelson, for his mentoring, support, encouragement, and patience. Staff members Winthrop F. Watts, Jr. and Darriek D. Zarling, both from the University's Center for Diesel Research, also provided me valuable support. The extremely helpful support I received from fellow students—both current and former—was crucial in my finishing my studies. That being said, I am particularly grateful to Helmer Acevedo, Anil Singh Bika, Grace Chan, Aaron M. Collins, John M. Dixon, Luke M. Franklin, David D. Gladis, Matthew R. Kenitzer, Adam C. Ragatz, Matthew F. Schumacher, Jacob J. Swanson, Andy Tan, and Lei Tian.

The Minnesota Corn Growers Association provided funding for the present work.

Last but not least, I would like to take this opportunity to convey very special acknowledgments to Álvaro P. Coppieters, João Paulo Sena, and Pietro Cardone.

A.L.O.

*Minneapolis, Minnesota*

*September 2010*

# In Memoriam

I dedicate the present work to the memory of my mother, TERESA CRISTINA SANTOS, who died in June 2009 after succumbing to cancer. Her tenacity, endurance, open-mindedness, sense of humor and irreverence, have all played a fundamental role in defining me as a person and in building my character. With her untimely death, I lost not only a parent but also a mentor, a best friend, a confidante, and—most of all—a companion in struggle through the incessant maelstroms of life. Due to everything my mother had done for me, I dedicate to her not merely this thesis, but also my eternal gratitude.

She should have died hereafter;  
There would have been a time for such a word.  
Tomorrow, and tomorrow, and tomorrow,  
Creeps in this petty pace from day to day  
To the last syllable of recorded time,  
And our yesterdays have lighted fools  
The way to dusty death. Out, out, brief candle!  
Life's but a walking shadow, a poor player  
That struts and frets his hour upon the stage  
And then is heard no more: it is a tale  
Told by an idiot, full of sound and fury,  
Signifying nothing.

(*Macbeth*, Act 5, Scene 5, 19–30)

# **The Effect of Ethanol-Water Fumigation on the Performance and Emissions from a Direct-Injection Diesel Engine**

by **André Louis Olson**

## **ABSTRACT**

The effect of ethanol fumigation and water injection on the performance and exhaust emissions from a 1.9-liter Volkswagen TDI diesel engine was investigated. The engine tests were conducted at a speed of 1700 rpm, and at loads of 40, 80, and 120 N-m. One hundred-proof ethanol, 200-proof ethanol, and distilled water were used as fumigants; they were injected into the intake air through a single air-atomizing nozzle mounted in the engine's intake manifold. Two flowrates of fumigant were used: 25% and 40% of the volumetric diesel fuel flowrate at the corresponding baseline operation. The atomizing nozzle was mounted either downstream or upstream of the aftercooler, and it was found that the upstream configuration resulted in more consistent results—probably due to improved evaporation and mixing of the fumigant with the intake air. In general, when compared to baseline operation, both ethanol and water resulted in reductions in the emissions of  $\text{NO}_x$ , total particle number, and total particle volume concentrations. At 1700 rpm and 80 N-m, the most significant (up to 25%) reductions in  $\text{NO}_x$  emissions were obtained with water injection, whereas ethanol resulted in more pronounced reductions in total particle number (about 40%) and total particle volume concentrations (about 30%). The HC emissions were dramatically increased with ethanol fumigation, particularly with 200-proof ethanol. The brake thermal efficiency was slightly decreased with both proofs of ethanol. As far as the emissions of  $\text{NO}_x$  and PM are concerned, the fumigation of 100-proof ethanol yielded better results than the fumigation of 200-proof ethanol.

# Contents

|   |             |
|---|-------------|
| <b>Acknowledgments</b>                                    | <b>i</b>    |
| <b>In Memoriam</b>  | <b>ii</b>   |
| <b>Abstract</b>   | <b>ii</b>   |
| <b>List of Tables</b>                                     | <b>vii</b>  |
| <b>List of Figures</b>                                    | <b>viii</b> |
| <b>1 Introduction</b>                                     | <b>1</b>    |
| 1.1 Chapter Overview . . . . .                            | 3           |
| <b>2 Theory and Background</b>                            | <b>4</b>    |
| 2.1 Combustion in Diesel Engines . . . . .                | 4           |
| 2.1.1 The Phases of Diesel Combustion . . . . .           | 5           |
| 2.2 Diesel Engine Exhaust Emissions . . . . .             | 8           |
| 2.2.1 Particulate Matter . . . . .                        | 8           |
| 2.2.2 Oxides of Nitrogen . . . . .                        | 16          |
| 2.2.3 Unburned Hydrocarbons and Carbon Monoxide . . . . . | 20          |
| 2.3 Diesel Fuel Oxygenates . . . . .                      | 21          |
| 2.3.1 Mechanism of Action . . . . .                       | 22          |
| 2.3.2 Types of Oxygenates . . . . .                       | 23          |
| 2.3.3 Review of Oxygenates . . . . .                      | 24          |

|          |  |           |
|----------|--|-----------|
| 2.4      | Utilization of Alcohols in Internal-Combustion Engines . . . . .                   | 28        |
| 2.4.1    | Ethanol Fumigation . . . . .   | 30        |
| 2.5      | Water Injection in Diesel Engines . . . . .  | 42        |
| 2.5.1    | Effects of Water on NO <sub>x</sub> Emissions . . . . .                            | 43        |
| 2.5.2    | Effects of Water on PM Emissions . . . . .   | 43        |
| <b>3</b> | <b>Experimental Apparatus and Procedures</b>                                       | <b>45</b> |
| 3.1      | Experimental Apparatus . . . . .   | 45        |
| 3.1.1    | Engine and Dynamometer . . . . .   | 47        |
| 3.1.2    | Fumigation System . . . . .  | 48        |
| 3.1.3    | Sampling of Exhaust Gaseous Emissions . . . . .                                    | 48        |
| 3.1.4    | Sampling of Exhaust Particulate Matter . . . . .                                   | 50        |
| 3.1.5    | Measurement of Flow Rates . . . . .  | 54        |
| 3.1.6    | Data Acquisition System . . . . .  | 55        |
| 3.2      | Experimental Procedures . . . . .  | 55        |
| 3.2.1    | Test Matrix . . . . .  | 55        |
| 3.2.2    | Test Procedure . . . . .   | 56        |
| 3.3      | Test History . . . . .   | 57        |
| <b>4</b> | <b>Analysis of Results</b>   | <b>60</b> |
| 4.1      | Introduction . . . . .   | 60        |
| 4.2      | Part I — Effect of Atomizing Nozzle Position . . . . .                             | 61        |
| 4.2.1    | Effect on PM Emissions . . . . .   | 62        |
| 4.2.2    | Effect on NO <sub>x</sub> Emissions . . . . .                                      | 78        |
| 4.3      | Part II — Effect of Injection Pump Repair on Baseline Engine Performance . . . . . | 84        |
| 4.3.1    | Effect on PM Volume Emissions . . . . .  | 84        |
| 4.3.2    | Effect on PM Number Emissions . . . . .  | 87        |
| 4.3.3    | Effect on NO <sub>x</sub> Emissions . . . . .                                      | 90        |

|          |  |            |
|----------|--|------------|
| 4.4      | Part III — Summary of Effects at 1700 rpm and 80 N-m . . . . .       | 91         |
| 4.4.1    | Effect on Engine Brake Thermal Efficiency . . . . .                  | 92         |
| 4.4.2    | Effect on PM Volume Emissions . . . . .                              | 93         |
| 4.4.3    | Effect on NO <sub>x</sub> Emissions . . . . .                        | 98         |
| 4.4.4    | Effect on NO <sub>2</sub> /NO <sub>x</sub> Ratios . . . . .          | 99         |
| 4.4.5    | Effect on Unburned Hydrocarbons Emissions . . . . .                  | 100        |
| 4.4.6    | Effect on Intake Manifold Temperature . . . . .                      | 101        |
| 4.5      | Sources of Inconsistencies in the Results . . . . .                  | 102        |
| 4.5.1    | Poor Cylinder-to-Cylinder Distribution . . . . .                     | 102        |
| 4.5.2    | Engine Speed Instabilities . . . . .                                 | 103        |
| <b>5</b> | <b>Conclusion and Recommendations</b>                                | <b>107</b> |
| 5.1      | Summary of Effects of Fumigation on Engine Performance and Emissions | 107        |
| 5.1.1    | Overall Conclusions . . . . .  | 108        |
| 5.2      | Suggestions for Future Work . . . . .                                | 109        |
|          | <b>References</b>  | <b>110</b> |
|          | <b>Appendix A.</b>   | <b>127</b> |



# List of Tables

|     |  |    |
|-----|--|----|
| 3.1 | Technical data of the Volkswagen 1.9-L TDI engine [23] | 47 |
| 3.2 | Test matrix  | 56 |
| 3.3 | Test history—Part I                                    | 58 |
| 3.4 | Test history—Part II                                   | 59 |
| 3.5 | Test history—Part III                                  | 59 |

# List of Figures

|      |   |    |
|------|---|----|
| 2.1  | Typical DI engine heat-release-rate diagram [65]                                    | 6  |
| 2.2  | Typical particle composition for a 1998 (and earlier) heavy-duty diesel engine [75] | 9  |
| 2.3  | The conceptual model of DI diesel combustion proposed by Dec [30]                   | 11 |
| 2.4  | Typical engine exhaust size distributions [75]                                      | 13 |
| 2.5  | Artist's conception of diesel particulate matter [92]                               | 15 |
| 2.6  | The shift in the NO <sub>x</sub> -PM trade-off curve produced by oxygenates [29].   | 27 |
| 3.1  | Schematic of the experimental setup   | 46 |
| 4.1  | Volume-weighted particle size distributions; 40 N-m; upstream nozzle.               | 63 |
| 4.2  | Volume-weighted particle size distributions; 80 N-m; upstream nozzle.               | 63 |
| 4.3  | Volume-weighted particle size distributions; 120 N-m; upstream nozzle.              | 64 |
| 4.4  | Volume-weighted particle size distributions; 40 N-m; downstream nozzle.             | 64 |
| 4.5  | Volume-weighted particle size distributions; 80 N-m; downstream nozzle.             | 65 |
| 4.6  | Volume-weighted particle size distributions; 120 N-m; downstream nozzle.            | 65 |
| 4.7  | Total particle volume concentrations; 40 N-m.                                       | 68 |
| 4.8  | Total particle volume concentrations; 80 N-m.                                       | 68 |
| 4.9  | Total particle volume concentrations; 120 N-m.                                      | 69 |
| 4.10 | Number-weighted particle size distributions; 40 N-m; upstream nozzle.               | 71 |

|      |  |    |
|------|--|----|
| 4.11 | Number-weighted particle size distributions; 80 N-m; upstream nozzle.            | 72 |
| 4.12 | Number-weighted particle size distributions; 120 N-m; upstream nozzle. . . . .   | 72 |
| 4.13 | Number-weighted particle size distributions; 40 N-m; downstream nozzle. . . . .  | 73 |
| 4.14 | Number-weighted particle size distributions; 80 N-m; downstream nozzle. . . . .  | 73 |
| 4.15 | Number-weighted particle size distributions; 120 N-m; downstream nozzle. . . . . | 74 |
| 4.16 | Total particle number concentrations; 40 N-m. . . . .                            | 76 |
| 4.17 | Total particle number concentrations; 80 N-m. . . . .                            | 76 |
| 4.18 | Total particle number concentrations; 120 N-m. . . . .                           | 77 |
| 4.19 | Total exhaust $NO_x$ concentrations; 40 N-m. . . . .                             | 79 |
| 4.20 | Total exhaust $NO_x$ concentrations; 80 N-m. . . . .                             | 79 |
| 4.21 | Total exhaust $NO_x$ concentrations; 120 N-m. . . . .                            | 80 |
| 4.22 | Intake manifold temperatures; 40 N-m. . . . .                                    | 82 |
| 4.23 | Intake manifold temperatures; 80 N-m. . . . .                                    | 82 |
| 4.24 | Intake manifold temperatures; 120 N-m. . . . .                                   | 83 |
| 4.25 | Volume-weighted particle size distributions; 40 N-m. . . . .                     | 85 |
| 4.26 | Volume-weighted particle size distributions; 80 N-m. . . . .                     | 85 |
| 4.27 | Volume-weighted particle size distributions; 120 N-m. . . . .                    | 86 |
| 4.28 | Total particle volume concentrations. . . . .                                    | 87 |
| 4.29 | Number-weighted particle size distributions; 40 N-m. . . . .                     | 88 |
| 4.30 | Number-weighted particle size distributions; 80 N-m. . . . .                     | 88 |
| 4.31 | Number-weighted particle size distributions; 120 N-m. . . . .                    | 89 |
| 4.32 | Total particle number concentrations. . . . .                                    | 90 |
| 4.33 | $NO_x$ concentrations. . . . .   | 91 |
| 4.34 | Engine Brake Thermal Efficiencies. . . . .                                       | 92 |

|      |  |     |
|------|--|-----|
| 4.35 | Volume-weighted particle size distributions; 25% flowrate. . . . .   | 94  |
| 4.36 | Volume-weighted particle size distributions; 40% flowrate. . . . .   | 94  |
| 4.37 | Total particle volume concentrations. . . . .  | 95  |
| 4.38 | Number-weighted particle size distributions; 25% flowrate. . . . .   | 96  |
| 4.39 | Number-weighted particle size distributions; 40% flowrate. . . . .   | 97  |
| 4.40 | Total particle number concentrations. . . . .  | 98  |
| 4.41 | Exhaust NO <sub>x</sub> concentrations. . . . .  | 99  |
| 4.42 | Exhaust NO <sub>2</sub> /NO <sub>x</sub> Ratios. . . . .   | 100 |
| 4.43 | Concentrations of unburned hydrocarbons (dry). . . . .   | 101 |
| 4.44 | Intake manifold temperatures. . . . .  | 102 |
| 4.45 | Sudden drop in engine speed; 80 N-m, 25% 200-proof ethanol; 53 s. . .  | 104 |
| 4.46 | Sudden drop in engine speed; 40 N-m, 40% 200-proof ethanol; 2 min. .   | 104 |
| 4.47 | Sudden drops in engine speed; 40 N-m, 25% 200-proof ethanol; 15 min.   | 105 |
| 4.48 | Sudden drops in engine speed; 40 N-m, 25% 200-proof ethanol; 15 min.   | 105 |
| 4.49 | Sudden drops in engine speed; 40 N-m, 40% water; 15 min. . . . .   | 106 |
| A.1  | Performance curves of the Volkswagen 1.9L TDI engine [23] . . . . .  | 128 |
| A.2  | Sectional view of the Volkswagen 1.9L TDI engine [23] . . . . .  | 129 |
| A.3  | The instruments which comprise the SMPS: the electrostatic classifier<br>(top) [3] and the water-based condensation particle counter (bottom)<br>[1] . . . . . | 130 |
| A.4  | Data for Part I . . . . .  | 131 |
| A.5  | Data for Part I (cont.) . . . . .  | 132 |
| A.6  | Data for Part I (cont.) . . . . .  | 133 |
| A.7  | Data for Part II . . . . .   | 134 |
| A.8  | Data for Part III . . . . .  | 135 |

# Chapter 1

## Introduction

In recent years, diesel engines have become increasingly popular—not only among trucks and heavy-duty vehicles but among passenger cars as well: For instance, in some European countries about half of the new cars sold are diesel-powered, and in the United States the share of diesel vehicles is also expected to increase [109]. This trend is partly due to the high efficiency and fuel economy characteristic of diesel engines [71, 60]—important features in a world with fluctuating oil prices and energy insecurity. However, in spite of their inherent thermodynamic advantages over their spark-ignited counterparts, diesel engines are still prone to produce much higher levels of particulate matter (PM) and oxides of nitrogen ( $\text{NO}_x$ ) [66, 110, 111]. At the same time, ever-increasingly stringent emissions standards are forcing the diesel engine industry to devise new ways to remedy that issue [79, 126]. The emissions target levels are often difficult to achieve solely through engine design. The required levels of PM and  $\text{NO}_x$  emissions can be achieved by a combination of several different techniques, including optimized fuel injection techniques—such as high-pressure common-rail systems, unit injectors— exhaust gas recirculation (EGR), exhaust pipe aftertreatment devices, etc [61]. Moreover, other strategies can be employed when it comes to further curb the exhaust pollutant emissions from diesel engines, and this can be accomplished through the utilization of cleaner-burning fuels—such as ethanol.

Ethanol (ethyl alcohol) is a well-known alternative fuel for internal-combustion engines and it has been extensively used in spark-ignition (Otto) engines [96, 78, 142]. The utilization of ethanol in compression-ignition (Diesel) engines has not achieved the same degree of success [10, 97], and the reasons will be further explained in Section 2.4 ahead. In spite of being not suitable for use as a fuel for diesel engines, ethanol can nevertheless be used in these engines by means of a number of techniques [34]. *Fumigation* is one of such techniques, and this method will be reviewed in Section 2.4. As a method of ethanol fuel utilization, fumigation is usually simple, it can be applied to existing engines, and it also results in significant decreases in PM emissions—the exhaust smoke levels are notably decreased. With absolute (200-proof) ethanol fumigation, the emissions of  $\text{NO}_x$  can either increase or decrease, depending on a number of factors.

Aqueous (low-proof) ethanol, in particular, has the advantage of being much cheaper and easier to produce than absolute ethanol. Small, farm-level distillation plants can economically produce aqueous ethanol, typically in proofs around 150 (75% ethanol, 25% water). The fumigation of aqueous ethanol has been reported to exhibit the same potential in decreasing PM emissions as absolute ethanol does. In addition to that, aqueous ethanol fumigation usually decreases the  $\text{NO}_x$  emissions to a greater extent than does absolute ethanol. This extra benefit can be explained by the presence of water in lower-proof alcohols: Indeed, water injection has been considered an effective method aimed at decreasing the emissions of  $\text{NO}_x$ . Moreover, water can also be effective in decreasing the PM emissions. A number of studies addressing the use of water injection as a pollutant-decreasing method have been published, and some of them are reviewed in Section 2.5.

The purpose of this research was to investigate the effects of fumigating 100-proof (50% ethanol, 50% water by volume) and 200-proof (absolute) on the performance and emissions of a Volkswagen 1.9L TDI engine. The effects of the injection of water into the intake manifold of the engine was also investigated. A simple and

easily retrofittable fumigation system consisting of a single atomizing nozzle mounted in the intake manifold was used for injecting ethanol and water. The results were compared to the baseline data obtained with regular ultra low-sulfur No. 2 diesel fuel. Conclusions were drawn regarding the effectiveness of the fumigation of both absolute and aqueous ethanol and also water injection in reducing exhaust pollutant emissions—primarily the emissions of PM and NO<sub>x</sub>.

## 1.1 Chapter Overview

The subjects in the present work are divided through the remaining sections as follows:

**Chapter 2** reviews diesel emissions, diesel oxygens, and the techniques of water injection and ethanol fumigation.

**Chapter 3** describes the experimental apparatus used for the engine experiments and the test procedures.

**Chapter 4** covers the experimental results. Comparisons are made between the results obtained from the fumigation techniques and from regular diesel operation.

**Chapter 5** presents a final discussion on the results obtained and concludes with suggestions for future work on the subject.

# Chapter 2

## Theory and Background

Background information on fumigation as a means to decrease diesel emissions will be presented in this section, along with references on the subject. Most of the references contain information on aqueous ethanol fumigation and a subsection dealing with water injection is also included. However, in order to help understand the mechanisms of action of those techniques on decreasing diesel pollutant emissions, some basic information on diesel engine combustion will be presented first. Subsequently, background material about emissions from diesel engines will be presented and discussed. Particular attention is given to PM and NO<sub>x</sub>—the pollutants from diesel engines which are hardest to control.

### 2.1 Combustion in Diesel Engines

The chemical reactions involved in diesel combustion are very similar to the reactions during combustion in spark-ignition engines. However, the *physical aspects* are very different in both combustion processes [132]. In a conventional spark-ignition engine, the processes of fuel metering and mixing with air take place upstream of the inlet valve(s), and the fuel-air mixture (along with some residual gas) reaches the cylinder essentially in gaseous phase and homogeneously mixed. Then the ignition by the spark



plug causes a well-defined *flame front* to spread through the cylinder charge, until it is burned. In contrast, in a diesel engine, fuel is injected into the cylinder towards the end of the compression stroke, when both in-cylinder pressure and temperature are very high. And because the fuel enters the cylinder in liquid phase, ignition does not start until a portion of it has vaporized and mixed with air. As a result, the flame develops under extremely nonuniform conditions of fuel in the air. Even though the overall fuel-air ratio is always lean in a diesel engine, there are large variations in equivalence ratio across the combustion chamber, on both a large and small scale [125]. This heterogeneous distribution of fuel within the cylinder and the corresponding heterogeneous burning process are the hallmark characteristics of diesel combustion. They are also the main reasons why diesel engines have a tendency to emit high levels of their most prominent pollutants, namely PM and NO<sub>x</sub>.

### 2.1.1 The Phases of Diesel Combustion

The overall process of combustion in diesel engines was originally conceived by Ricardo [112] to be divided into three distinct phases. The letters refer to the diagram in Figure 2.1:

- ignition delay (A–B)
- rapid combustion (premixed combustion) (B–C)
- mixing-controlled combustion (diffusion combustion) (C–D)

In Figure 2.1, SOI and EOI stand for "start of injection" and "end of injection", respectively. In addition to these, Heywood [65] defined also a fourth phase, the *late combustion phase* (D–E).

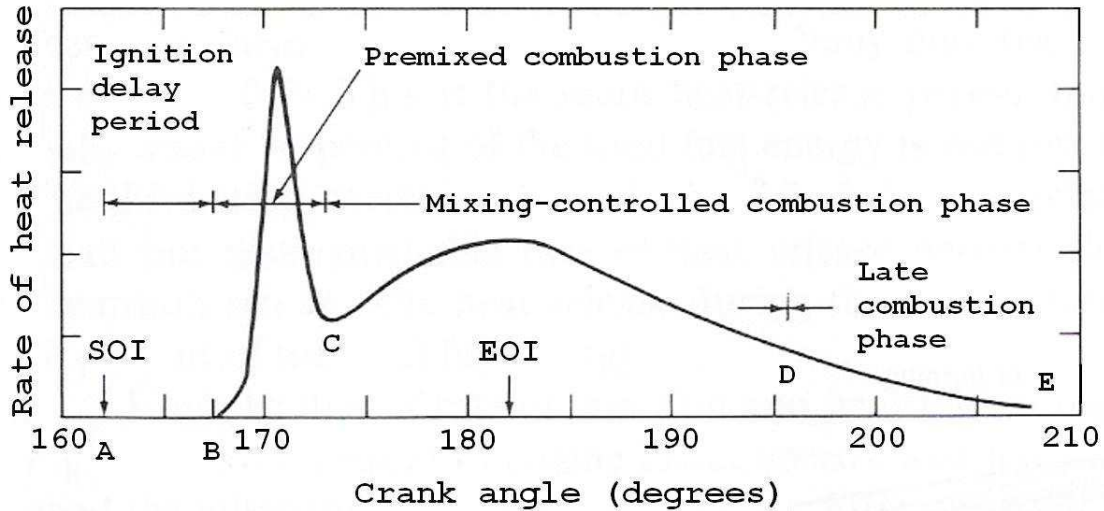


Figure 2.1: Typical DI engine heat-release-rate diagram [65]

As the fuel-air mixture burns, the chemical energy of the reactants is converted into sensible energy of the products through the combustion process, thus raising cylinder pressure and producing useful work. The rate at which this chemical energy is released is usually called *rate of heat release*, and it can be calculated from cylinder pressure data (see references [80] and [39] for further details).

Figure 2.1 above shows a typical heat-release-rate diagram for a DI diesel engine according to Heywood [65]. It illustrates the four phases of the overall diesel combustion process described below.

### 2.1.1.1 Ignition Delay

Fuel is injected into the cylinder towards the end of the compression stroke. The high-pressure jet of fuel being injected breaks up into tiny droplets which vaporize and mix rapidly with the surrounding hot air. However, combustion does not start until a visible flame or a measured in-cylinder pressure rise can be detected [132]. This period between the start of fuel injection and start of combustion is referred to as the *ignition delay*. The magnitude of the ignition delay depends on several factors,

such as: injection pressure, compression ratio, and fuel cetane number—fuels with poor self-igniting properties take longer to ignite, thus increasing the ignition delay.

#### 2.1.1.2 Rapid Combustion

As soon as the premixed fuel-air charge starts to ignite, the combustion reactions proceed extremely rapidly, burning the mixture of fuel and air that had been prepared during the ignition delay period. Therefore, the rate and length of this phase are closely related to the length of the delay period. This is the *rapid combustion* phase, which is also referred to as the *premixed combustion* phase. The large number of ignition points results in a very sharp rise in cylinder pressure, which in turn is responsible for the "knocking" sound characteristic of diesel engines. Indeed, this phase is characterized by the high rates of pressure rise and heat release. It is in the high-temperature, fuel-rich regions inside this premixed flame that soot precursors are originated before soot itself is nucleated and grown in the richer regions of the subsequent diffusion flame. More information about soot will be provided in Section 2.2.1.

#### 2.1.1.3 Mixing-Controlled Combustion

After the rapid combustion phase, when the premixed mixture of fuel and air has burned, combustion continues until all the remaining fuel is consumed. This is the *mixing-controlled combustion* phase, and the rate of the combustion reactions is now controlled by the rate at which fuel-air mixtures are formed—that is, this burning rate is governed by the *diffusion* processes of fuel into air and vice-versa. This phase is also known as the *diffusion combustion* phase. The diffusion flames are also responsible for the formation and growth of soot particles.

#### 2.1.1.4 Late Combustion

As described by Heywood [65], this combustion phase develops in the expansion stroke, when the reaction rates slow down as a result of the decreasing in-cylinder temperatures. Yet a small fraction of fuel is still burned, and oxidation of soot and fuel-rich combustion products can also take place.

## 2.2 Diesel Engine Exhaust Emissions

When compared to spark-ignition engines, diesel engines are known for their higher efficiency and lower levels of fuel consumptions—consequently, lower emissions of carbon dioxide ( $\text{CO}_2$ ). Moreover, their emissions of unburned hydrocarbons (HC) and carbon monoxide (CO) are in general much lower than those from an equivalent SI engine. However, diesel engines are still capable of producing high emission levels of PM and  $\text{NO}_x$ , and strict emissions standards are currently imposed to decrease the production of those pollutants from such engines [88, 126, 89, 47].

### 2.2.1 Particulate Matter

For the Environmental Protection Agency (EPA) regulation purposes, PM can be defined as any solid or liquid, excluding water, that can be collected on a filter when filtering diluted exhaust. The dilution ratio must be such that the temperature of the filter is not higher than  $52^\circ\text{C}$  ( $125^\circ\text{F}$ ) [17]. Particles produced by diesel engines are basically a complex mixture of elemental carbon, hydrocarbons, sulfur compounds, and ash. They can vary greatly in size, composition, solubility, and also in toxicity [27]. A typical composition for diesel particles was presented by Kittelson [75] and is illustrated in Figure 2.2 below.

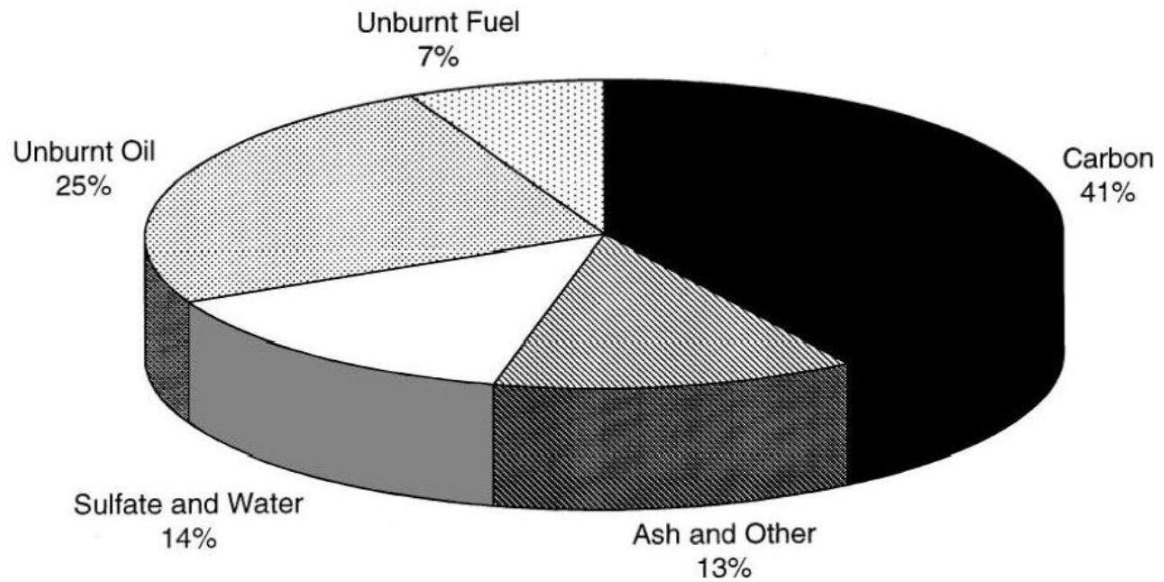


Figure 2.2: Typical particle composition for a 1998 (and earlier) heavy-duty diesel engine [75]

In general, the composition of diesel exhaust PM is divided into two major parts: a *solid fraction* and a *volatile fraction*:

- the solid fraction consists of:
  - carbonaceous agglomerates (soot)
  - inorganic ash
- the volatile fraction consists of:
  - organic compounds (hydrocarbons)
  - inorganic compounds (sulfuric acid and sulfates)

### 2.2.1.1 Solid Fraction

The solid fraction is responsible for most of the total particle mass, and its constituents (soot and ash) are formed directly by the combustion process.

**Soot** Over the years, *soot* has been the foremost and most characteristic pollutant emitted by diesel engines. Its formation is a very complex process, involving a large number of chemical reactions and intermediate compounds. Still, the process has been extensively studied, and a number of models for soot formation have been devised. One of such models is presented in the studies by Dec [30] and Flynn et al. [38]. Based on their findings, the soot formation process originates in the fuel-rich regions of the premixed flame (see Figure 2.3). Typical conditions are characterized by temperatures between about 1000 and 2800 K, and pressures of 50 to 100 atm [65]. In such regions, large hydrocarbon molecules from the fuel undergo thermal decomposition (cracking), due to the high temperatures and the relative absence of oxygen. This process is analogous to a pyrolysis process and it produces compounds that are precursors to soot formation. These *soot precursors* typically include unsaturated hydrocarbons, such as ethylene, acetylene, etc., and the so-called polycyclic aromatic hydrocarbons (PAHs) [65, 58]. Once formed, these compounds originate soot particles in a region between a standing fuel-rich premixed flame and the outer diffusion flame of the burning fuel jet [29]. In this region, soot precursors cause the nucleation and growth of soot particles through a complex process which involves oxidation, condensation, coagulation, agglomeration, and growth. Yet not all soot precursors become soot: the remaining precursors are emitted in the form of volatile compounds that comprise the soluble organic fraction (SOF) (see below). After formation, soot starts to oxidize when it reaches the leaner periphery of the flame and it undergoes further oxidation during the expansion stroke. Estimates have suggested that over 90% of the soot eventually oxidizes [65]. However, as the temperature inside the cylinder

drops, oxidation ceases, and the remaining soot is emitted through the exhaust manifold and tailpipe in the form of agglomerates of very small individual carbonaceous spherical particles. Amann and Siegl [17] named these primary particles "spherules". According to their work, most spherules fall into the 15–30 nm diameter range.

In the case of pure hydrocarbon fuels, soot formation may be correlated to fuel properties such as hydrogen-to-carbon ratio, aromatic content, and the number of carbon-carbon bonds. Indeed, a work by Takahashi and Glassman [131] concluded that, in laboratory flame studies, the H to C ratio and the number of C-C bonds in the molecule were the most important properties that determine the tendency for soot formation.

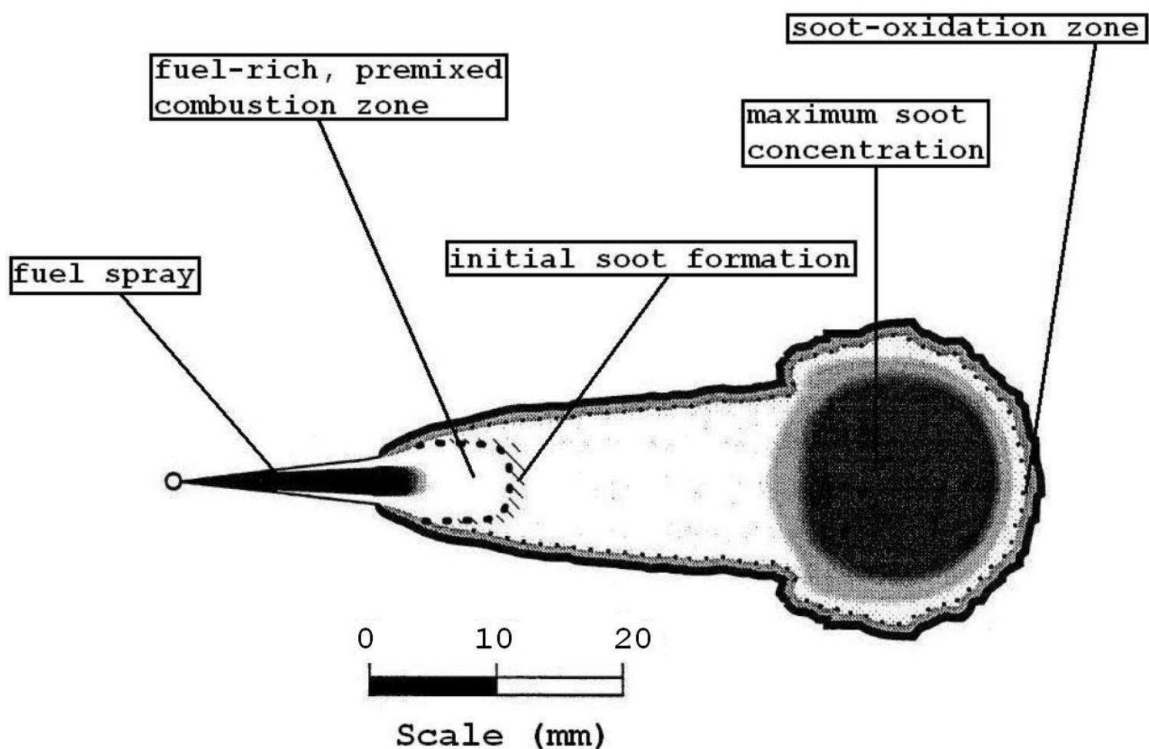


Figure 2.3: The conceptual model of DI diesel combustion proposed by Dec [30]

**Inorganic Ash** Ash constitutes only a small portion of the entire solid particulate fraction, and it originates mostly from metal compounds in the fuel and lubricant oil.

### 2.2.1.2 Volatile Fraction

The volatile fraction is responsible for most of the particle number and does not originate directly from combustion. Instead, these particles originate from volatile precursors by nucleation and adsorption as the exhaust undergoes dilution and cooling. The extent to which the precursors can nucleate to form new particles depends strongly on the dilution and cooling conditions. Furthermore, nucleation to form new particles is not the only process the volatile materials can undergo during dilution and cooling of the exhaust: they can also remain in the gas phase or they can condense onto droplets or adsorb onto solid particles (e.g., soot). Indeed, high concentrations of solid particles inhibit the nucleation of new volatile ones, due to a higher total surface area available for condensation and adsorption. Most of the volatile particles are composed of organic and inorganic compounds [7]:

**Organic Compounds** This fraction originates primarily from lubricating oil and fuel [115] and is comprised mainly of unburned fuel-bound hydrocarbons, oxygenated hydrocarbons (ketones, esters, ethers, organic acids), and PAHs. Most of the volatile compounds in the exhaust of modern diesel engines are comprised of hydrocarbons.

**Inorganic Compounds** The basic components of the volatile inorganic fraction are sulfur compounds originating from sulfur present in the fuel; these compounds are essentially sulfuric acid ( $\text{H}_2\text{SO}_4$ ) and various sulfates. This inorganic volatile fraction is also roughly proportional to the sulfur content of the diesel fuel [75].

The organic and inorganic volatile compounds are collectively known as *soluble organic fraction* (SOF) and *soluble inorganic fraction*, respectively. These fractions can be separated with extraction solvents, such as dichloromethane and blends of benzene ( $\text{C}_6\text{H}_6$ ) and ethanol. The remaining, "dry" fraction is the solid fraction—primarily soot.



In appearance, diesel PM is conceived as being formed by large clusters or aggregates of soot spherules onto which volatile compounds have adsorbed and condensed. Metallic ash may often appear embedded into these clusters. An illustration of the morphology of a typical diesel particle shown in Figure 2.5.

### 2.2.1.3 Particle Size Distributions

The concentration of the particles emitted by a diesel engine is typically distributed by size according to Figure 2.4 [75]. The figure shows both number- and mass-weighted particle size distributions. Three modes can be identified in an idealized distribution:

- accumulation mode
- nucleation mode
- coarse mode

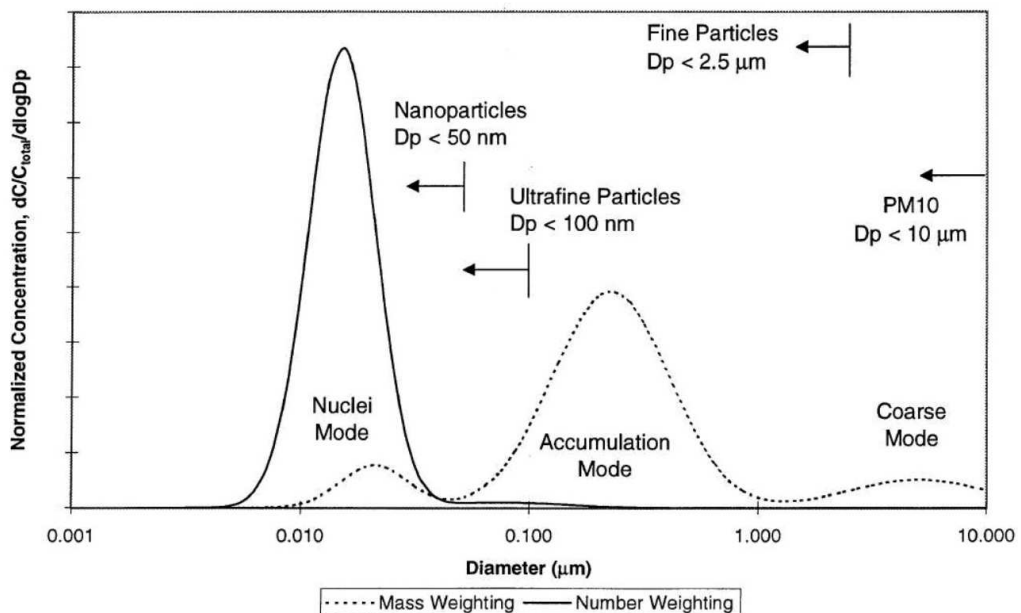


Figure 2.4: Typical engine exhaust size distributions [75]

The *accumulation mode* is typically responsible for 90% of the total particle mass, and is essentially comprised of agglomerates of soot spherules, embedded ash, and associated adsorbed and condensed volatile materials. Most of the total number of particles, on the other hand, is in the *nucleation mode*—also referred to as *nuclei mode*. This mode includes volatile particles that originate from organic and inorganic compounds through nucleation during as the exhaust dilutes and cools. The nucleation mode can also contain small amounts of solid particles, such as ash particles and individual spherules. Lastly, the *coarse mode* is formed by reentrained particles from the accumulation mode that have been collected on the surfaces of the cylinder and exhaust system. A study by Harris and Maricq [51] provides further information on particle size distributions from both diesel and gasoline engines.

A work by Maricq [92] presents an artist's conception of diluted and cooled diesel PM. Figure 2.5 below illustrates this conception.

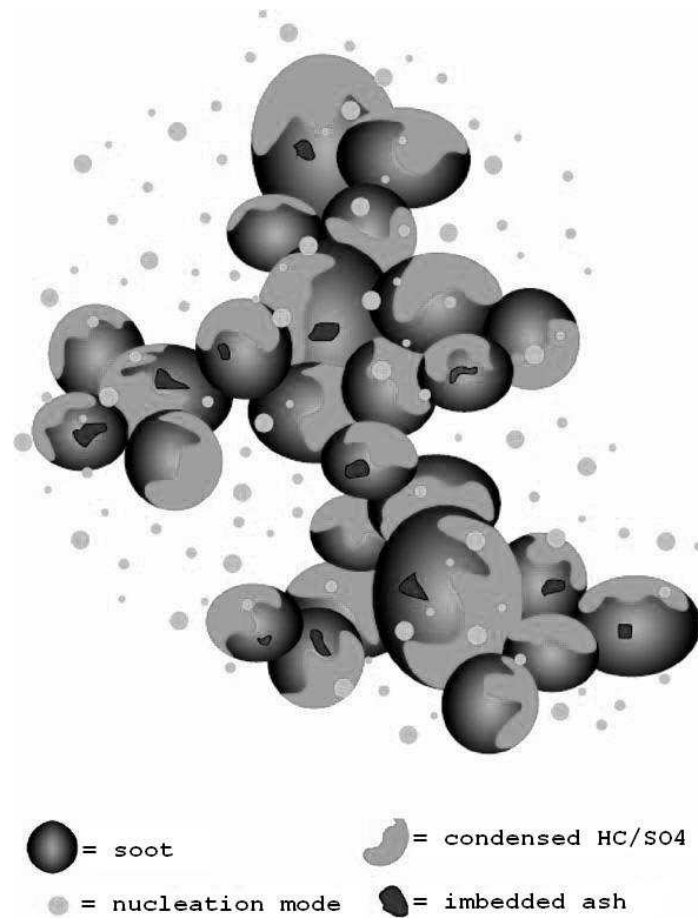


Figure 2.5: Artist's conception of diesel particulate matter [92]

#### 2.2.1.4 PM-Reducing Techniques

Some commonly-used techniques for decreasing the emissions of PM in diesel engines are discussed below:

**Engine Design** The emissions levels of PM (smoke in particular) are nowadays reduced by techniques that aim at precisely controlling the mixing process of diesel and air in the cylinder. Such techniques include: high-pressure, electrically-controlled fuel injection (such as unit injectors or common-rail systems) , turbocharging, and aftercooling. A study by Russell [114] shows how the control of fuel injection rate and profiling influences pollutant formation.

**Aftertreatment Devices** PM emissions can also be effectively reduced with aftertreatment devices, such as oxidation catalysts and particulate traps—filters that require high temperatures for soot oxidation [37, 56, 136]. An example of a device that combines both a catalyst and a trap is the continuously regenerating trap (CRT) [8].

**Fuel Oxygenates** Fuel-borne oxygen generates certain radicals during combustion that have the ability to inhibit the inception of PM—particularly soot. The addition of an oxygenate also causes the fuel-air mixture to burn leaner, which tends to reduce pollutant emissions. The issue of oxygenates and their method of action are further discussed ahead, in Section 2.3.

## 2.2.2 Oxides of Nitrogen

The term  $NO_x$  refers to a mixture of both nitric oxide (NO) and nitrogen dioxide ( $NO_2$ ). The majority of  $NO_x$  formed during combustion in diesel engines is comprised of NO, although at light loads a significant  $NO_2$  fraction is present. After NO is emitted in the exhaust it suffers an oxidation process in the atmosphere, in the presence of non-methane hydrocarbons and ultraviolet light. This process results in NO being converted into  $NO_2$ , and the latter is an important component responsible for the photochemical smog—a major form of pollution [125].

### 2.2.2.1 Chemical Pathways for NO Formation

NO is formed in flames mainly by the following mechanisms [99]:

- prompt
- thermal
- nitrous oxide

**Prompt Mechanism** The formation of NO through the prompt mechanism occurs in the flame region as the CH radical reacts with molecular nitrogen according with the reaction [99]:



This mechanism is usually not relevant for combustion at the conditions found in compression-ignition engines. Therefore, the chemistry of NO in diesel engines can be assumed to be controlled by the thermal and nitrous oxide mechanisms only [99].

**Thermal Mechanism** This is the foremost mechanism for  $NO_x$  formation in diesel engines and it occurs in the hot combustion gases at sufficiently high temperatures ( $>1800$  K). The thermal mechanism is based on the so-called *extended Zeldovich mechanism* [143], in which NO is formed as atomic oxygen reacts with nitrogen in the presence of free radicals (O, N, H, and OH) [99], according to the following reactions:



Zeldovich was the first to suggest the importance of reactions 2.2 and 2.3; Lavoie et al. [86] added reaction 2.4 to the mechanism.

**Nitrous Oxide Mechanism** The formation of NO by the nitrous oxide mechanism is particularly significant in high-pressure premixed and diffusion flames. At the pressures typically found in diesel engines, the nitrous oxide mechanism takes the form:



By adding the reaction:



all the above reactions can be balanced so that the *overall reaction* is:



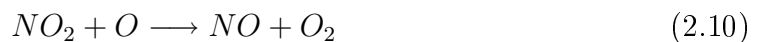
Therefore, the so-called "skeletal" mechanism for  $NO_x$  chemistry in diesel engines is comprised of reactions 2.2 through 2.7 [99].

#### 2.2.2.2 $NO_2$ Formation

Unlike spark-ignition engines, diesel engines can produce a measurable amount of  $NO_2$ , and the fraction of  $NO_2$  in the total exhaust  $NO_x$  typically varies from 10 to 30% [67]. Merryman and Levy [100] presented the following mechanism for the formation of  $NO_2$  in diesel engines, in which  $NO$  is converted to  $NO_2$  via reactions such as:



Unless the  $NO_2$  formed in the flame zone is quenched, however, it is converted back to  $NO$  via the reaction:



This quenching of  $NO_2$  explains why the  $NO_2/NO$  ratios in diesel engines are highest under low load conditions, when the cycle temperatures are lower [67].

High temperatures are the main driving force for the formation of  $NO_x$  in diesel engines, with oxygen concentration and duration of combustion also playing a significant role. Because temperature has such a strong influence, the in-cylinder techniques used to decrease  $NO_x$  emissions do so by attempting to ultimately reduce peak combustion temperatures in one way or another.

#### 2.2.2.3 $NO_x$ -Reducing Techniques

Some commonly-used techniques for decreasing the emissions of  $NO_x$  in diesel engines are:

**Injection Timing** Retarding the timing of fuel injection is an effective method used to decrease  $\text{NO}_x$  emissions from a diesel engine. By doing so, the combustion events are shifted towards the expansion stroke, causing a reduction in peak flame temperature and pressure, thus slowing down the reactions of the  $\text{NO}_x$  mechanism. On the other hand, this technique also causes an increase in PM emissions and fuel consumption, because by delaying the fuel injection the duration of the diffusion combustion phase is extended and the resulting lower temperatures during the expansion stroke impair the oxidation of the soot that has been formed. The change in fuel injection timing provides a classic example of the  $\text{NO}_x$ -PM trade-off which is characteristic of diesel engines [64, 141].

**Exhaust Gas Recirculation** Exhaust gas recirculation (EGR) is another common technique currently used to decrease  $\text{NO}_x$  emissions from internal-combustion engines—both spark- and compression-ignited [5]. It consists in introducing exhaust gases into the intake manifold of an engine as a way to reduce the peak flame temperatures, consequently slowing down the formation of  $\text{NO}_x$ . The  $\text{NO}_x$ -reducing ability of the EGR method is essentially due to three effects [81, 82, 83, 84, 79]:

- dilution
- chemical
- thermal

**Dilution Effect** This effect is caused by the displacement of oxygen by inert gases, such as  $\text{CO}_2$ ,  $\text{N}_2$ , and water vapor drawn from the exhaust. This displacement decreases the availability of oxygen required for combustion, and as a consequence, the peak combustion temperature is lowered.

**Chemical Effect** The chemical effect happens as a result of the dissociation of compounds like CO<sub>2</sub> and water vapor at the high in-cylinder temperatures. The dissociation of such compounds is highly endothermic, which causes the peak temperatures to drop.

**Thermal Effect** This effect helps lower combustion temperatures by introducing into the cylinder compounds with high specific heats. Both CO<sub>2</sub> and water have specific heats that are higher than the specific heat of air. This change in the overall thermal capacity of the charge helps cooling down in-cylinder temperatures.

All of the above effects cause an increase in ignition delay, and a decrease in both peak cylinder pressure and temperature, thus lowering NO<sub>x</sub> emissions. Ladommatos et al. [85] investigated the effects above in detail and they came to the conclusion that, in diesel engines, dilution is the foremost NO<sub>x</sub>-reducing effect when EGR is used.

## 2.2.3 Unburned Hydrocarbons and Carbon Monoxide

### 2.2.3.1 Unburned Hydrocarbons

The emissions of HC are usually not as high in diesel engines as they are in spark-ignition engines. In the latter, there are several sources of unburned HC, the most prominent being the flame-quenching phenomenon that occurs on cylinder and piston surfaces, and crevices. In diesel engines, the complex and heterogeneous nature of combustion is responsible for the two major mechanisms that result in diesel HC emissions. These HC-forming mechanisms are a consequence of the wide distribution of equivalence ratios that exists across the fuel spray: *Overmixing* (overleaning) occurs during the ignition delay, in the regions in the spray periphery that are too lean to sustain combustion. This is the predominant mechanism for HC emissions during normal engine operation and it becomes more prominent at idle and low-load



conditions, when the ignition delay is longer [141, 45]. On the other hand, *undermixing* occurs in the fuel-rich regions in the fuel spray that are too rich to burn. This mechanism occurs more frequently during the injection of fuel after the delay period, and during overfueling conditions, such as engine accelerations at high loads. Advancing fuel injection timing tends to cause higher combustion temperatures and pressures, thus promoting the oxidation of hydrocarbons. However, this increase in temperatures also causes an increase in  $\text{NO}_x$  emissions, and the increase in rate of pressure rise results in higher engine noise levels [141].

### 2.2.3.2 Carbon Monoxide

The emissions of CO are a direct consequence of incomplete combustion. Accordingly, the fuel-air ratio is the main factor controlling CO emissions in engines. In spark-ignition engines, which operate close to stoichiometric fuel-air ratios at part-load and fuel-rich at full load, CO emissions increase with increasing equivalence ratio [50]. If the CO levels are to be kept low, spark-ignition engines require the use of exhaust gas treatment, such as oxidation catalysts. In contrast, diesel engines operate with excess air. The overall lean combustion ensures very low levels of CO emissions. In the case of well-regulated diesel engines, CO emissions are low enough and thus can be considered not relevant.

## 2.3 Diesel Fuel Oxygenates

In attempting to reduce PM emissions from diesel engines, a method which is commonly employed is the combination of oxygen-bearing compounds along with regular diesel fuel. Compounds which contain oxygen are referred to as *oxygenates*. Their usage has become more common as a result of more stringent emissions standards and the promotion of the use of renewable fuels—which usually contain oxygen—in diesel engines.

### 2.3.1 Mechanism of Action

It was previously discussed that soot precursors originate in the fuel-rich areas of premixed flames and the nucleation and growth of soot itself occurs in the subsequent diffusion flames during the diesel combustion process. Part of the soot undergoes oxidation in leaner zones of diffusion flames and also during the expansion stroke. However, the oxidation is not complete, and soot is emitted as a black smoke.

Basically, the introduction of fuel-borne oxygen into the combustion process decreases the formation of soot precursors during the thermal cracking of the fuel. Results obtained by numerical simulations from a study conducted by Cheng et al. [29] show that the ability of an oxygenate to decrease soot emissions in general can be attributed to some important mechanisms:

- Fuel-borne oxygen shifts the products of thermal cracking by displacing the long carbon chains that exist in regular diesel fuel. In general, different fuels originate different cracking products, with different tendencies for soot formation
- During the premixed combustion phase, oxygenates can dramatically increase the concentration of free radicals such as O, OH, and HCO. These radicals help oxidize carbon to CO and CO<sub>2</sub>. As a result, the availability of carbon to form soot precursors is decreased
- High concentrations of those free radicals (OH in particular) can also oxidize soot precursors in the diffusion flame, limiting the formation and growth of PAHs and inhibiting the inception of soot particles

It was reported in a modeling study carried out by Benvenuti et al. [21] that the methyl radical (CH<sub>3</sub>) is also an important precursor for the formation of soot-oxidizing radicals, such as OH.

As it can be noted, the formation and growth of soot precursors are essential for the subsequent inception and growth of soot particles. Cheng et al. also pointed

out in their study [29], that the relative concentration of species in the fuel-rich premixed flame plays an important role in the soot formation process by controlling the subsequent processes of formation of aromatics, growth of PAHs, and inception of soot particles.

### 2.3.2 Types of Oxygenates

Several types of oxygen-containing compounds have been used as fuel oxygenates. According to their chemical nature, oxygenates usually belong to one of the following groups:

- alcohols
- ethers
- esters
- carbonates
- acetals

Oxygenates can range widely in molecular weight, from light molecules such as methanol to heavy methyl or ethyl esters of fatty acids with up to 20 carbon atoms.

**Biodiesel** Vegetable oils have long been considered as alternative fuels for diesel engines [119]. However, the use of vegetable oils as diesel fuels has also been precluded by many factors, such as their high viscosity, polyunsaturated character, and very low volatility [14, 12, 13]. In order to overcome these problems different techniques are employed that allow vegetable oils to be used as fuels for diesel engines. Typically, these techniques are: dilution, pyrolysis, microemulsions, and transesterification [14]. Biodiesel is the term commonly applied to the alternative fuel obtained from the transesterification of vegetable oils or animal fats. Transesterification (also known as alcoholysis) is a method through which an alcohol substitutes glycerol, splitting the

vegetable molecules into lighter molecules [12]. It is defined as a mixture of monoalkyl esters of long-chain fatty acids, derived from either vegetable oils or animal fats. It is typically comprised of alkyl fatty acid esters of short-chain alcohols, such as methanol or ethanol. Commercial biodiesel is currently mainly obtained from soybean, rapeseed, and palm oils [32]. When compared to petroleum-based diesel fuels, biodiesel has several advantages, such as renewability, higher combustion efficiency, lower sulfur and aromatic content, higher cetane number, and higher biodegradability. It also reduces greenhouse gas emissions, helps reduce dependence on imported petroleum, and strengthens agriculture [32]. Also, biodiesel typically contains 11% oxygen by weight—and no sulfur. Because of these advantages, biodiesel has gained broader acceptance and market share as a diesel fuel in both Europe and the United States. It can be used in diesel engines in neat form, but its utilization is more common in the form of blends with regular diesel fuel—blends of up to 20% biodiesel with diesel can virtually be used in any diesel engine [32].

Although oxygenates are usually used in the form of blends with diesel fuel, alcohols, for instance, can also be used in other forms. Depending on the level of engine modifications required, alcohols can be used through the methods of fumigation, dual fuel injection, and even neat alcohol operation—the latter two requiring extensive engine modifications. Fumigation is a particularly attractive method because it allows the utilization of alcohols in engines with little modifications and without the issues associated with the limited miscibility of alcohols (methanol and ethanol in particular) with diesel fuel. Further background information on ethanol fumigation will be presented below.

### 2.3.3 Review of Oxygenates

The utilization of oxygenates in diesel engines has been extensively investigated over the years and the literature on the field is vast. The actual mechanisms through which oxygenated compounds affect pollutant formation in diesel engines are still

widely debated by researchers. In particular, there is controversy about the role of molecular structure in the PM-reducing abilities of an oxygenate: some believe that structure does play a significant role whereas others affirm that oxygen content is by far the sole determining factor on the performance of an oxygenate:

A study of oxygen content on engine smoke emissions was conducted by Nabi et al. [105]. Their study investigated the effects of six different oxygenates on the emissions from a single-cylinder DI diesel engine, and they found that the smoke emissions decreased linearly as a function of oxygenate oxygen content only. Near-zero smoke levels were attained at an oxygen content of 38% (wt.) and higher.  $\text{NO}_x$  emissions were significantly reduced not directly, but indirectly, by using higher EGR levels.

An earlier study that attributed oxygenate soot-reduction effectiveness to oxygen content was carried out by Miyamoto et al. [101].

The aforementioned work by Cheng et al. [29] also reported that the reduction in PM levels was largely influenced the oxygen content of the fuel blend. In their study the effect of oxygenate chemical structure was found to be small.

On the other hand, several investigators agree that besides fuel oxygen content, the *chemical structure* of an oxygenate also plays a significant role in determining its effectiveness in reducing PM emissions.

For instance, Yeh et al. [139] tested a wide variety of blends using fourteen different oxygenates. The comparison between blends was made with all blends having the same oxygen content (% wt.). They reported "very large PM emissions differences" between oxygenated blends containing the same oxygen content. In their study, the most effective oxygenates were found to be the higher alcohols, which outperformed ethers, esters, and carbonates in PM reduction. In particular, the more volatile compounds exhibited superior performance than the heavier ones.

In a study by Sison et al. [124], rapeseed methyl ester (RME) and diglyme (an ether) were used as oxygenated blending agents. Both blends had an oxygen content of 3% by mass. Although they reported a PM-reducing behavior for both oxygenates,

their results also showed "significant differences in soot generation" between the two compounds. Also, there was "some indication" that oxygenated fuel blends had a tendency to burn with lower flame temperatures than the base diesel fuel.

A study conducted by Mueller et al. [103] made use of engine tests and numerical simulations in order to better assess the effect on engine PM emissions of the oxygenated compounds di-butylmaleate (DBM) and tri-propylene glycol methyl ether (TPGME). The results of both their experiments and numerical modeling concluded that fuel blends with TPGME were more effective at reducing soot levels than the DBM blends. This behavior was observed for all testing conditions. The numerical simulations showed that over 30% of the oxygen in the DBM molecules is not available for inhibiting the formation of soot precursors. Indeed, it was shown that DBM exhibited a tendency to form acetylene—a soot precursor. These particular results suggest that some oxygenates do not possess molecules that are very prone for the elimination of soot precursors. Some oxygen-containing compounds, by virtue of their molecular structure, are unable to make all of their oxygen available for precursor oxidation.

Therefore, whether chemical structure plays a larger or a lesser role is by no means a trivial issue. Oxygen content is not the only diesel fuel variable that changes when an oxygenate is added to it—the physical and chemical properties of a fuel can be somewhat modified when oxygen-bearing compounds are blended with it. Furthermore, all changes in fuel properties have an influence on the way the engine operates, the combustion develops, and consequently the way particles are formed. As Hallgren and Heywood stressed in their study [47]:

"It is difficult to attribute emission changes to the addition of molecular oxygen when several fuel properties are changed simultaneously".

And the extent to which those variables affect engine behavior is very often *engine- and test-specific*. As an example, in their investigation [47], Hallgren and Heywood observed that intake air temperature had a significant influence on PM emissions. They also concluded that oxygenate structure had an impact on those emissions.

Although there is a consensus about the PM-reducing benefits of diesel oxygenates, the same cannot be said about their  $\text{NO}_x$ -reducing capabilities. The effect of fuel-bound oxygen on  $\text{NO}_x$  emissions is not very clear: some studies report a small increase in  $\text{NO}_x$  whereas others conclude that the emissions of oxides of nitrogen remain essentially unchanged. Again, the addition of oxygen modifies the fuel as a whole and the changes in  $\text{NO}_x$  formation cannot be attributed solely to oxygen content. Moreover, testing conditions and engine characteristics probably have a significant influence in  $\text{NO}_x$  emissions.

Nevertheless, because the addition of oxygen into diesel fuel produces a shift in the  $\text{NO}_x$ -PM trade-off behavior, once the PM emissions had been reduced by the presence of an oxygenate the emissions of  $\text{NO}_x$  can be *indirectly* decreased by further utilization of a technique such as exhaust gas recirculation. This shift in the  $\text{NO}_x$ -PM trade-off curve is illustrated in Figure 2.6 [29]. For instance, a discussion about the use of higher EGR rates combined with oxygenated fuels can be found on a study by Hilden et al. [66].

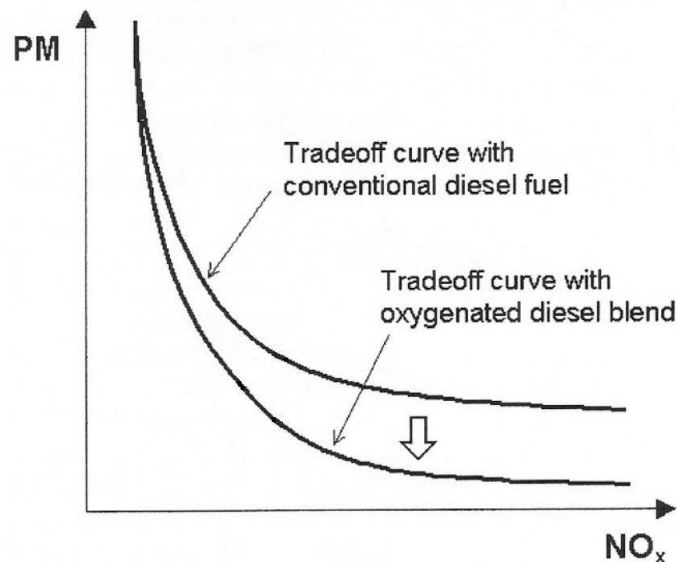


Figure 2.6: The shift in the  $\text{NO}_x$ -PM trade-off curve produced by oxygenates [29].

The effect of using oxygenated fuels to reduce PM mass emissions can be verified on a mass-weighted particle size distribution by noting the decrease in particle concentration. This decrease may be accompanied by a shift in mode toward smaller particle diameters. If a nucleation mode is present, an increase in particle number concentration may also occur as a result of oxygenate addition. An example of a shift in particle diameter is illustrated in a study by Maricq et al. [93], where a diesel passenger car was coupled to a chassis dynamometer and the diesel fuel was oxygenated by the addition of dimethoxymethane (DMM). The car was powered by a four-cylinder, 1.8-L, indirect-injection (IDI) turbocharged diesel engine. Besides the reduction in particle mass concentrations and the shift towards smaller particles, their results found that the  $\text{NO}_x$  emissions were relatively unchanged when the DMM-blend was compared to regular diesel fuel.

## 2.4 Utilization of Alcohols in Internal-Combustion Engines

The worldwide petroleum crises of the 1970s also triggered the awareness for seeking alternative, renewable energy sources, and ethanol (ethyl alcohol) from biomass has been widely proposed as a renewable fuel for internal-combustion engines—due to its renewable nature and cleaner-burning combustion. Bioethanol—from either corn grain (starch) or sugar cane (sucrose)—is nowadays the most common renewable fuel [43, 33], and the idea of using it as an alternative engine fuel is not recent—as an example, see the 1907 study by Lucke and Woodward [91]. In more recent years, ethanol fuel has been used primarily in Brazil, where ethanol-fueled automobiles have been sold since 1979 [127, 42, 102, 78]. In the United States, the utilization of ethanol in spark-ignition engines has gained momentum as well. This is particularly the case in the Midwest, where a blend comprised of 85% anhydrous ethanol and 15% gasoline (referred to as "E85") has found widespread use as a fuel for the so-called Flex Fuel



Vehicles (FFV) [133, 94, 135]. The use of ethanol as a motor fuel can result in several benefits, such as:

- lower levels of pollutant emissions
- decreased demands for imported crude oil
- improved utilization of domestic, renewable energy sources
- strengthened energy security

Whereas the use of ethanol as spark-ignition engines has been generally successful [10, 96, 78, 106], its use as a fuel for compression-ignition engines has been precluded by several factors. Among those are the physico-chemical characteristics of ethanol that make it unsuitable as a fuel for diesel engines [97], for instance:

- ethanol has poor autoigniting properties (i.e., low cetane number)
- ethanol has very poor lubricating characteristics
- ethanol is corrosive

The foremost drawback for the utilization of ethanol in diesel engines is probably its low cetane number which, depending on the measurement method, typically ranges from 2 to 12 [104]. These values are well below the minimum cetane number of 40 required by the ASTM standard [4]. In spite of these drawbacks ethanol has nevertheless been used in diesel engines in primarily one the following methods:

- ethanol-diesel fuel blends
- dual injection ethanol-diesel fuel
- neat ethanol with ignition improvers
- ethanol fumigation

A further review on the utilization of alcohols in diesel engines can be found in references [10], [96], [34], and [140].

The technique of obtaining blends of ethanol with conventional diesel fuel (sometimes called “e-diesel”) has been extensively investigated over the years and the literature in this field is vast [128, 138, 120, 98, 15, 22, 35, 107, 48]. However, in spite of its relative popularity, blends of diesel fuel and ethanol have some well-known drawbacks—miscibility is one of them: ethanol, being a polar compound, does not mix well with diesel fuel. The problem of phase separation becomes even worse when the ethanol (which is hydrophilic) contains even minute amounts of water [97, 40, 70]. Actually, the feasibility of diesel-ethanol blends has been made possible only by the addition of surfactants in order to form micro-emulsions, rather than real solutions. The use of two separate fuel injection systems—for alcohol and diesel fuel—is more complicated because it involves significant engine modifications, whereas the use of neat ethanol in diesel engines usually requires the addition of relatively large amounts of expensive ignition-improving compounds and very high compression ratios [49, 117, 123].

### 2.4.1 Ethanol Fumigation

Another method of utilizing ethanol in diesel engines is by means of *fumigation*, i.e., the introduction of ethanol into the intake manifold of a diesel engine. It is a form of dual-fuel operation where part of the fuel is premixed with the intake air, and part is injected into the cylinder as in a regular diesel engine [36]. This injection of alcohol can be accomplished by means of a carburetor, atomizing nozzles, electronically-controlled fuel injectors, etc. Alcohol fumigation is a relatively simple and uncomplicated method which also features some important advantages: it can be made easily retrofittable to existing engines and it easily allows the engine to switch back to neat diesel operation at any time. Unlike diesel-ethanol blends, miscibility does not pose a problem and in general, depending on several factors, the fumigation

technique is able to replace up to about 50% of energy from diesel fuel.

#### 2.4.1.1 Background

In an early study, Havemann et al. [54] attempted to utilize ethanol in diesel engines in the form of ethanol-diesel blends; because the results were not very satisfactory—due to the poor miscibility of ethanol in diesel fuel—they decided to try fumigation instead. The fumigation tests were carried out in a Ricardo research engine and in a Petter AV1 Series II production engine. Their results showed that at full load the fumigation of ethanol could provide up to 36% of fuel energy in the Ricardo engine, whereas in the Petter engine up to nearly 70% of fuel energy could be provided by the ethanol at full load. It was reported that the maximum amount of alcohol that could be inducted was limited by the occurrence of knocking (in the Ricardo engine) and misfiring (in the Petter engine). In both engines alcohol fumigation led to higher air utilization, which made it possible to use ethanol to provide a power boost (overfueling) without sacrificing the smoke limit. The smoke density was considerably reduced as a result of the fumigation of ethanol in both engines, and the reductions in smoke levels were proportional to the amount of ethanol inducted. The Ricardo engine also exhibited a slight increase in thermal efficiency with ethanol fumigation at high loads. More early results obtained with ethanol fumigation can be found in references [55] and [53].

In 1958, Alperstein et al. [16] introduced atomized supplementary fuels into the intake air of a single-cylinder, naturally-aspirated diesel engine, in an attempt to reduce exhaust smoke levels. Their study reported a reduction of up to 70% in smoke levels, increased power output, and slightly increased thermal efficiency with ethanol fumigation.

In a 1975 study by Barnes et al. [20] the utilization of alcohols as supplemental fuels by means of fumigation was examined. The alcohols used were methanol, ethanol, and isopropanol. Their work was conducted on a six-cylinder, 5.1-L turbocharged DI

diesel engine. Fumigation was achieved by a single alcohol atomizing nozzle located *upstream* of the turbocharger compressor. This particular location was chosen to "take full advantage of charge cooling". Their results showed that engine efficiency decreased with increasing flow of alcohol. They attributed this loss in efficiency to insufficient compression heating, which impaired full alcohol evaporation. Also, due to alcohol evaporation, the intake manifold temperature was shown to decrease significantly. The gaseous exhaust emissions were not greatly affected in their study, whereas the smoke density decreased with increasing alcohol amounts, as had been expected. The in-cylinder pressure traces revealed that alcohol caused sharper pressure peaks when compared to regular diesel operation. The sharpest pressure peaks were observed at the highest engine loads; lower loads resulted in lower peak pressure—probably due to misfire. No engine knock was observed.

Bro and Pedersen [24] carried out fumigation tests on a single-cylinder, naturally-aspirated diesel engine. They reported improved thermal efficiency at high loads, decreased smoke levels, and increased levels of HC emissions when ethanol was fumigated. They also found that the maximum amount of fumigated ethanol was limited by excessive rates of combustion, leading to engine knock.

Chen et al. [28] tested the fumigation of 200- and 160-proof ethanol in a four-cylinder, 5.5-L turbocharged diesel engine. The alcohol was fumigated by means of a simple atomizing nozzle mounted in the intake air duct *downstream* of the compressor, in order to avoid liquid droplet impingement on its blades. It was reported that engine thermal efficiency would either exhibit a slight increase at high loads or a slight decrease at low loads. Ethanol fumigation would cause an increase in both ignition delay and in-cylinder rates of pressure rise. Worth noting is the fact that they did not observe any noticeable change in engine performance with ethanol proof (a similar result had been reported in a previous study by Holmer et al. [68]). At all tests conditions, they reported decreases in smoke levels with increased alcohol flowrates. Ethanol fumigation also decreased the levels of  $\text{NO}_x$ , whereas HC and CO

emissions increased with ethanol, as compared to regular diesel fuel operation. A problem which was detected was uneven ethanol distribution among the cylinders, as indicated by the marked differences in the exhaust temperatures among them.

Similar emissions results were also reported by the work of Heisey and Lestz [59]. In their study, the fumigation of ethanol in different proofs (200, 180, 160, and 140) was carried out in a single-cylinder DI diesel engine using a simple atomizing nozzle which was mounted in the intake manifold. Their results also showed that NO emissions were reduced when fumigating the lower proofs. Also, engine thermal efficiency, and rate of pressure rise were not significantly affected by lower ethanol proofs. However, use of lower-proof ethanols resulted in longer ignition delays.

Broukhiyan and Lestz [25] conducted ethanol fumigation tests on an Oldsmobile 5.7-L V8 diesel engine. This was a naturally-aspirated, indirect-injection engine introduced by General Motors in 1978 (see Jones et al. [73]). They used a simple air-atomizing nozzle in a specially-designed mixing chamber to fumigate the alcohol among the eight cylinders. Their results showed increases in thermal efficiency with ethanol fumigation at higher loads. Engine roughness or the occurrence of knock, however, limited the maximum amount of ethanol that could be fumigated. The emissions of  $\text{NO}_x$  generally decreased below baseline levels as the amount of fumigated ethanol was increased; ethanol also decreased the PM emissions on a mass basis. The biological activity of both the raw PM and its SOF were screened using the Ames *Salmonella typhimurim* assay [18]; it was found that the biological activity of the particulates seemed to increase with ethanol fumigation. Similar results were also reported in a study by Houser et al. [69] in which the fumigation of methanol was carried out on a similar Oldsmobile diesel engine.

Sullivan and Bashford [129] tested a commercially-available retrofittable fumigation kit on an Allis-Chalmers 7040 diesel tractor. The fumigation system sprayed ethanol upstream of the turbocharger and the flowrate of ethanol delivered was controlled by means of the boost pressure. The results showed improved diesel fuel

economy, but the impingement of ethanol droplets resulted in excessive damage on the turbocharger compressor blades after only 30 hours of testing.

Goering and Wood [41] carried out ethanol fumigation tests under *overfueling* conditions (i.e., when the alcohol is used to augment total engine power, rather than substituting diesel energy) on a 3-cylinder, naturally-aspirated tractor engine. Aqueous ethanol (100- and 160-proof) was used as fumigant and the intake air was heated in order to vaporize the alcohol. Ethanol was able to supply up to 40% of the total energy at idle and 16% at full load. Their results also showed increased power, slightly decreased thermal efficiency, increased emissions of smoke, CO, and HC.

Shropshire and Goering [122] performed fumigation tests on a 4-cylinder, direct-injection, 3-L Case 188D diesel engine fitted with four fuel injection nozzles—one mounted at each intake port. Ethanol in three different proofs (100, 150, and 190) was used as fumigant. At full engine load, their results showed an energy replacement of up to 66% when 190-proof ethanol was fumigated; at low loads, they reported a 30% replacement. Brake thermal efficiency increased slightly at full load, but tended to decrease at lighter loads. As it was reported in previous studies, ethanol proof did not cause any significant effect on thermal efficiency. As far as emissions were concerned, ethanol fumigation caused reductions in smoke levels, whereas the exhaust levels of HC and CO were increased.

One of the major limitations of fumigation is the problem of obtaining a uniform distribution of fumigant among the cylinders. The intake manifolds of diesel engines are usually not designed to handle a multiphase flow of air, liquid droplets and fuel vapor. As a consequence, there may be significant variations in the amount of fumigant that is delivered to each cylinder, which can lead to discrepancies and inconsistencies in the results. A study by Shropshire and Bashford [121] compared the effectiveness of different ethanol-fumigation systems on the same engine, a 6-cylinder, turbocharged, direct-injection, 6.6-L John Deere 6404TR-13 diesel engine. Atomizing nozzles of different sizes were arranged and tested in either a simpler, single-nozzle

configuration or a multiple-nozzle arrangement. The latter configuration used three nozzles mounted in the intake manifold in order to achieve a better distribution of ethanol among the cylinders. Aqueous ethanol (191-proof) was used in all tests. As expected, the three-nozzle configuration gave better cylinder-to-cylinder ethanol distribution than the single-nozzle arrangement. This was confirmed by comparing the exhaust temperature data from each individual cylinder: the differences in exhaust temperatures were more uniform when multiple nozzles were used, suggesting a better distribution of ethanol.

Baranescu [19] performed alcohol fumigation experiments on a six-cylinder, turbocharged, direct-injection, 7.1-L diesel engine. The alcohols used were methanol, 190-, and 160-proof ethanol. Her results reported that alcohol fumigation caused a substantial increase in maximum in-cylinder rates of pressure rise and peak in-cylinder pressures when compared to regular diesel operation. She concluded that this should be a limiting factor to be taken into account when alcohol fumigation is to be used. The study reported a maximum fuel energy replacement of 30%. The fumigation of all alcohols also resulted in significant increases in the exhaust levels of HC and CO, especially at lower loads. The  $\text{NO}_x$  emissions were lowered. Smoke levels and PM emissions were not measured in the study.

Because the fumigation of an alcohol results in significant changes to the combustion process, it is sometimes desirable to optimize the timing of alcohol injection to obtain the best results from the fumigation technique. These optimum results may not occur when fumigation is used on an engine without any modification in the injection parameters. However, the advantages come at the expense of increased system complexity and cost. The effect of varying alcohol injection timing on fumigation performance was investigated by Savage et al. [116]. This was accomplished by using an electronically-controlled, multi-point ethanol injection system installed on a six-cylinder, turbocharged, direct-injection, 7.1-L Navistar DT-436B diesel engine. The timing was varied in the sense that the injection of fumigants occurred at different

times in the cycle; the total duration of injection (the injection profile) could also be varied. Methanol and 190-proof ethanol were used as fumigants, and the test matrix included a combination of three speeds and three loads. The results obtained showed that large differences in alcohol tolerance and knock threshold could be achieved by varying the alcohol injection timing cycles: up to 90% in alcohol replacement energy was attained at low loads; at high loads the maximum ethanol replacement on an energy basis was around 35%. Only small changes in engine thermal efficiency were reported.

Low-proof ethanol fumigation is economically advantageous, since aqueous ethanol is easier and cheaper to manufacture, which can be done in small distillation facilities. This important issue of ethanol proof was addressed by Hayes et al. [57]. Their study investigated the effect of ethanol proof on the fumigation results obtained from a six-cylinder, turbocharged, direct-injection, 7.1-L Navistar DT-436B diesel engine equipped with a multi-point electronic ethanol injection system (the same engine set-up used in the previous reference). The engine was tested at 2400 rpm and at three loads (200, 500, and 800 kPa bmep). The following results were obtained when fumigating lower ethanol proofs: The maximum rate of in-cylinder pressure rise was reduced (up to 20%) when compared to absolute (200-proof) ethanol; similarly, the peak in-cylinder pressure levels were reduced; NO emissions were reduced below diesel levels with low-proof ethanol (proof below 150); although the emissions of HC were greatly increased, ethanol proof did not have any significant effect on it; similarly, the emissions of CO were substantially increased, without any influence from ethanol proof. According to their results, the optimum ethanol proof under the test circumstances lay within the 100- to 150-proof range.

In a study by Griffith et al. [46] an electronically-controlled multi-point ethanol fumigation system was installed on an International Harvester 5288 farm tractor equipped with a 6-cylinder, turbocharged, direct-injection, 7.6-L diesel engine. The purpose of their study was to evaluate the effect of ethanol fumigation through both



laboratory and field testing. In the dynamometer tests, the fumigated ethanol could supply fuel energy up to 28% at low loads, and 13% at full load. The field tests reported a fuel replacement of about 14% with ethanol fumigation. The tractor field tests also reported an increased engine wear with ethanol fumigation, as it was indicated by lubricating oil analyses and also by optical borescopic inspections of the cylinder walls. It was argued that the ethanol might have affected the lubrication of the cylinder walls, thus causing abnormal wear.

A study by Jiang et al. [72] addressed the effects of ethanol fumigation on the performance and emissions from a 4-cylinder, turbocharged, direct injection, 4.5-L John Deere 4276T diesel engine. The main emphasis of their work was to reduce the emissions of  $\text{NO}_x$  through ethanol fumigation. They concluded that, in general, it is possible for the  $\text{NO}_x$  emissions to be substantially reduced by alcohol fumigation. This reduction in  $\text{NO}_x$  is more pronounced with lower ethanol proofs, as the increased amounts of water help decrease the peak combustion temperatures. They also concluded that the emissions of HC and CO tend to increase with alcohol fumigation. Finally, they showed that it is possible to correlate the exhaust  $\text{NO}_x$  emissions to the stoichiometric adiabatic flame temperature.

Abu-Qudais et al. [9] investigated the effects of ethanol fumigation on the performance and emissions from a single-cylinder, naturally-aspirated, direct-injection, 0.582-L diesel engine. The results obtained with fumigation were then compared to the results obtained when ethanol-diesel blends were tested on the same engine. They concluded that both fumigation and blends affect the engine in similar ways, but the benefits of ethanol utilization were more pronounced when the fumigation method was utilized. They reported that up to 20% diesel fuel substitution from ethanol could be achieved through fumigation, whereas the optimum percentage of ethanol in an ethanol-diesel blend was found to be 15%. Further, the fumigation method was able to decrease the soot mass concentrations by 51%; with the 15% ethanol-diesel blend, this reduction was 32%. Both methods resulted in increased emissions of HC

and CO.

Surawski et al. [130] conducted a study in order to investigate the effect of ethanol fumigation on PM emissions, volatility, and toxicity. Their experiments were carried out on a 4-cylinder Ford 2701C diesel engine and the fumigation system featured an electronically-controlled ethanol injector. A Scanning Mobility Particle Sizer (SMPS) was employed to obtain particle size distributions. Their results showed that ethanol fumigation caused reductions in total particle *mass* concentrations when compared to the baseline diesel operation. However, the particle size distributions also exhibited a shift towards smaller particle diameters (nucleation-mode particles), with a corresponding increase in total particle *number* concentrations with ethanol fumigation. Further, the volatility of the exhaust particles was measured with a Volatilization Tandem Differential Mobility Analyzer (V-TDMA). Their tests reported an increase in particle volatility with increased levels of ethanol fumigation, which may explain the tendency to form nucleation-mode particles as the exhaust gases undergo dilution and cooling. Finally, their study addressed the issue of particle toxicity by using a profluorescent nitroxide probe (BPEAnit). It was shown that ethanol fumigation increased the concentrations of free radicals and the so-called reactive oxygen species (ROS)—compounds that have the ability of inducing oxidative stress and mitochondrial damage at the sites of deposition, resulting in potentially deleterious health effects [31, 87].

#### 2.4.1.2 Summary of the Effects of Ethanol Fumigation

The general effects of ethanol fumigation on a diesel engine behavior can be summarized as follows:

**Ignition Delay, In-Cylinder Rate of Pressure Rise and Peak Pressure** Ethanol has a high resistance to autoignition; that is a major reason why it is a very suitable

fuel for spark-ignition engines. On the other hand, its poor autoignition characteristics—evidenced by its low cetane number—have precluded its widespread use as a fuel for compression-ignition engines. The high heat of vaporization of ethanol (about four times higher than that of regular diesel fuel) also contributes to delay the start of ignition in diesel engines: The vaporization of ethanol tends to cause a pronounced charge cooling which lowers the in-cylinder temperatures prior to ignition, thus increasing the ignition delay. A long ignition delay may result in a large amount of ethanol being introduced into the cylinder before ignition occurs. Under such conditions, the combustion of a large mass of fuel results in very rapid burning rates with high rates of in-cylinder pressure rise and high in-cylinder peak pressures. Under extreme conditions, the combustion proceeds so rapidly that an audible knocking sound can be discerned—the so-called "diesel knock". Under low engine loads, however, the ignition delay caused by the ethanol can become so large that the combustion occurs very late in the expansion stroke. This results in the quenching of the combustion process, resulting in low peak pressures and temperatures, incomplete combustion, reduced power output, low thermal efficiency, and increased HC and CO emissions (see below). Engine knocking (at high loads) and misfire (at low loads) are usually the factors that limit the maximum amount of ethanol that can be fumigated into a diesel engine. The water contained in lower-proof alcohols appears to inhibit pre-combustion reactions that cause engine knocking.

**Thermal Efficiency** At sufficiently high engine load conditions—with the corresponding high in-cylinder temperatures—when the longer ignition delay causes a larger mass of fuel to burn rapidly, the combustion of the premixed charge tends to proceed in a nearly constant-volume combustion that usually results in slight increases in thermal efficiency. On the other hand, at loads the low in-cylinder temperatures further increase the ignition delay, resulting in a combustion process which extends further into the expansion stroke, causing misfire, lowering efficiency and decreasing

engine output. Various studies on fumigation have not found any noticeable effect of ethanol proof on thermal efficiency.

**Unburned Hydrocarbons** Ethanol fumigation usually results in higher HC emissions due to two main mechanisms:

- *Flame quenching* caused when the premixed-like ethanol flame quenches at cylinder walls, piston top surfaces, and crevices—similar to the quenching which occurs in spark-ignition engines
- *Short-circuiting* occurring when fresh air-ethanol mixture flows into the exhaust during the valve overlap period

With alcohol fumigation, the HC emissions tend to increase at low loads, when the flame-quenching and short-circuiting phenomena are aggravated. The water in lower-proof alcohols does not seem to affect HC emissions appreciably.

**Carbon Monoxide** Ethanol fumigation can result in less efficient overall combustion processes, due to the unfavorable conditions for ethanol combustion found in diesel engines. Consequently, the emissions of CO are usually higher than those from regular diesel operation. The CO emissions tend to increase at low loads (due to poorer combustion), and higher engine speeds (due to less time available for complete combustion). As in the case of unburned HC emissions, the water in lower-proof alcohols does not seem to cause any significant effect on CO emissions.

**Oxides of Nitrogen** The effect of ethanol fumigation on  $\text{NO}_x$  emissions is not as clear as it is in the case of other gaseous emissions. Ethanol fumigation has been shown to either increase or decrease  $\text{NO}_x$  emissions. Further, this effect seems to be quite engine- and test-dependent. Engine load conditions and alcohol proof play an important role in determining how ethanol fumigation affects  $\text{NO}_x$ . Absolute (200-proof) ethanol may decrease  $\text{NO}_x$  by displacing some of the inlet charge oxygen that

is available for combustion (dilution effect), thus lowering peak temperatures and decreasing  $\text{NO}_x$  formation. This ethanol dilution effect may not be significant, however, and several studies have reported an increase in  $\text{NO}_x$  with fumigation of absolute ethanol at high engine loads. Lower-proof ethanol has shown to be more effective than absolute ethanol in decreasing  $\text{NO}_x$  emissions because of its water content. The presence of inert water helps decrease  $\text{NO}_x$  by providing additional oxygen reduction (enhanced dilution effect). Further, water also tends to cool the inlet charge (thermal effect). Lastly, albeit to a lesser degree, the dissociation of water vapor can modify the combustion process, inhibiting the  $\text{NO}_x$ -forming reactions (chemical effect). Under low engine load conditions, the fumigation of ethanol usually results in long ignition delays and low peak temperatures. Therefore, at such conditions, ethanol fumigation usually decreases  $\text{NO}_x$  emissions irrespective of alcohol proof. In any case, as it was previously discussed,  $\text{NO}_x$  emissions can be decreased indirectly by higher utilization of  $\text{NO}_x$ -reducing techniques, such as EGR—once the PM emissions have been reduced by ethanol fumigation.

**Particulate Matter** Ethanol is an oxygenated compound and, as it was previously discussed, it has the potential for decreasing the emissions of PM on a *mass* basis. The combustion of ethanol, in particular, provides a pathway for the production of soot-oxidizing radicals, such as the OH radicals. Indeed, the decrease in smoke levels with alcohol fumigation has been widely reported in the literature. On the other hand, whether ethanol fumigation can decrease particle *number* concentrations or not, is less clear. It has been shown [76] that soot agglomerates, because of their relatively large surface area, act as sites for the condensation and adsorption of volatile compounds that may be present in the exhaust gases. Once the formation of soot has been inhibited (by means of an oxygenate, for instance) those volatile materials become deprived of the surfaces they can condense onto. As a result, as the exhaust gases undergo dilution and cooling, the volatile compounds can nucleate in the form of

very small particles, typically in the ultrafine and nanoparticle range. Frequently this shift in particle size towards the very small diameters is accompanied by a noticeable increase in total particle number concentration. This phenomenon was observed in the study by Surawaski et al. [130] discussed above. Therefore, it becomes harder to predict the number-based particle behavior which may result from the fumigation of ethanol.

**Aldehydes** The use of ethanol in internal-combustion engines has reportedly resulted in marked increases in the emissions of aldehydes. Aldehydes are unregulated exhaust emissions which are found in relatively abundance in the exhaust gases of a diesel engine. In this case, formaldehyde and acetaldehyde are particularly important: Both are regarded as probable human carcinogens; furthermore, aldehydes can react with hydrocarbons in the atmosphere to form smog. A study by Haupt et al. [52] investigating the emissions of aldehydes from an ethanol-fueled Scania diesel engine found that the engine-out emissions of acetaldehyde and formaldehyde were respectively 9.8 and 1.6 times higher than the emissions from the equivalent diesel-fueled engine.

## 2.5 Water Injection in Diesel Engines

Water has been primarily used as a means to decrease pollutant emissions from diesel engines ( $\text{NO}_x$  in particular), and water introduction is usually carried out by the following methods [44, 74, 134]:

- Water-diesel fuel emulsions
- Stratified water injection into the cylinder
- Water injection into the cylinder with a separate injector
- Water injection into the intake manifold ("fumigation")

### 2.5.1 Effects of Water on NO<sub>x</sub> Emissions

The NO<sub>x</sub>-reducing mechanisms brought about by water are similar to the ones caused by EGR, viz.[118]:

- dilution effects
- chemical effects
- thermal effects

The effects above were previously discussed on Section 2.2.2, regarding NO<sub>x</sub> formation in diesel engines.

The studies by Brusca and Lanzafame [26], Udayakumar et al. [134], and Shah et al. [118] present experiments investigating the influence of water injection as a NO<sub>x</sub>-reducing strategy. And the results from these works conclude that water is an effective way to reduce NO<sub>x</sub> emissions from diesel engines. A study by Greeves et al. [44] also reported reductions up to 70% in NO<sub>x</sub> emissions by introducing water through different methods. In summary, water is effective in displacing oxygen available for combustion (dilution effect) and it also cools the intake charge because of its higher specific heat (thermal effect). Both effects tend to lower cycle temperatures, thus inhibiting the formation of NO. As drawbacks, water was also reported to cause a slight increase in HC and CO emissions, and a slight reduction in engine thermal efficiency, along with an accompanying increase in fuel consumption.

### 2.5.2 Effects of Water on PM Emissions

As far as the emissions of PM are concerned, the effect caused by water addition cannot be easily predictable. There are studies that claim that water injection decreases PM emissions, whereas there are others which claim the opposite. In a manner analogous to the effect of ethanol fumigation on NO<sub>x</sub>, the effect of water injection on PM emissions also seems to be sensitive to engine characteristics and testing conditions.

As an example, the study by Greeves et al. [44] mentioned above reported a slight increase in smoke levels when water was injected into the intake manifold. They attributed this increase in smoke to a worsening in the fuel-air mixing when water was introduced. The presence of atomized water reduced the rate of *air entrainment* due to the dilution effect, consequently decreasing the rate at which oxygen reaches the fuel. This poorer air utilization provides an explanation for an increase in PM with water injection. On the other hand, there are instances where water injection can be beneficial in reducing PM emissions. For instance, Wilson et al. [137] reported reduced levels of smoke with increasing amounts of water injection on an indirect-injection diesel engine.

There are studies that provide a theoretical explanation for the benefits of water injection as a PM-reducing method. One of such studies was presented by Roberts et al. [113]. According to their work, whenever water reduces soot, it can do so via a combination of physical, thermal, and chemical effects—the details of which are not yet well-understood. Their study attempted to identify and understand those mechanisms by means of both experimental burner experiments and numerical modeling. Because soot precursors are believed to originate in rich premixed flames during diesel combustion [30, 38], they tried to focus their attention on the effects of water in those flames in bunsen-type burners, and through numerical simulations. In summary, their results suggested that both the thermal and chemical effects are prominent, and the dissociation of water in the flame reaction zone originates free radicals (especially OH) that may act on hydrocarbon precursors to the formation of  $C_6H_6$ . The action of those radicals may thus inhibit the formation and growth of PAHs and the subsequent inception of soot particles.



# Chapter 3

## Experimental Apparatus and Procedures

In this chapter the engine test bench, along with the instrumentation for measuring exhaust emissions—both gaseous and particulate—and data acquisition system will be described. The apparatus will be addressed in the first section and the test matrix will be presented in the second section of the chapter.

### 3.1 Experimental Apparatus

In this first section the description of the experimental apparatus will be divided as follows:

- engine and dynamometer (engine test bench)
- gaseous emissions-measuring instrumentation
- particulate emissions-measuring instrumentation
- data acquisition system

A schematic of the experimental set up is presented in Figure 3.1

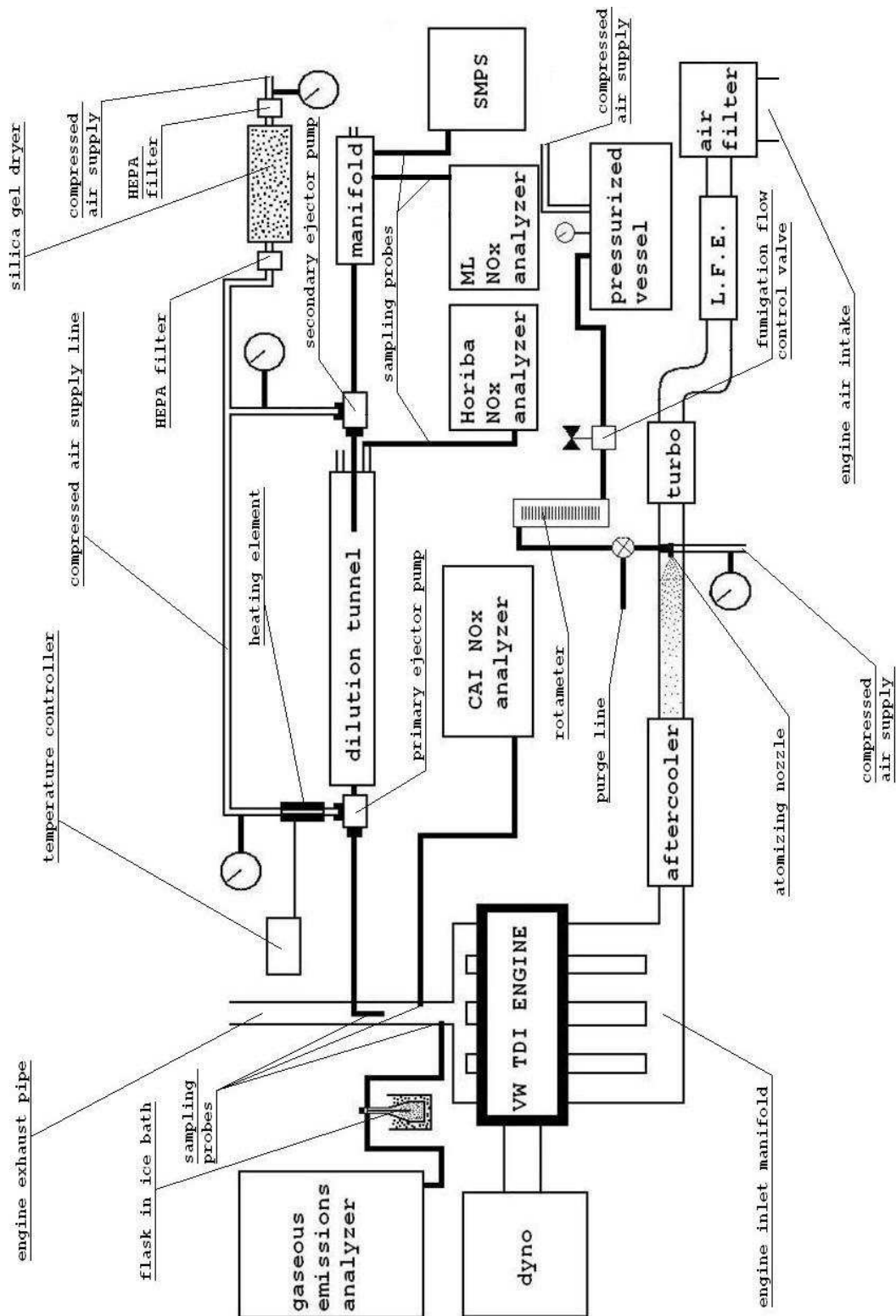


Figure 3.1: Schematic of the experimental setup

### 3.1.1 Engine and Dynamometer

#### 3.1.1.1 The 1.9-L Volkswagen TDI Engine

All tests were performed on a 66-kW 1999 Volkswagen 1.9-L TDI engine. This four-cylinder, turbocharged, direct-injected diesel engine is a popular member of the large TDI (Turbocharged Direct Injection) engine family, which belongs to Volkswagen AG. In the United States, the 1.9-L TDI engine is used on the diesel-powered versions of the VW New Beetle, Jetta, Golf, and Passat models. Further information on this particular engine can be found in a paper by Bosch et al. [23]. Some relevant engine technical specifications are presented in the table 3.1. In the present tests, the EGR system was disabled, in an attempt to eliminate a variable affecting  $\text{NO}_x$  emissions.

|                                |                    |
|--------------------------------|--------------------|
| type                           | 4-stroke diesel    |
| no. of cylinders               | 4 in-line          |
| displacement ( $\text{cm}^3$ ) | 1896               |
| bore x stroke (mm)             | 79.5 x 95.5        |
| compression ratio              | 19.5               |
| induction                      | turbocharged       |
| turbocharger                   | VNT (Garrett)      |
| valve configuration            | OHC 2 valves/cyl.  |
| injection pump                 | Bosch VE VP 37     |
| max. output                    | 66 kW @ 3750 rpm   |
| max. torque                    | 210 N-m @ 1900 rpm |
| max. MEP (kPa)                 | 1400               |

Table 3.1: Technical data of the Volkswagen 1.9-L TDI engine [23]

The performance curves and a sectional view of the the VW 1.9-L TDI engine can be found in Appendix A, in Figures A.1 and A.2, respectively.

### 3.1.1.2 Dynamometer

The engine was coupled to an Eaton Dynamatic model AD-806 DG eddy-current dynamometer, which is rated at 75 HP (56 kW) at 3400 rpm. At 1700 rpm—the speed at which the tests were conducted—this dynamometer is able to absorb up to about 152 N-m, whereas at that speed the engine can deliver a maximum torque of about 208 N-m. Therefore, *the maximum engine load that can be attained at 1700 rpm is dynamometer-limited*, and this load is  $(152/208) \times 100 = 73\%$ . The AD-806 DG is not capable of motoring the engine. The dynamometer was controlled by a Digalog model 1022A-STD dynamometer controller.

### 3.1.2 Fumigation System

The introduction of atomized fumigant (water or ethanol) into the intake manifold was accomplished by a Spraying Systems no. SU1A atomizing nozzle. This nozzle has two ports, to which both liquid and compressed air lines are fitted. It provides a continuous spray of liquid. In the present study, the fumigant was pressurized by means of a 2-gallon (7.6 L) 304-stainless steel vessel manufactured by Alloy Products Corp., Waukesha, Wisconsin. The vessel was kept at a constant gauge pressure of about 140 kPa, and the flow rate of fumigant was controlled by both a Swagelok 31 Series metering valve, and the valve furnished with the Omega flowmeter.

### 3.1.3 Sampling of Exhaust Gaseous Emissions

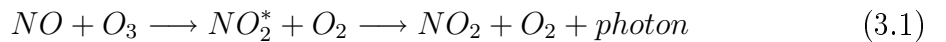
Gaseous emissions (HC, and  $\text{NO}_x$ ) were measured as explained in the following sections:

### 3.1.3.1 Unburned Hydrocarbons

The emissions of unburned hydrocarbons (HC) were measured using a Beckman Industrial model 400A analyzer, according to the *flame ionization detection* (FID) technique. In such detectors, the unburned hydrocarbons are burned in a hydrogen flame with an electric field applied by electrodes, thus creating a current flow which accurately corresponds to the number of carbon atoms present [125]. The analyzer was fitted with an unheated sample line, which means that the concentrations of heavier hydrocarbons could not be accurately taken into account due to condensation onto the inner walls of the sample line.

### 3.1.3.2 Oxides of Nitrogen

The concentrations of oxides of nitrogen ( $\text{NO}_x$ ) are measured according to the *chemiluminescence* method, which detects the emission of light produced when NO reacts with ozone ( $\text{O}_3$ ) to produce nitrogen dioxide in an excited state ( $\text{NO}_2^*$ ). Subsequently, the  $\text{NO}_2$  reverts to its normal state by emitting light according to the reaction below [125]:



In the present study, besides the raw  $\text{NO}_x$  concentrations in the engine exhaust gases, the concentrations of nitric oxide (NO) were also measured in order to determine both the primary and overall dilution ratios of the PM-sampling dilution system (see section 3.1.4 below).

**Raw NO and  $\text{NO}_x$**  The  $\text{NO}_x$  concentrations of both NO (only) and  $\text{NO}_x$  (combined) in the raw exhaust were measured with a California Analytical Instruments (CAI) model 600 HCLD, fitted with a heated line.

**Primary-Dilution NO** The concentrations of nitric oxide in the exhaust after the primary dilution were measured using a Horiba model CLA-510SS/ES-C510SS  $\text{NO}_x$

analyzer.

**Overall-Dilution NO** A Monitor Labs model 8840/8850 high-sensitivity NO<sub>x</sub> analyzer was used in order to measure the NO concentrations after the secondary dilution, downstream of the dilution tunnel.

The gas analyzers were zeroed and spanned several times a day to minimize error.

### 3.1.4 Sampling of Exhaust Particulate Matter

As it was explained in Section 2.2.1.2, nucleation-mode particles originate mostly from volatile compounds, both organic and inorganic, such as hydrocarbons and sulfur compounds. Unlike solid particles, that are formed during combustion, most nucleation-mode particles nucleate and grow as a result of the dilution and cooling of the exhaust gases. Note that the *compounds* that originate these particles—the particle *precursors*—are formed during combustion, but the particles themselves do not form until adequate dilution and cooling conditions have occurred. Further, small changes during dilution and cooling can have a pronounced effect on the concentration of particles formed. Moreover, even after dilution and cooling of the exhaust, not all precursors nucleate into particles—a fraction escapes into the atmosphere in gas phase. Due to the complex nature of nucleation-mode particles, and because their nucleation is very sensitive to the dilution/cooling parameters, their sampling presents challenges [6, 95]. Therefore, a dedicated *dilution system* should be employed, and the dilution and cooling conditions should be carefully monitored.

#### 3.1.4.1 Dilution System

The dilution system used in the present study was similar to a system described by Abdul-Khalek et al. [6]. The function of such a system is to attempt to simulate the dilution conditions that occur in the atmosphere. It does so by diluting a sample of raw exhaust with clean air, and then sending the diluted stream into a chamber

where the particle precursors are allowed to form particles by nucleation and growth. This first dilution process is carried out by the *primary ejector pump*, a simple device that draws a continuous sample of raw exhaust and mixes it with dry and clean compressed air. The chamber where the diluted exhaust gases undergo cooling is called the *dilution tunnel*. Downstream of this tunnel, usually a second dilution takes place to further dilute the stream down to concentrations that are suitable for the particle-measuring instruments and also stabilize particle growth. When necessary, this second dilution is accomplished by a *secondary ejector pump*. The dilution tunnel is usually made of a metal pipe on whose ends the ejector pumps are fitted. The volume of the tunnel depends upon the desired *residence time*—the time a volume of sample "resides" inside the tunnel. It is a function of the outlet flow of the primary dilution pump. The average residence time ( $t_R$ ) is thus given by:

$$t_R = V_T/Q_P \quad (3.2)$$

In the equation above,  $V_T$  is the dilution tunnel volume, and  $Q_P$  is the flow out of the primary dilution pump. According to Abdul-Khalek et al., "the residence time is like a waiting period that allows the nucleated particles to grow to a detectable size" [6].

**Dilution System Specifications** In the present study, the specifications of the elements comprising the dilution system are as follows:

**Primary Dilution Pump** The primary dilution pump dilutes the exhaust gases with air upstream of the dilution tunnel. An Air-Vac model TD260H ejector pump was used for primary dilution. This pump operated with compressed air at a gauge pressure of 295 kPa. The corresponding flowrate out of the pump was 229 L/min.

**Secondary Dilution Pump** For the secondary stage of dilution, an Air-Vac model TD110H was used. The operating pressure was 300 kPa, and the flowrate was 10.6 L/min.

**Dilution Tunnel** A galvanized steel pipe, with diameter of approximately 5.46 cm and length of 100 cm was used as a dilution tunnel. The volume of this tunnel is therefore 2342 cm<sup>3</sup>. This tunnel had on both ends pipe fittings which allowed connection with the ejector pumps.

**Residence Time** According to equation 3.2, the residence time given by a primary ejector pump flowrate of 229 L/min and the above tunnel dimensions is therefore approximately 0.6 s.

**Dilution Ratios** The *primary dilution ratio* is an important controlling parameter for the formation of nucleation-mode particles. In the present study, it is defined as the ratio of the NO concentration *downstream* of the primary ejector pump to the NO concentration in the *raw* exhaust gases:

$$PDR = [NO]_{primary}/[NO]_{raw} \quad (3.3)$$

Note that the above equation assumes a concentration of background NO<sub>x</sub> equal to zero.

Similarly, the *secondary dilution ratio* can be defined as the ratio of the NO concentration downstream of the secondary ejector pump to the NO concentration in the gases inside the dilution tunnel:

$$SDR = [NO]_{secondary}/[NO]_{primary} \quad (3.4)$$

Consequently, the *overall dilution ratio* is defined as:

$$ODR = [NO]_{secondary}/[NO]_{raw} = PDR \times SDR \quad (3.5)$$

In the present experiments, the overall dilution ratios varied between 329 and 818. The overall dilution ratios for each test condition are shown in the Appendix.



### 3.1.4.2 The Scanning Mobility Particle Sizer

Once the exhaust sample has been "conditioned" by dilution and cooling, it becomes necessary to classify the particles according to their size and concentration—that is, a *particle size distribution* should be obtained (see Section 2.2.1.3). The Scanning Mobility Particle Sizer (SMPS) Spectrometer is a particle-measuring instrument used for that purpose. Its main components are the Electrostatic Classifier (EC) and the Condensation Particle Counter (CPC). The Differential Mobility Analyzer (DMA) constitutes the core of the EC. An SMPS system is able to classify particles according to a detection technique based on their electrical mobility.

In the present work, the SMPS spectrometer used was the TSI model 3936 [2]. This system was comprised of:

- TSI model 3080 Electrostatic Classifier—fitted with a TSI model 3081 long DMA
- TSI model 3782 water-based CPC

Figure A.3 shows a scheme of the instruments comprising the SMPS system.

**Electrostatic Classifier (TSI model 3080)** The EC consists of a neutralizer and a mobility section. In the neutralizer, the particles are charged to a known charge level called the *Boltzmann distribution*. This is done by passing the aerosol by a radioactive source (Po-210 in the present study). The mobility section is represented by the DMA column, and it is where the charged aerosol is classified according to its ability to traverse the electrical field inside it, according to the electrical mobility theory developed mainly by Knutson and Whitby [77], and Liu and Pui [90].

**Water-Based Condensation Particle Counter (TSI model 3782)** The electrically-classified aerosol is then sent to a CPC, where they are counted. The model 3782 is a water-based CPC, i.e., it uses water as the condensing fluid. In this instrument

the aerosol first enters a region surrounded by wetted media to saturate it with water vapor. Then the aerosol enters a growth section where the wetted walls are heated, producing a high vapor pressure and supersaturated conditions. In this growth section the particles act as nuclei for condensation: Water condenses onto the particles, which consequently grow to a size that allows them to be detected and counted by an optical system [1]. This technology was invented by Susanne V. Hering and Mark R. Stolzenburg, and its patent is assigned to Aerosol Dynamics Inc., Berkeley, Calif. [11, 62, 63].

### **3.1.5 Measurement of Flow Rates**

The fluids entering the engine are:

- diesel fuel
- fumigant (water or ethanol, when operating in fumigation mode)
- air

The measurement of their respective volumetric flow rates is discussed below.

#### **3.1.5.1 Diesel Fuel Flow Rate**

The flow rate of diesel fuel into the engine was measured with a Brooks model BM01ARSPA2RVA micro-oval flowmeter.

#### **3.1.5.2 Ethanol and Water Flow Rates**

The flow rate of fumigated ethanol or water was measured with an Omega model FL-2045 liquid-flow rotameter.

#### **3.1.5.3 Measurement of Volumetric Air Flow Rate**

The volumetric flow rate of air (in std. L/min) inducted into the engine was measured with a Meriam laminar flow element (LFE) model 50MC2-4.

### 3.1.6 Data Acquisition System

A 16-bit, 200 kS/s National Instruments model SCXI-1600 USB data acquisition module mounted on a National Instruments model SCXI-1001 chassis. The data inputs were processed using LabVIEW 8.6.

## 3.2 Experimental Procedures

In this section, the engine conditions used during the tests (i.e., the test matrix) and the test procedures are presented.

### 3.2.1 Test Matrix

In the present study, three fumigants were investigated:

- water
- 100-proof ethanol
- absolute (200-proof) ethanol

The three fumigants above were introduced into the intake manifold in two different proportions:

- 25%
- 40%

*These fractions are based on the volumetric diesel fuel flow rate under diesel-only (baseline) operation.*

Three engine loads were used, at a speed of 1700 rpm:

- 40 N-m (2.65 bar BMEP, 19% of engine max. load)
- 80 N-m (5.30 bar BMEP, 38% of engine max. load)

- 120 N-m (7.95 bar BMEP, 58% of engine max. load)

The speed of 1700 rpm and the three loads above were chosen because they are representative of the driving conditions for a passenger car in city driving, for instance.

The test conditions are summarized on table 3.2 below:

| FUMIGANT                        | FUMIGANT FLOWRATE LEVEL | LOAD    |
|---------------------------------|-------------------------|---------|
| water                           | 25%                     | 40 N-m  |
| 100-proof ethanol               | 40%                     | 80 N-m  |
| 200-proof ethanol               |                         | 120 N-m |
| diesel—50 ppm sulfur (baseline) | —                       |         |

Table 3.2: Test matrix

### 3.2.2 Test Procedure

The engine test procedure was divided into the following events:

- high-load burn-off
- load stabilizing
- data acquisition

**High-Load Burn-Off** This is a period when the engine load was brought to its highest test level (120 N-m) for a period of about 5 minutes. This was done in-between different load conditions. The purpose of this procedure is to help burn off any excess of volatile materials in the exhaust which could affect particle measurements and impair adequate data repeatability.

**Load Stabilization** Following the burn-off period, the engine load was set to the desired value until steady-state operation was attained. This was carried out by monitoring parameters such as exhaust mean temperature, oil temperature, and raw NO<sub>x</sub> emissions. Typically, a period of 15 minutes was sufficient to attain this steady-state operation.

**Data Acquisition** When steady-state operation was achieved at the desired load, the acquisition of engine data would take place. For that purpose, the LabVIEW program was set in data acquisition mode, when all of the engine test parameters would be logged by the computer and stored in a spreadsheet.

As previously stated, the gas-measuring analyzers were routinely zeroed and spanned (calibrated) before switching to a different engine load condition. This was done to minimize errors in the acquired data.

### **3.3 Test History**

The chronological order of all engine experiments is listed in Tables 3.3, 3.4, and 3.5 below:

| DATE         | TEST CONDITION                   | COMMENTS              |
|--------------|----------------------------------|-----------------------|
| July 7, 2009 | 120 N-m baseline                 |                       |
|              | 80 N-m baseline                  |                       |
|              | 40 N-m baseline                  |                       |
| July 8, 2009 | 120 N-m 25% water downstream     |                       |
|              | 120 N-m 40% water downstream     |                       |
|              | 80 N-m 25% water downstream      |                       |
|              | 80 N-m 40% water downstream      |                       |
|              | 40 N-m 25% water downstream      |                       |
|              | 40 N-m 40% water downstream      |                       |
|              | 120 N-m 25% 100-proof downstream |                       |
|              | 120 N-m 40% 100-proof downstream |                       |
|              | 80 N-m 25% 100-proof downstream  |                       |
|              | 80 N-m 40% 100-proof downstream  |                       |
| July 9, 2009 | 40 N-m 25% 100-proof downstream  |                       |
|              | 40 N-m 40% 100-proof downstream  |                       |
|              | 120 N-m 25% 100-proof upstream   |                       |
|              | 120 N-m 40% 100-proof upstream   | engine speed unstable |
|              | 80 N-m 25% 100-proof upstream    |                       |
|              | 80 N-m 40% 100-proof upstream    | engine speed unstable |
|              | 40 N-m 25% 100-proof upstream    |                       |
|              | 40 N-m 40% 100-proof upstream    |                       |
|              | 120 N-m 25% water upstream       | engine speed unstable |
|              | 120 N-m 40% water upstream       |                       |
|              | 80 N-m 25% water upstream        |                       |
|              | 80 N-m 40% water upstream        |                       |
|              | 40 N-m 25% water upstream        |                       |
|              | 40 N-m 40% water upstream        |                       |

Table 3.3: Test history—Part I

| DATE             | TEST CONDITION            | COMMENTS |
|------------------|---------------------------|----------|
| July 31, 2009    | 120 N-m baseline (before) |          |
| August 4, 2009   | 80 N-m baseline (before)  |          |
|                  | 40 N-m baseline (before)  |          |
| October 16, 2009 | 120 N-m baseline (after)  |          |
|                  | 80 N-m baseline (after)   |          |
|                  | 40 N-m baseline (after)   |          |

Table 3.4: Test history—Part II

| DATE             | TEST CONDITION       | COMMENTS              |
|------------------|----------------------|-----------------------|
| December 3, 2009 | 80 N-m baseline      |                       |
|                  | 80 N-m 25% 100-proof |                       |
|                  | 80 N-m 40% 100-proof |                       |
|                  | 80 N-m 25% water     |                       |
|                  | 80 N-m 40% water     |                       |
|                  | 80 N-m 25% 200-proof | engine speed unstable |
|                  | 80 N-m 40% 200-proof | engine speed unstable |
| December 4, 2009 | 80 N-m baseline      |                       |
|                  | 80 N-m 25% 200-proof | engine speed unstable |
|                  | 80 N-m 40% 200-proof |                       |
|                  | 80 N-m 25% 100-proof |                       |
|                  | 80 N-m 40% 100-proof |                       |
|                  | 80 N-m 25% water     |                       |
|                  | 80 N-m 40% water     |                       |

Table 3.5: Test history—Part III

# Chapter 4

## Analysis of Results

### 4.1 Introduction

In this chapter, the experimental results obtained with ethanol fumigation and water injection are presented and compared to the results obtained with regular diesel fuel operation. The effect of both techniques on engine performance and emissions (primarily  $\text{NO}_x$  and PM) are addressed. Thus, conclusions are drawn regarding the utilization of ethanol fumigation and water injection using a simple, inexpensive, and retrofittable air atomizing injector. The limitations of such system are also pointed out.

The engine tests whose results are presented here were obtained during the months of July, October, and December 2009. The experimental testing from each month had different characteristics and are henceforth referred to as Part I, Part II, and Part III, respectively.

**Part I** In this first part, the effect of installing the atomizing nozzle either *downstream* or *upstream* of the aftercooler is investigated. Testing was carried out in both arrangements and the results were compared. The upstream configuration resulted in better liquid atomization and evaporation, and this was the arrangement used for the remainder of the engine tests.



**Part II** During engine testing in July the engine's fuel injection pump had a gasket failure, resulting in a massive leak of diesel fuel. After the pump was repaired its behavior was changed: The injection timing of diesel fuel had been slightly advanced, and the total amount of fuel the pump could deliver was also altered. The differences in engine behavior resulting from these modifications are shown in Part II.

**Part III** In this final part, the experimental results were obtained by running the VW TDI engine at an intermediate load of 80 N-m; this section also features the utilization of 200-proof (absolute) ethanol as a fumigant, in addition to 100-proof ethanol and water; the emissions of HC were also measured. The atomizing nozzle was mounted *upstream* of the aftercooler. Part III thus provides an overall summary and a conclusion of the effects of ethanol fumigation and water injection on engine performance and emissions, namely  $\text{NO}_x$ , PM, and HC.

In neither part engine knock due to ethanol fumigation occurred, and the maximum ethanol fuel-energy substitution achieved was about 20%.

## 4.2 Part I — Effect of Atomizing Nozzle Position

The use of a single atomizing nozzle in a multi-cylinder engine usually leads to a poor cylinder-to-cylinder distribution of fumigant (alcohol or water), therefore it was decided to conduct tests to evaluate nozzle position *upstream* of the intake air aftercooler. In this case, the injection of fumigant into the hot air coming out of the turbocharger would result in enhanced evaporation and mixing of the liquid, thus minimizing the problem of poor distribution of fumigant among the cylinders. Therefore, in this first part tests were carried out with the atomizing nozzle being positioned either downstream or upstream of the aftercooler. Both distilled water and 100-proof (non-denatured) ethanol were used as fumigants, in amounts of 25% and 40% of the

corresponding baseline diesel fuel flowrate. The effect of both nozzle configurations on exhaust emissions was investigated. The PM emissions were analyzed with an SMPS; the emissions of  $\text{NO}_x$  were also measured. Due to instrument malfunction, the emissions of HC could not be measured in this first part of engine testing.

### 4.2.1 Effect on PM Emissions

The effect of nozzle position with 100-proof ethanol fumigation and water injection on PM emissions is shown in the following number- and volume- based particle size distributions. It is worth noting that the volume-weighted measurements correlate with the mass-weighted particle size distributions through the *effective density* of the particulate matter [108].

#### 4.2.1.1 Volume-Weighted Particle Size Distributions

The volume-weighted particle size distributions for all three loads (40, 80, and 120 N-m) and 1700 rpm—for both upstream and downstream nozzle configurations—are shown in Figures 4.1–4.6:

## Upstream Nozzle

40 N-m

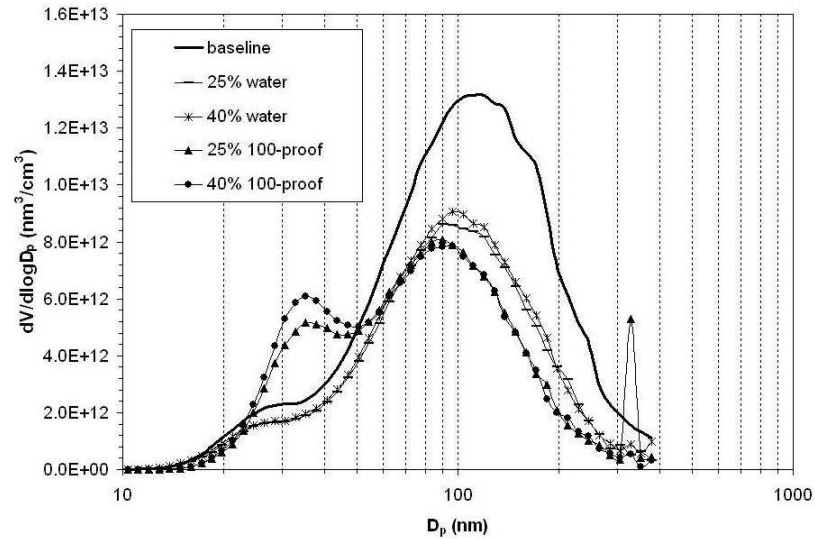


Figure 4.1: Volume-weighted particle size distributions; 40 N-m; upstream nozzle.

80 N-m

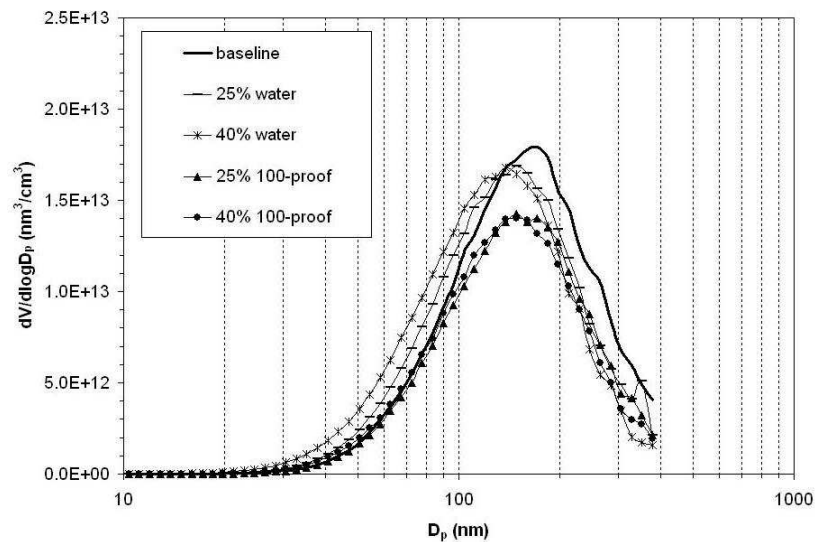


Figure 4.2: Volume-weighted particle size distributions; 80 N-m; upstream nozzle.

## 120 N-m

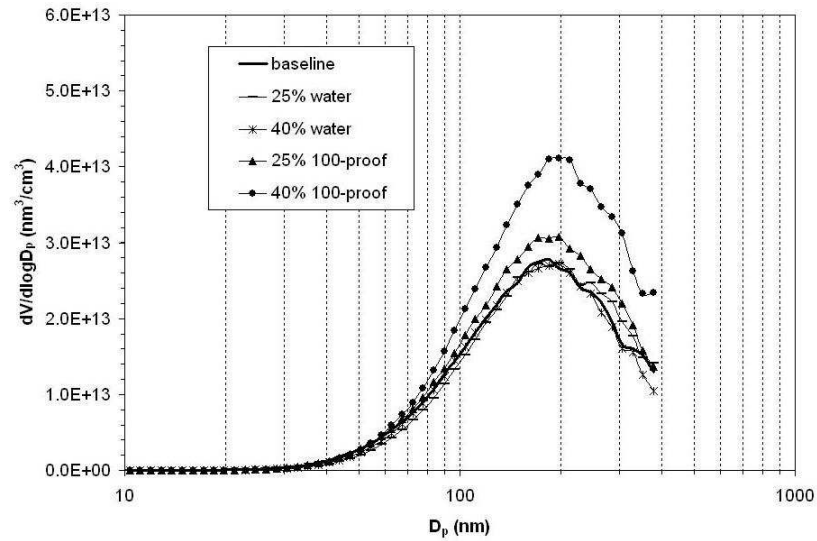


Figure 4.3: Volume-weighted particle size distributions; 120 N-m; upstream nozzle.

## Downstream Nozzle

## 40 N-m

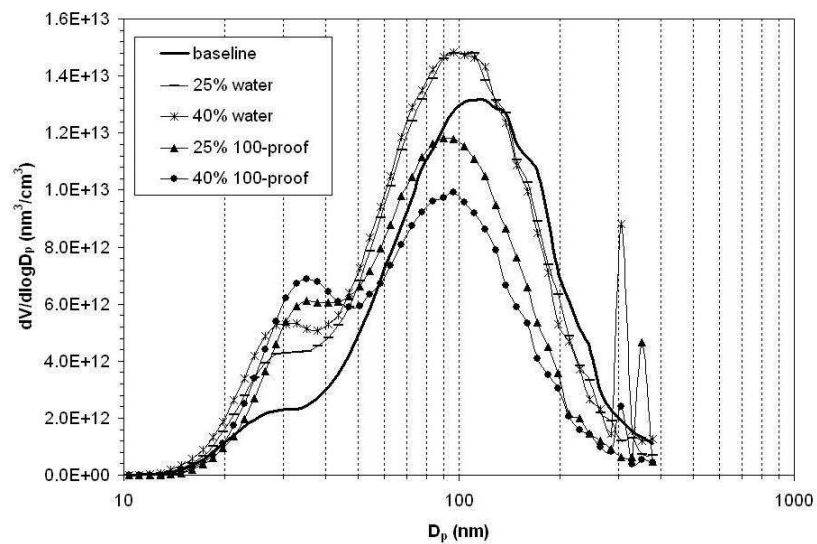


Figure 4.4: Volume-weighted particle size distributions; 40 N-m; downstream nozzle.

## 80 N-m

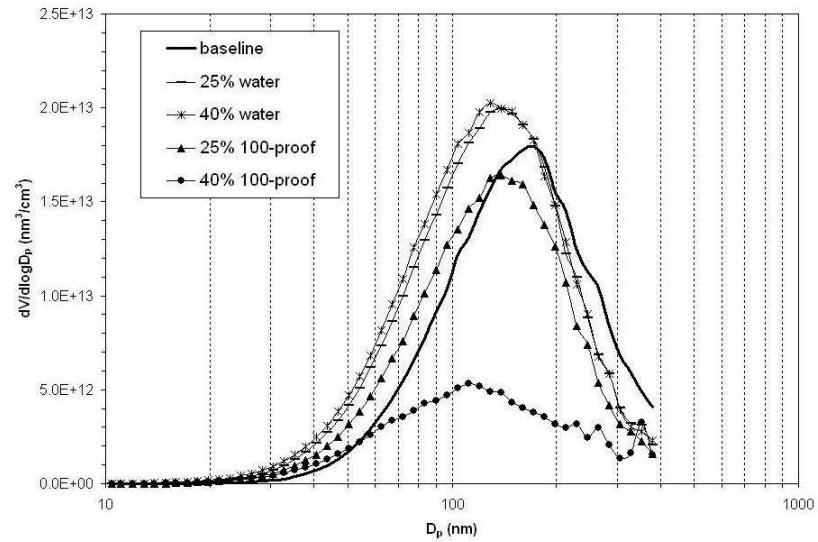


Figure 4.5: Volume-weighted particle size distributions; 80 N-m; downstream nozzle.

## 120 N-m

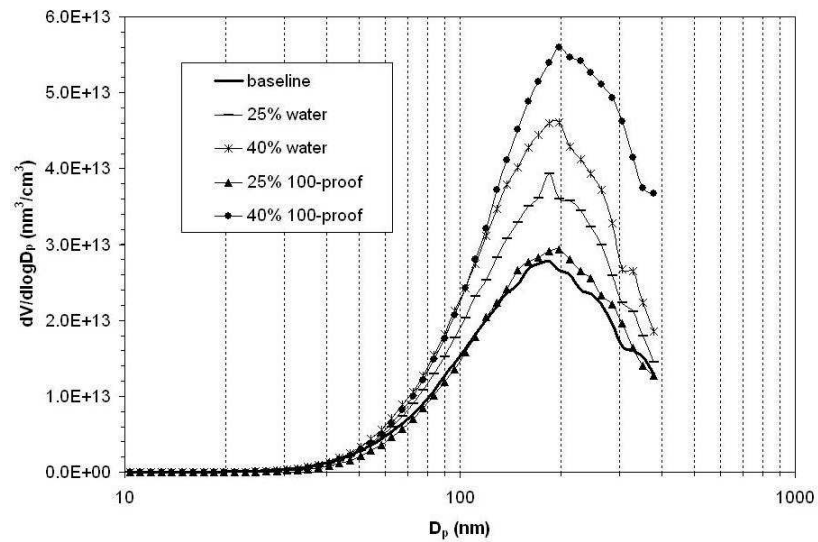


Figure 4.6: Volume-weighted particle size distributions; 120 N-m; downstream nozzle.

**Discussion: 40 N-m** When compared to baseline operation (solid line), the results obtained with the downstream nozzle configuration show a decrease in peak particle volume concentrations with 100-proof ethanol fumigation, whereas the injection of water caused a slight increase in peak volume concentrations. While the fumigation of a larger amount (40%) of ethanol resulted in a further peak volume reduction, the injection of water in both flowrates (25 and 40%) did not cause any noticeable difference in these particle concentrations. On the other hand, when the atomizing nozzle was located upstream of the aftercooler the size distributions show a reduction in peak particle volume concentrations for both water and 100-proof ethanol. The alcohol exhibited a slightly larger reduction in peak volume concentrations when compared to water; for both fumigants, the difference in flowrates did not cause any significant difference in peak volume concentrations. The introduction of either water or ethanol resulted in a slight shift towards smaller particle diameters and—in the case of ethanol—a second mode can be discerned at particle diameters of about 33 nm.

These size distributions suggest that the injection of either water or ethanol *upstream* of the aftercooler resulted in larger reductions in particle volume concentrations. It was probably due to the better evaporation and mixing in the upstream configuration. The increase in peak particle volume concentrations with water injection with the downstream nozzle can be attributed to poor mixing and maldistribution of water among the cylinders: water injection can interfere with the proper mixing of diesel fuel with air (see Greeves et al. [44]), resulting in slight increases in PM mass emissions. This problem is aggravated when poor cylinder-to-cylinder distribution of fumigant occurs.

**Discussion: 80 N-m** With the downstream arrangement the injection of water caused an increase in peak particle volume concentrations, both at 25% and 40% water flowrates. This was probably due to poor mixing of diesel fuel with air, caused by poor

water distributions among the cylinders. The downstream fumigation of 100-proof ethanol, on the other hand, resulted in decreases in peak particle volume concentrations. Worth noting is the fact that an alcohol flowrate level of 40% produced a somewhat sharp decrease in particle volume concentrations, as shown in Figure 4.5—a surprising result that may have been due to other factors. Unfortunately, these tests were not repeated.

Similarly to what occurred with the 40 N-m engine load, the upstream configuration resulted in decreases in peak particle volume concentrations when either water or 100-ethanol was introduced. However, in the present 80 N-m case, the reductions were less marked than those at 40 N-m. The fumigation of 100-proof ethanol resulted in slightly larger decreases in peak particle volume concentrations, when compared to the reductions obtained with water injection. With the upstream configuration, the differences in flowrates of either water or alcohol did not cause any significant effect.

**Discussion: 120 N-m** At this higher load level of 120 N-m the injection of water and the fumigation of 100-proof ethanol both resulted in *increased* peak particle volume concentrations, regardless of whether the fumigation occurred downstream or upstream of the aftercooler. This may be partly explained by the higher overall fuel/air ratio at higher loads, with the consequently larger number of soot-producing fuel-rich regions inside the cylinder. This larger number of soot nucleation sites would make it more difficult for either water or alcohol to cause a reduction in particle volume concentrations. Indeed, the most significant overall reductions in particle volume concentrations were observed in the lowest-load case, namely 40 N-m.

**Total Particle Volume Concentrations** The areas under the volume-weighted particle size distributions shown above represent the *total* particle volume concentrations and the bar plots shown below compare the total particle volume concentrations for baseline, upstream and downstream nozzle configurations.

## 40 N-m

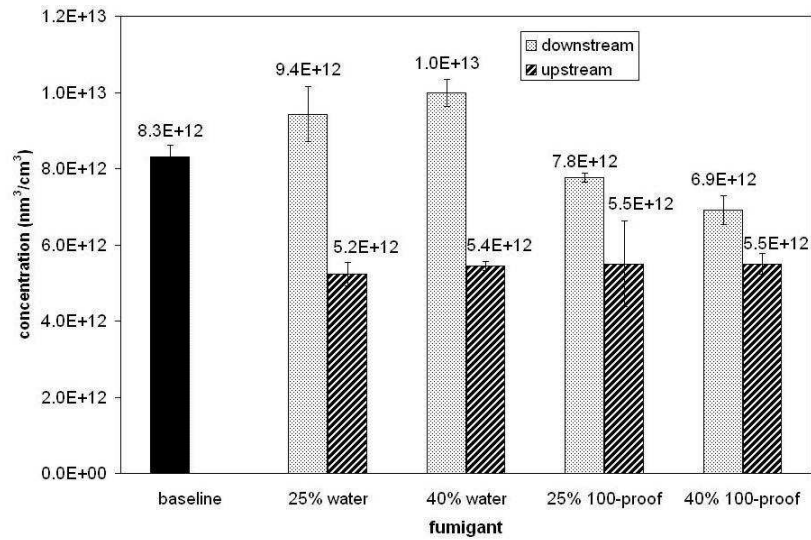


Figure 4.7: Total particle volume concentrations; 40 N-m.

## 80 N-m

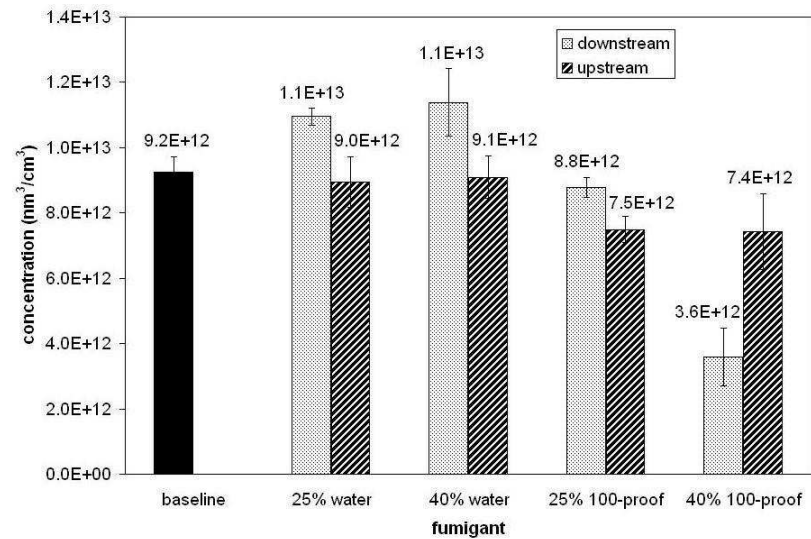


Figure 4.8: Total particle volume concentrations; 80 N-m.



## 120 N-m

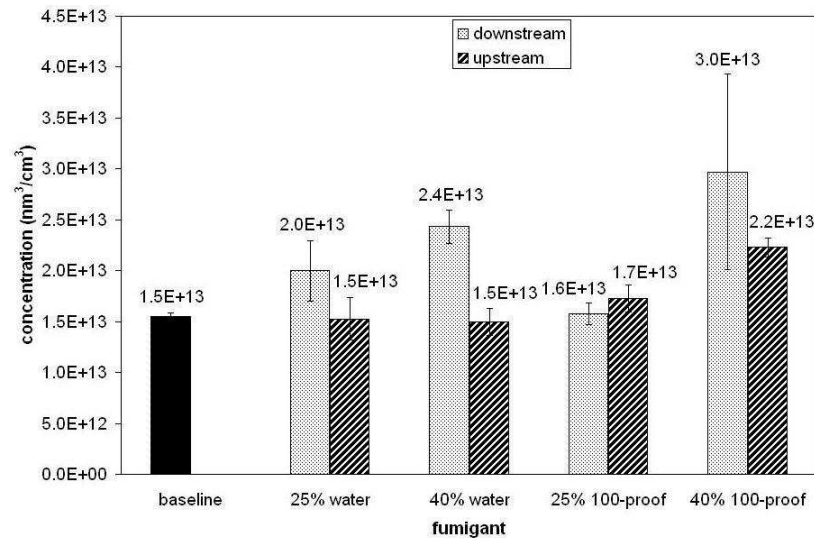


Figure 4.9: Total particle volume concentrations; 120 N-m.

**Discussion: 40 N-m** This bar plot summarizes the trends exhibited by the size distributions discussed above: it can be seen that the upstream atomizer configuration resulted in significant decreases in total particle volume concentration regardless of fumigant (water or 100-proof ethanol) or amount (25 or 40% flowrates). On the other hand, the introduction of water downstream of the aftercooler resulted in increased particle volume concentrations, when compared to the baseline levels. As stated before, water is less volatile than 100-proof ethanol and this would further make it difficult for the water to fully vaporize and mix with the intake air, resulting in even worse cylinder-to-cylinder distribution. The downstream fumigation of 100-proof ethanol caused reductions in total particle volume concentrations. Compared to water, this can be attributed to the oxygenate effect of the alcohol and to the relative ease with which it can evaporate and mix with air in the intake manifold. Further, the addition of ethanol results in an increase in ignition delay which is even more pronounced at lower loads. This longer delay provides more time for diesel fuel and air to fully mix, which helps achieve a more complete combustion with resulting

lower particle volume concentrations.

**Discussion: 80 N-m** This plot shows that the fumigation upstream of the aftercooler resulted in smaller total particle volume concentration across the board, similarly to what was observed in the 40 N-m case. However, the reductions at 80 N-m were less marked. Downstream injection of water caused increases in total particle volume concentrations, whereas only a very slight decrease was observed when water was injected upstream of the aftercooler. Again, the increases in particle volume caused by the downstream injection of water resulted probably from poor cylinder-to-cylinder distribution. Ethanol, being an oxygenate, has a greater potential for reducing particle volume emissions, and volume reductions were observed with the fumigation of 100-proof ethanol. As it was previously explained, the increase in ignition delay caused by the ethanol may also enhance the mixing of diesel fuel with air, resulting in lower PM volume emissions. Interesting to note is the sharp reduction which was obtained with the downstream fumigation of ethanol at the 40% flowrate.

**Discussion: 120 N-m** In this bar plot it becomes more evident the fact that neither fumigant nor fumigation method was able to cause any significant reductions in total particle volume concentrations. Even the upstream fumigation of 100-proof ethanol—which is an oxygenate—was not sufficient to decrease the total concentrations in particle volume. Besides the oxygenate effect, the ignition delay caused by the ethanol at this higher load level was probably not large enough in order to enhance the mixing of diesel fuel with air—which would had helped decrease PM volume emissions. Lastly, as an odd result, the downstream fumigation of 100-proof ethanol at 25% flowrate produced only a slight increase in total particle volume concentration—in sharp contrast with the other downstream results.

#### 4.2.1.2 Number-Weighted Particle Size Distributions

Now the corresponding number-weighted particle size distributions for all three loads (40, 80, and 120 N-m) and 1700 rpm—for both upstream and downstream nozzle configurations—are shown in the plots shown in Figures 4.10–4.15; the plots for total particle number concentration are shown in Figures ??–??:

#### Upstream Nozzle

##### 40 N-m

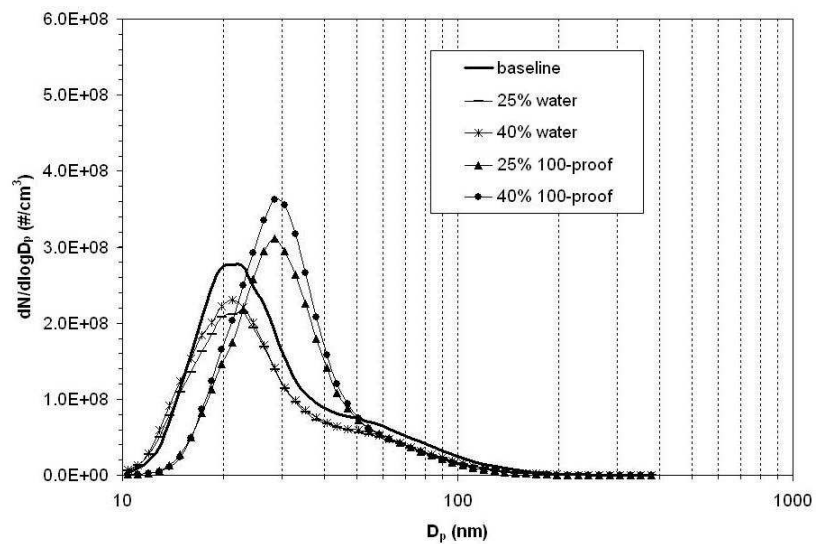


Figure 4.10: Number-weighted particle size distributions; 40 N-m; upstream nozzle.

## 80 N-m

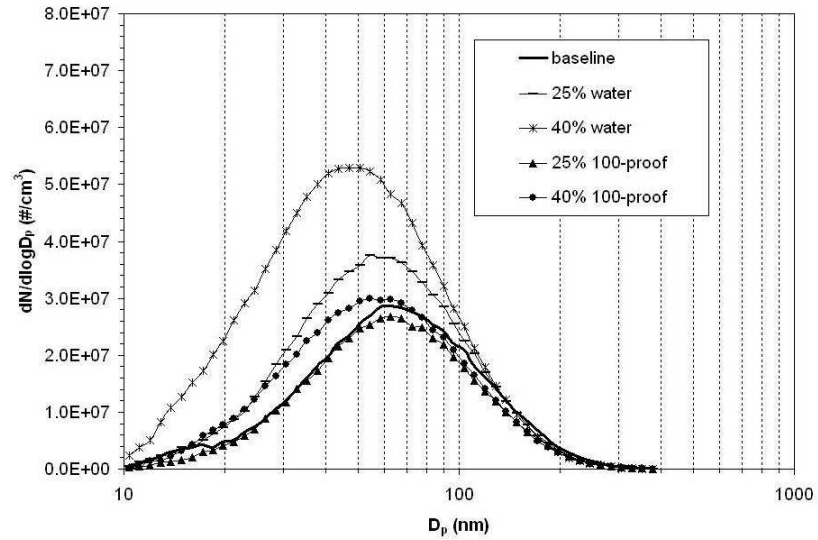


Figure 4.11: Number-weighted particle size distributions; 80 N-m; upstream nozzle.

## 120 N-m

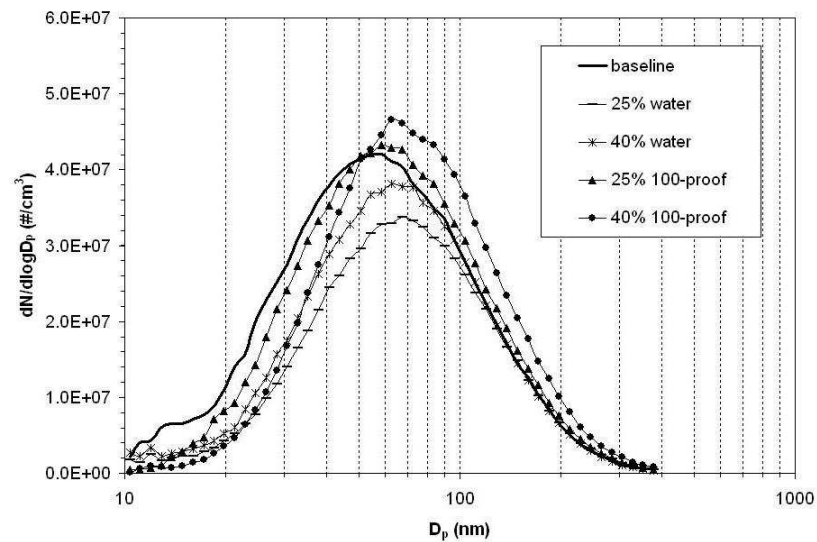


Figure 4.12: Number-weighted particle size distributions; 120 N-m; upstream nozzle.

## Downstream Nozzle

40 N-m

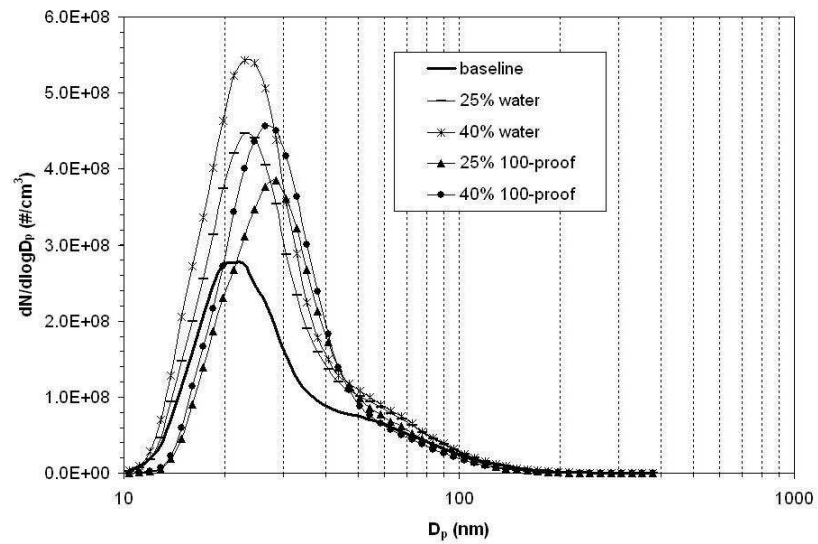


Figure 4.13: Number-weighted particle size distributions; 40 N-m; downstream nozzle.

80 N-m

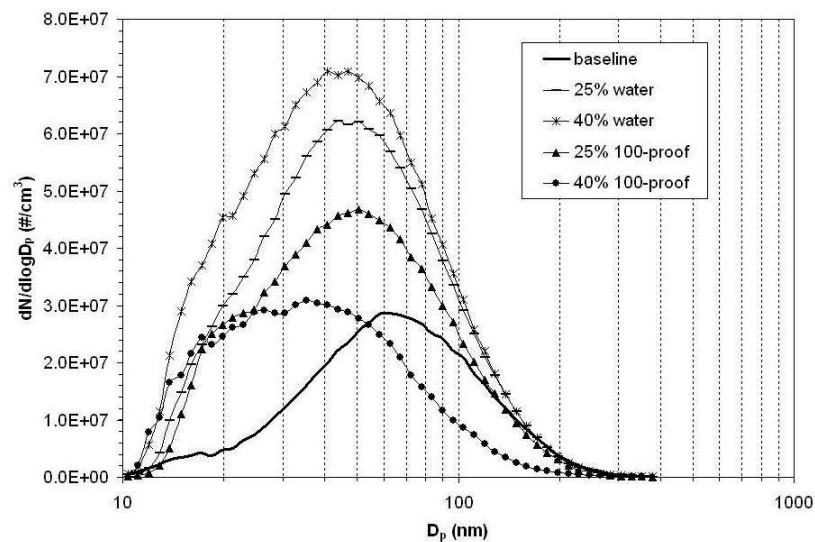


Figure 4.14: Number-weighted particle size distributions; 80 N-m; downstream nozzle.

## 120 N-m

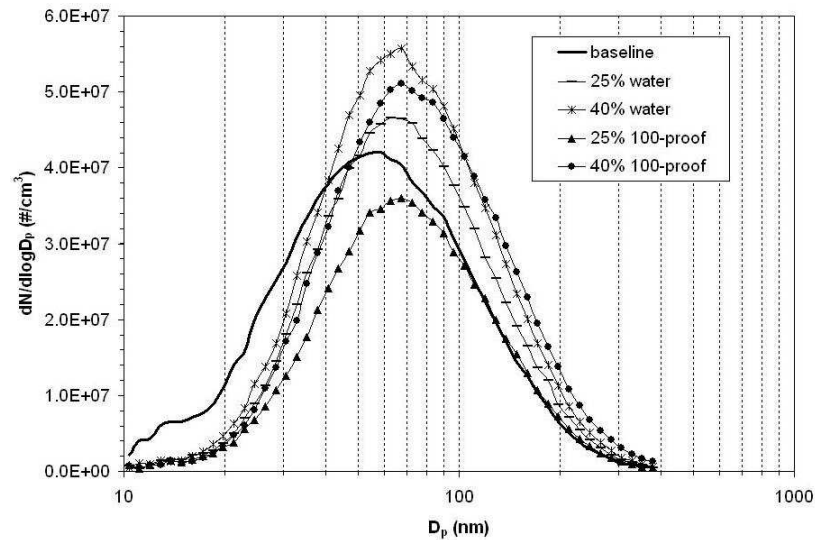


Figure 4.15: Number-weighted particle size distributions; 120 N-m; downstream nozzle.

**Discussion: 40 N-m** On a number-based comparison, the results suggest that the downstream nozzle configuration resulted in uneven cylinder-to-cylinder distribution of either water or 100-proof ethanol: Figure 4.13 shows marked increases in particle number concentrations with *both* water and alcohol downstream fumigation. Water produced the worst results, probably due to its lesser volatility, resulting in worse mixing and cylinder-to-cylinder distribution. In contrast, this problem was minimized when water was introduced upstream of the aftercooler, as the size distributions show a reduction in peak particle number concentration with water. With 100-proof ethanol, there were increases in peak number concentrations; this fact is probably due to the occurrence of the 33-nm mode that appeared in the volume-weighted particle size distributions (see Figure 4.1 above).

**Discussion: 80 N-m** The number-weighted particle size distributions obtained from 80 N-m engine load exhibit some interesting results. With downstream fumigation significant increases in peak particle number were observed, similarly to what

occurred in the 40 N-m case. Downstream injection of water produced the largest increases in peak particle number, and there were also shifts towards smaller particle diameters. The upstream fumigation, however, resulted in slightly different results: water injection caused large increases in peak particle number concentrations, and the upstream fumigation of 100-proof ethanol did not result in significant departures from the baseline condition.

**Discussion: 120 N-m** The trends observed in the number-weighted particle size distributions obtained at 120 N-m are in many instances similar to the ones observed in the volume-weighted particle size distributions discussed above. In general, at this load level, neither fumigant nor nozzle configuration resulted in appreciable reductions in peak particle number concentrations. Nevertheless, slightly better reductions were observed with upstream injection of water; upstream fumigation of 100-proof ethanol caused a slight increase in peak particle number concentrations. With the downstream nozzle configuration, increases in peak number concentrations were observed, except for a reduction which was caused by the fumigation of 100-proof ethanol at 25% flowrate.

**Total Particle Number Concentrations** Similarly to the volume case, the areas under the number-weighted particle size distributions shown above represent the *total* particle number concentrations and the bar plots shown below compare the total particle number concentrations for baseline, upstream and downstream nozzle configurations.

## 40 N-m

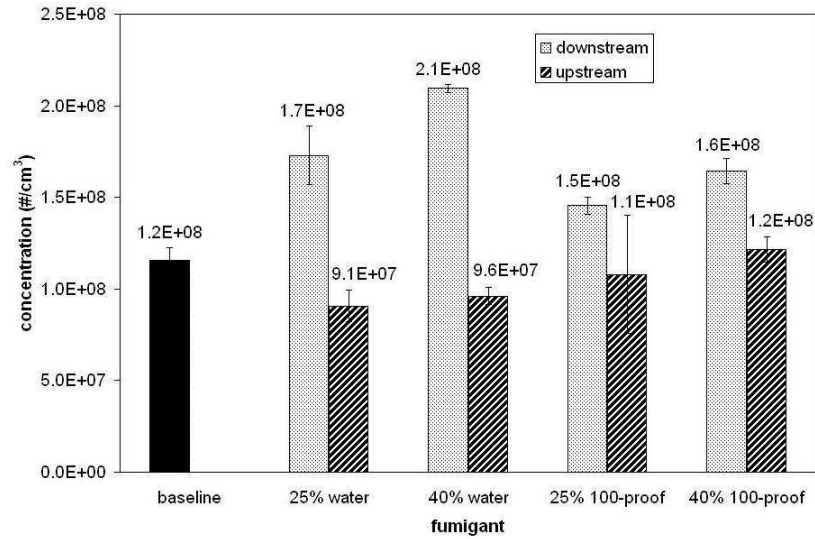


Figure 4.16: Total particle number concentrations; 40 N-m.

## 80 N-m

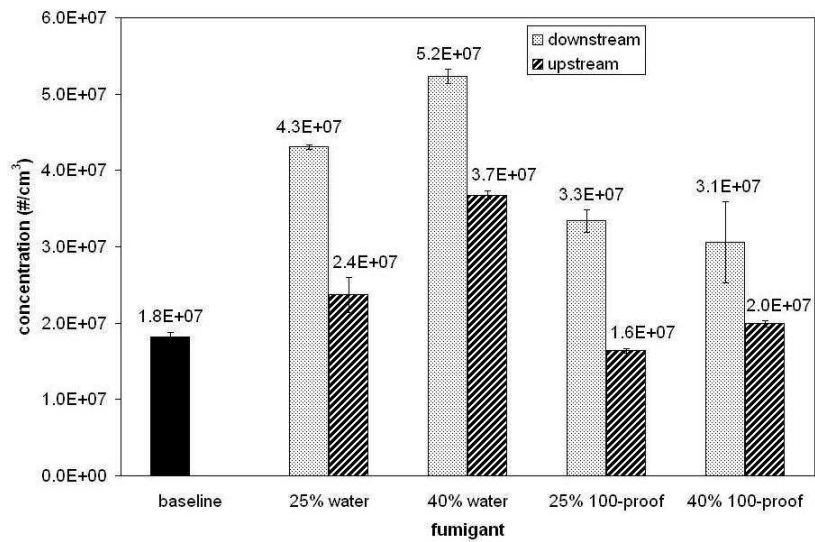


Figure 4.17: Total particle number concentrations; 80 N-m.



## 120 N-m

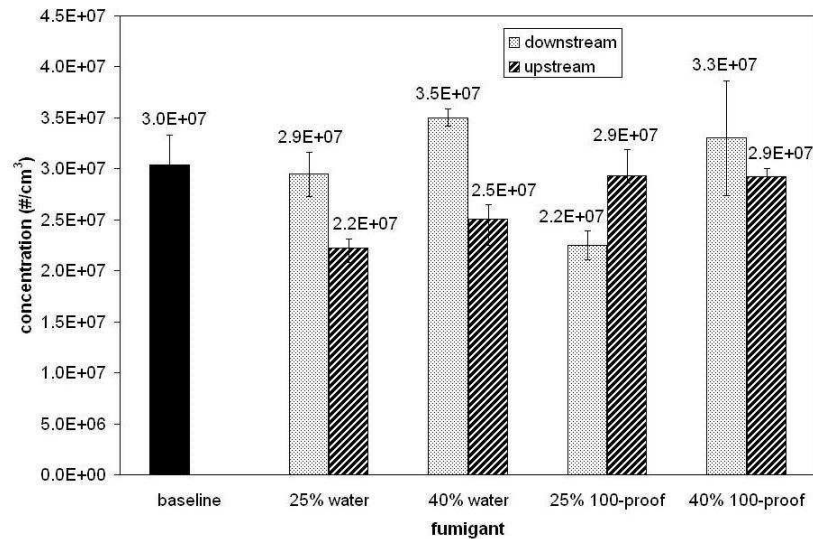


Figure 4.18: Total particle number concentrations; 120 N-m.

**Discussion: 40 N-m** This bar plot shows the significant increases in total particle number with downstream fumigation and, as explained above, this is probably due to the poor evaporating and mixing that occurs with that particular configuration. This maldistribution problem is aggravated by the water as it is evidenced by the even higher increases in number concentrations resulting from water injection. With the atomizing nozzle located upstream of the aftercooler, the mixing was enhanced and water injection could cause a reduction in both total particle number and volume concentrations. The slight increase in total particle number brought about by ethanol fumigation at 40% flowrate is probably related to the peak in particle volume concentration at particle diameters about 33 nm, as illustrated by Figure 4.1.

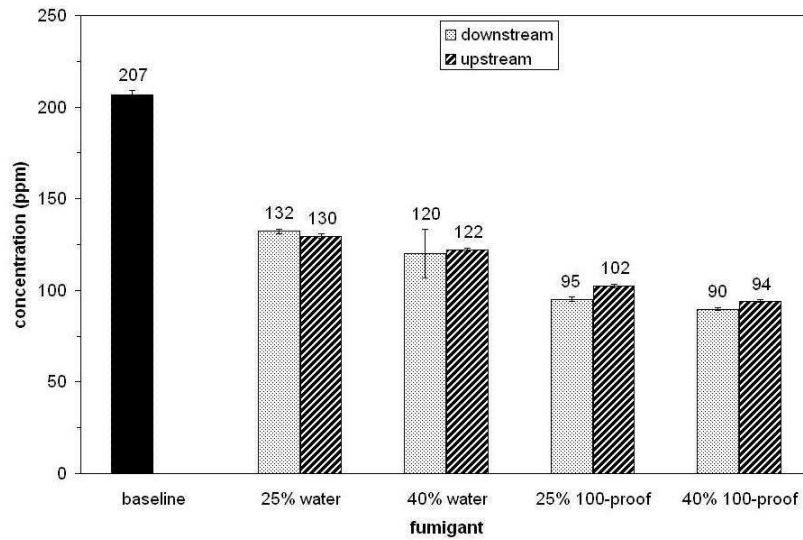
**Discussion: 80 N-m** This plot shows that an increase in total particle number concentrations occurred at all cases—except with 100-proof ethanol at 25% flowrate, when no significant reduction was observed. These results are in agreement with both downstream and upstream number-weighted particle size distributions, which also did not show any significant decrease in particle number concentrations.

**Discussion: 120 N-m** As it is illustrated by Figure 4.18, the upstream atomizing nozzle setup in smaller levels of total particle number concentrations. The smallest levels were observed when water was injected, whereas the reductions obtained with 100-proof ethanol were not quite significant. These results are in accordance with the number-weighted particle size distributions discussed above, which showed a decrease in particle number concentrations with upstream water injection. The results obtained with the downstream nozzle configuration exhibit a curious pattern: Both water and 100-proof ethanol were able to decrease total particle number at 25% flowrates, whereas at higher flowrates (40%) the total particle concentrations increased relative to the baseline concentration.

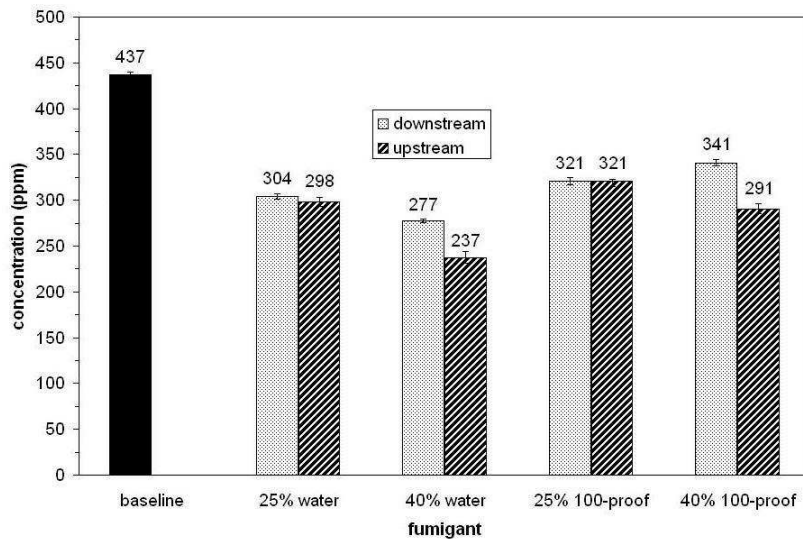
#### 4.2.2 Effect on $\text{NO}_x$ Emissions

The total exhaust  $\text{NO}_x$  concentrations, are illustrated in the bar plots 4.19, 4.20, and 4.21 below, which compare the total  $\text{NO}_x$  emissions for baseline, upstream and downstream nozzle configurations for all three engine loads.

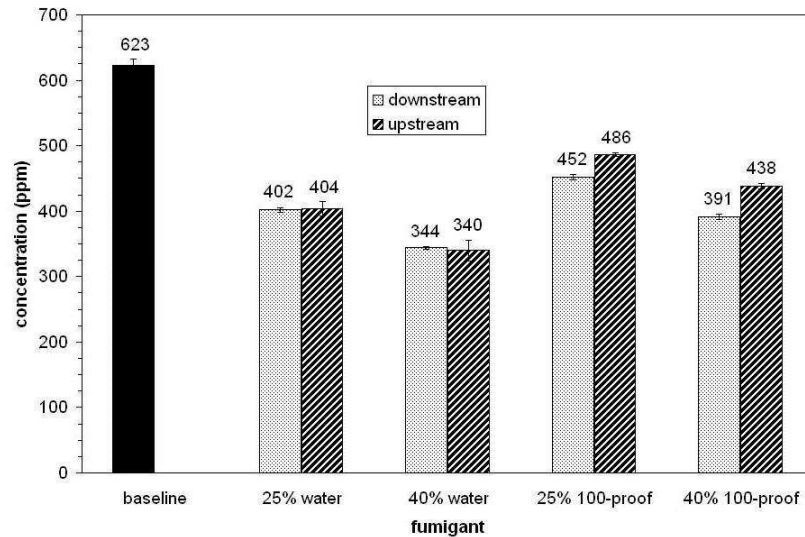
## 40 N-m

Figure 4.19: Total exhaust  $NO_x$  concentrations; 40 N-m.

## 80 N-m

Figure 4.20: Total exhaust  $NO_x$  concentrations; 80 N-m.

## 120 N-m

Figure 4.21: Total exhaust  $NO_x$  concentrations; 120 N-m.

**Discussion: 40 N-m** In this case, it can be seen that the  $NO_x$  emissions were reduced with the introduction of either water or 100-proof ethanol, at either 25% or 40% flowrates. Increasingly smaller levels were observed with increased content in alcohol: 100-proof ethanol was shown to be slightly more effective than pure water in curbing  $NO_x$  emissions. The decrease in  $NO_x$  caused by water is primarily due to a combination of dilution and thermal effects, whereas ethanol can accomplish that also by way of the increase in ignition delay and a subsequent reduction in peak combustion temperatures. In this low-load case the increase in ignition delay caused by the alcohol is more pronounced, which tends to result in lower cycle temperatures and lower  $NO_x$  emissions. The introduction of larger amounts of fumigant resulted in slightly increased reductions in  $NO_x$ . Lastly, the configuration of the atomizing nozzle did not seem to have a significant effect on the  $NO_x$  emissions, as the results from up- and downstream fumigation did not differ appreciably.

**Discussion: 80 N-m** The trends illustrated by Figure 4.20 are similar to the ones obtained at 40 N-m engine load: significantly smaller  $\text{NO}_x$  emissions were observed with both water and 100-proof ethanol; further, the location of the atomizing nozzle—downstream or upstream of the aftercooler—did not seem to influence the  $\text{NO}_x$  emissions significantly. Again, the effect of water injection on  $\text{NO}_x$  is believed to be primarily due to a dilution (oxygen substitution) effect and a thermal (cooling) effect. The reductions in  $\text{NO}_x$  produced by the alcohol are probably caused by the lower cycle temperatures resulting from an increase in ignition delay at this engine load level.

**Discussion: 120 N-m** As it was the case in the previously discussed engine load conditions (40 N-m and 80 N-m) the emissions of  $\text{NO}_x$  were reduced in all cases. At this engine load of 120 N-m, water injection at 40% flowrate was able to yield the greatest reduction in  $\text{NO}_x$  emissions (about 45%), when compared to the baseline levels. The fumigation of 100-proof ethanol at 25% flowrate resulted in the less pronounced  $\text{NO}_x$  reduction (around 25% less than baseline). Similarly to what was observed in the previously discussed load conditions, the reductions in  $\text{NO}_x$  emissions were usually shown to be somewhat insensitive to the configuration of the atomizing nozzle: For a given fumigant (water or 100-proof ethanol) introduction down- or upstream of the aftercooler usually did not result in marked differences.

#### 4.2.2.1 Effect on Intake Manifold Temperature

An indication of the degree of vaporization of the fumigant inside the intake manifold is shown in Figures 4.22, 4.23, and 4.24 below:

## 40 N-m

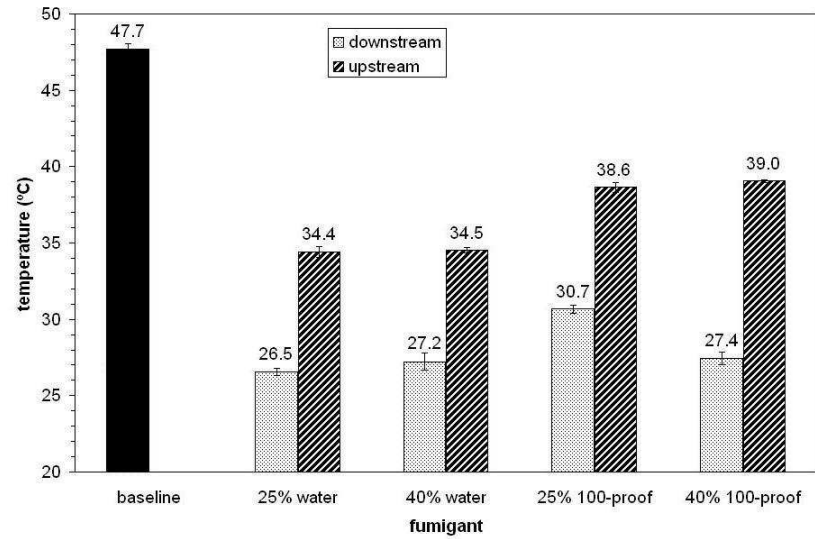


Figure 4.22: Intake manifold temperatures; 40 N-m.

## 80 N-m

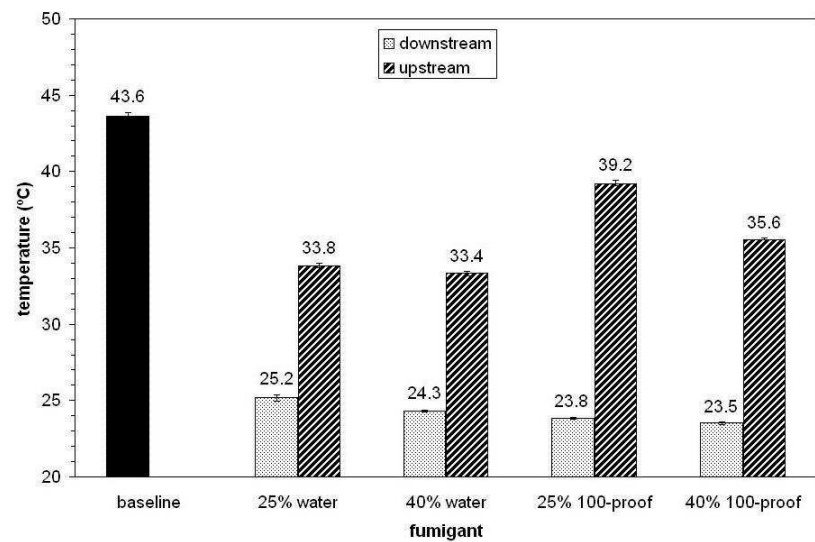


Figure 4.23: Intake manifold temperatures; 80 N-m.

## 120 N-m

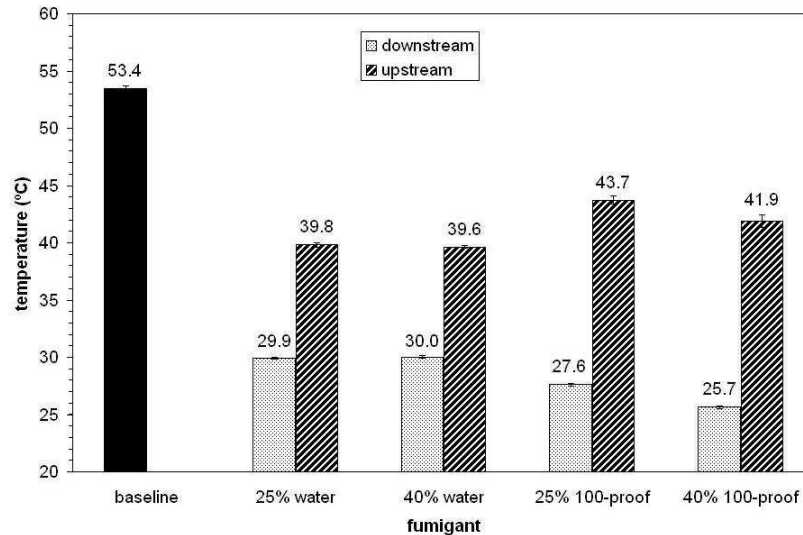


Figure 4.24: Intake manifold temperatures; 120 N-m.

**Discussion** At the engine loads of 40, 80, and 120 N-m, similar results were obtained: The bar plots above show a reduction in intake manifold temperatures with either water injection or ethanol fumigation, when compared to baseline operation. Compared to downstream fumigation, the introduction of fumigant into the hotter intake air upstream of the aftercooler resulted in higher intake temperatures; the introduction of the spray upstream cooled the intake air before entering the aftercooler, thus reducing its effectiveness. Therefore, the total cooling effect was less pronounced when compared to the downstream injection and the temperatures were higher. Therefore, the plot suggests that upstream fumigation resulted in better evaporation and mixing of the fumigant—which helps minimize cylinder-to-cylinder distribution problems.

It is interesting to note that all of the previously discussed  $\text{NO}_x$  reductions did not exhibit the same pattern observed in the intake air temperature data. That is, whereas air temperature changed appreciably with both nozzle configurations, the same pattern was not exhibited by the  $\text{NO}_x$  emissions data—which remained

essentially unchanged regardless of nozzle configuration.

### 4.3 Part II — Effect of Injection Pump Repair on Baseline Engine Performance

On September 17, 2009 the engine's fuel injection pump started to leak diesel fuel copiously. Testing was halted, the pump was fixed and the experiments were resumed one month later. However, after the repair the fuel injection timing of the pump changed—it became slightly more advanced. Therefore, the baseline behavior of the engine was altered and the present section examines those changes by comparing the PM and NO<sub>x</sub> emissions data *before* and *after* the pump was repaired.

#### 4.3.1 Effect on PM Volume Emissions

The effect of the pump repair on the volume-based PM emissions will be addressed below. Volume-weighted particle size distributions and total particle volume concentrations bar plots are presented. Particle data are presented for all engine loads tested: 40 N-m, 80 N-m, and 120 N-m. The engine speed is the usual 1700 rpm.

##### 4.3.1.1 Volume-Weighted Particle Size Distributions

The volume-weighted particle size distributions for *baseline operation* at 40 N-m, 80 N-m, and 120 N-m are shown in Figures 4.25, 4.26, and 4.27 below:



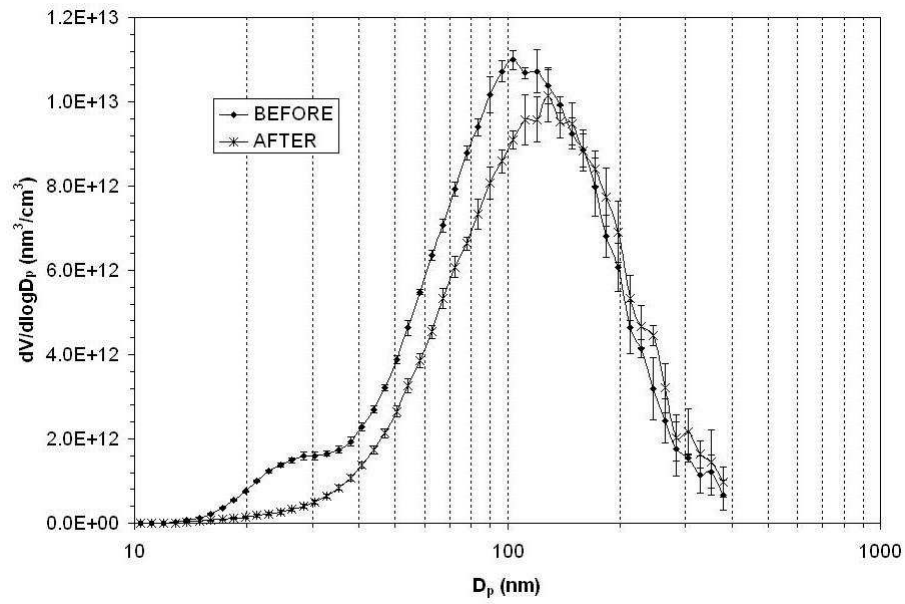


Figure 4.25: Volume-weighted particle size distributions; 40 N-m.

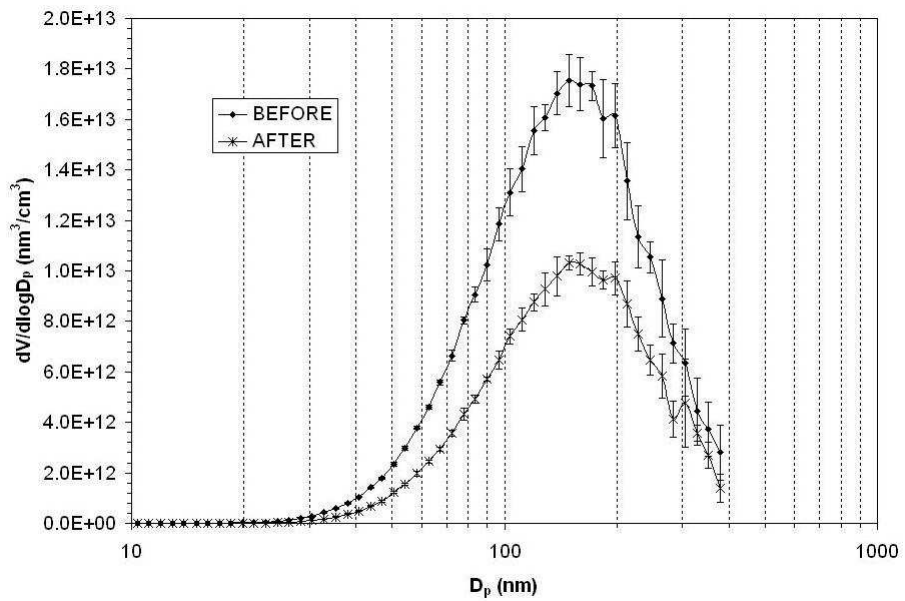


Figure 4.26: Volume-weighted particle size distributions; 80 N-m.

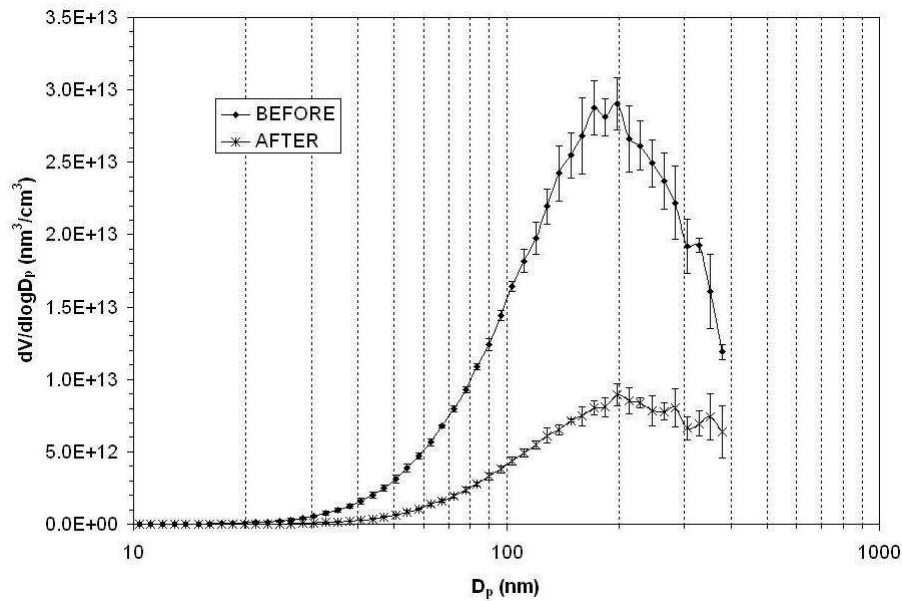


Figure 4.27: Volume-weighted particle size distributions; 120 N-m.

From the plots above it can be seen that after the injection pump was repaired the peak particle volume concentrations were significantly reduced, which is consistent with an advance in fuel injection timing: The advance in timing results in more fuel being burned in the premixed phase of the diesel combustion process, which inhibits the formation of soot particles in the subsequent diffusion-burning phase of combustion. This effect is more evident at higher engine loads, and this fact is confirmed by the higher reductions in peak particle volume concentrations at 80 N-m and 120 N-m.

#### 4.3.1.2 Total Particle Volume Concentrations

The total particle volume concentrations (in  $\text{nm}^3/\text{cm}^3$ ) for baseline operation before and after the pump repair is shown in Figure 4.28 below.

This plot confirms the fact that the total particle volume concentrations were significantly reduced as a result of pump repair. Further, the reductions in volume concentration increased with increasing engine load, reaching a maximum at 120 N-m.

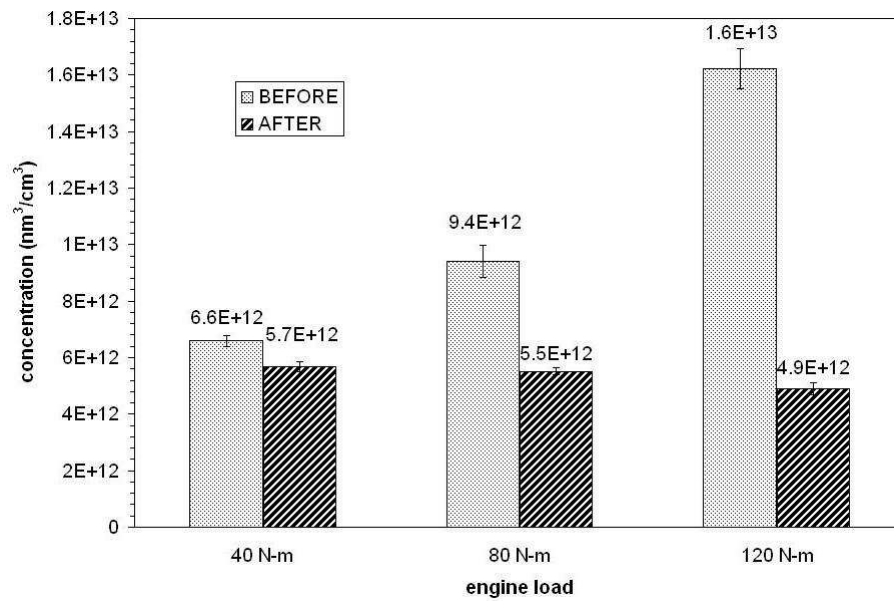


Figure 4.28: Total particle volume concentrations.

### 4.3.2 Effect on PM Number Emissions

Now the effect of the pump repair on the number-based PM emissions will be presented. Number-weighted particle size distributions and total particle number concentrations bar plots are shown below.

#### 4.3.2.1 Number-Weighted Particle Size Distributions

The number-weighted particle size distributions for baseline operation at 40 N-m, 80 N-m, and 120 N-m are presented in Figures 4.29, 4.30, and 4.31 as follows:

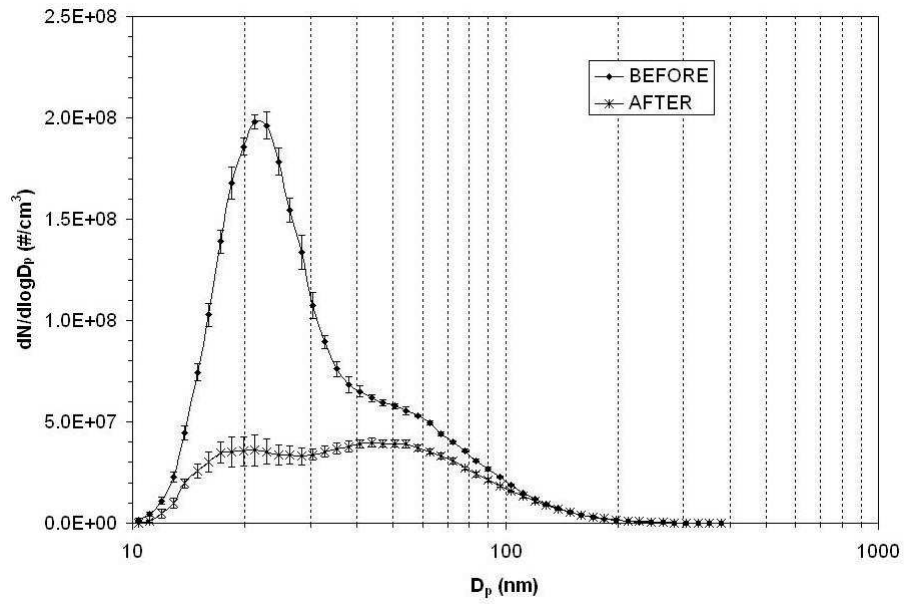


Figure 4.29: Number-weighted particle size distributions; 40 N-m.

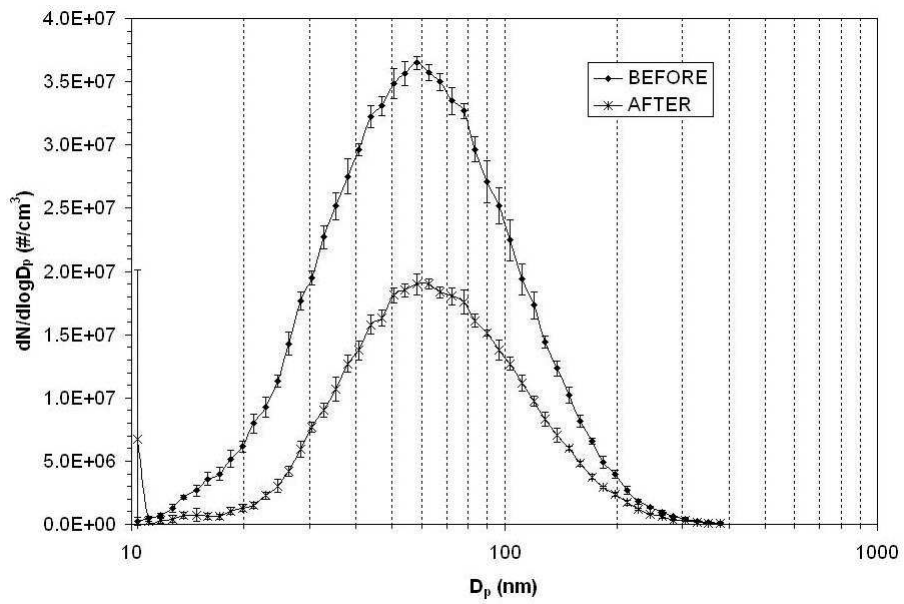


Figure 4.30: Number-weighted particle size distributions; 80 N-m.

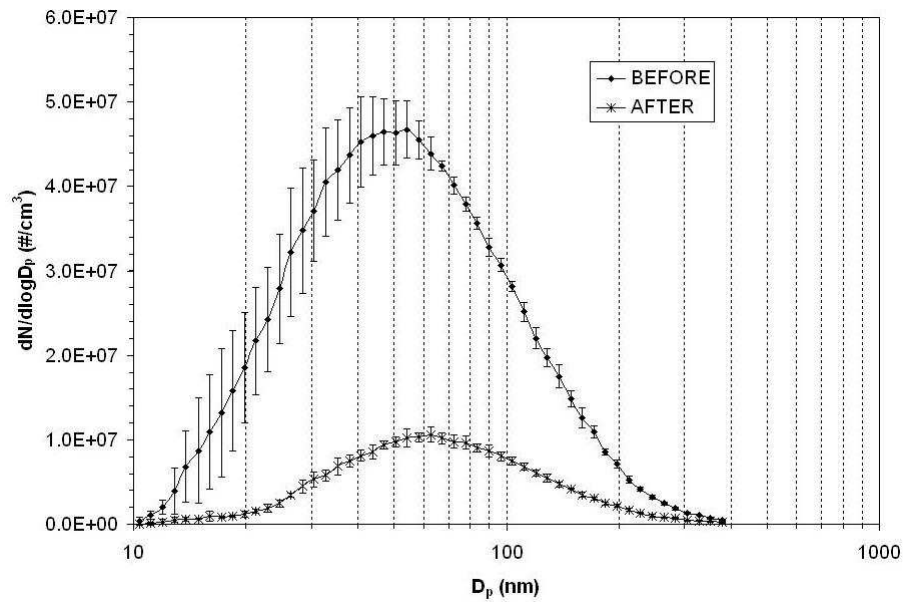


Figure 4.31: Number-weighted particle size distributions; 120 N-m.

As it was the case with the volume size distributions, the number-weighted particle size distributions also changed appreciably after the pump was repaired: a significant reduction in peak particle number concentrations resulted as the fuel injection timing became slightly advanced. The absolute reduction was most prominent at low engine load (40 N-m), although the percentage reduction was greatest at the highest load (120 N-m).

#### 4.3.2.2 Total Particle Number Concentrations

The total particle number concentrations (in particles/cm<sup>3</sup>) for baseline operation before and after the pump repair is presented in Figure 4.32 below.

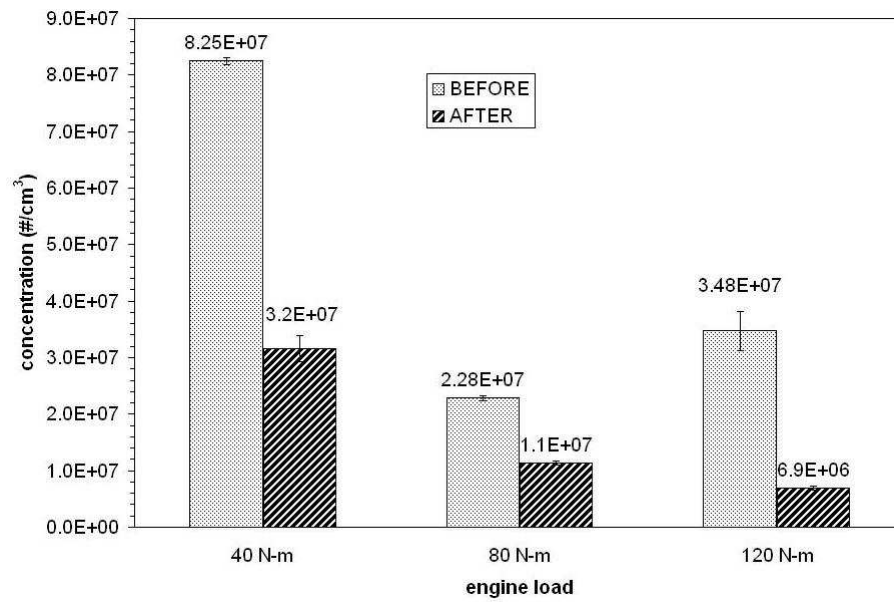


Figure 4.32: Total particle number concentrations.

As in the previous volume-based case, the total particle number concentrations were significantly reduced after the pump repair. However, in the present number-based case the reductions were more significant at 40 N-m load.

### 4.3.3 Effect on NO<sub>x</sub> Emissions

The effect of the pump repair on the NO<sub>x</sub> emissions (in ppm) is summarized in Figure 4.33 below:

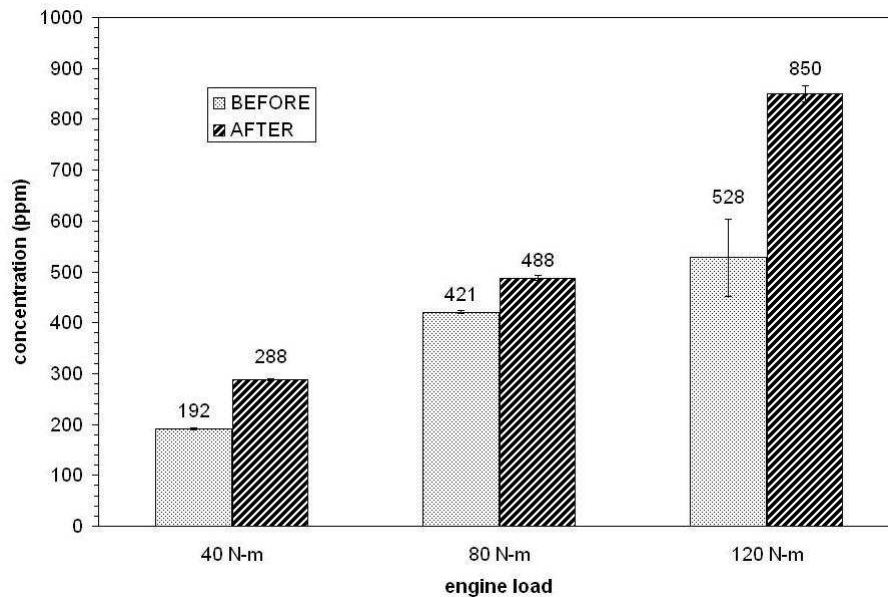


Figure 4.33:  $\text{NO}_x$  concentrations.

The advance in fuel injection timing—as it was discussed above—caused a larger amount of fuel to be burned in the premixed phase of the diesel combustion process. This leads to the occurrence of higher peak in-cylinder temperatures, which in turn favors the formation of NO. Therefore, the total  $\text{NO}_x$  emissions are increased, as the Figure 4.33 shows. This result is consistent with the trade-off between PM and  $\text{NO}_x$  emissions.

#### 4.4 Part III — Summary of Effects at 1700 rpm and 80 N-m

In this last part the overall effects of water injection and ethanol fumigation on engine performance and emissions are summarized. The engine load of 80 N-m was chosen for this last part of testing because—after the fuel injection pump was repaired—it had shown to be the most stable engine condition. Further, in addition to distilled

water and 100-proof ethanol, 200-proof (absolute) ethanol was also used as a fumigant. The same flowrate levels of 25% and 40% (of the corresponding baseline diesel fuel flowrate) were used in this last part. The atomizing nozzle was always mounted *upstream* of the aftercooler. This was done to enhance the evaporation and mixing of the fumigant—an attempt to minimize the problems with cylinder-to-cylinder distribution. A fuel-energy-based ethanol substitution of up to 20% was observed with 200-proof ethanol at 40% flowrate. No engine knock occurred. In this last part, the effect of water injection and ethanol fumigation on the HC emissions was also investigated.

#### 4.4.1 Effect on Engine Brake Thermal Efficiency

The plot in Figure 4.34 below shows the effect on average engine brake thermal efficiency resulting from the fumigation of ethanol, in both 100- and 200-proofs.

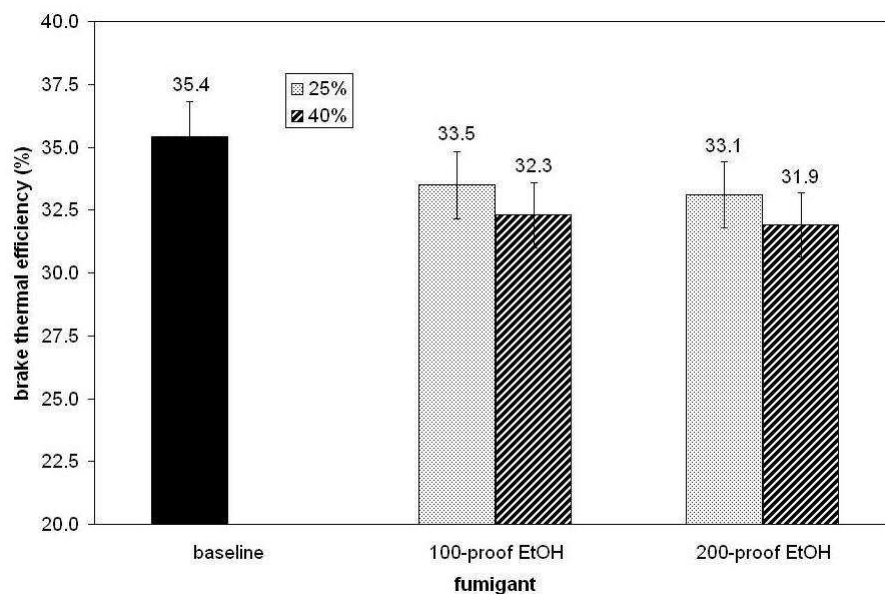


Figure 4.34: Engine Brake Thermal Efficiencies.

From the plot in Figure 4.34 it can be seen that the fumigation of ethanol resulted in a slight reduction in average thermal efficiency. The reduction was more noticeable



with the fumigation of 200-proof ethanol. This is probably due to the fact that—at this engine load of 80 N-m—the introduction of alcohol caused an increase in ignition delay such that the combustion process was shifted further into the expansion stroke, therefore producing less work and decreasing efficiency. Higher flows of both 100- and 200-proof ethanol also resulted in slight decreases in efficiency. Absolute ethanol probably caused a slightly longer ignition delay, thus worsening the break thermal efficiency. Nevertheless, the differences in thermal efficiency are not very pronounced. This is in agreement with the results obtained by several authors [28] [122] [57], who have reported that thermal efficiency is usually not significantly affected by ethanol proof.

#### 4.4.2 Effect on PM Volume Emissions

In this section the influence of the different fumigants on the volume-based particulate emissions is addressed. First, the volume-weighted particle size distributions are presented—for both 25% and 40% flowrates—followed by a bar plot showing the total particle volume concentrations.

##### 4.4.2.1 Volume-Weighted Particle Size Distributions

The effect of water, 100-proof, and 200-proof ethanol on the volume-weighted particle size distributions is shown below in Figures 4.35 and 4.36, for 25% and 40% flowrates, respectively.

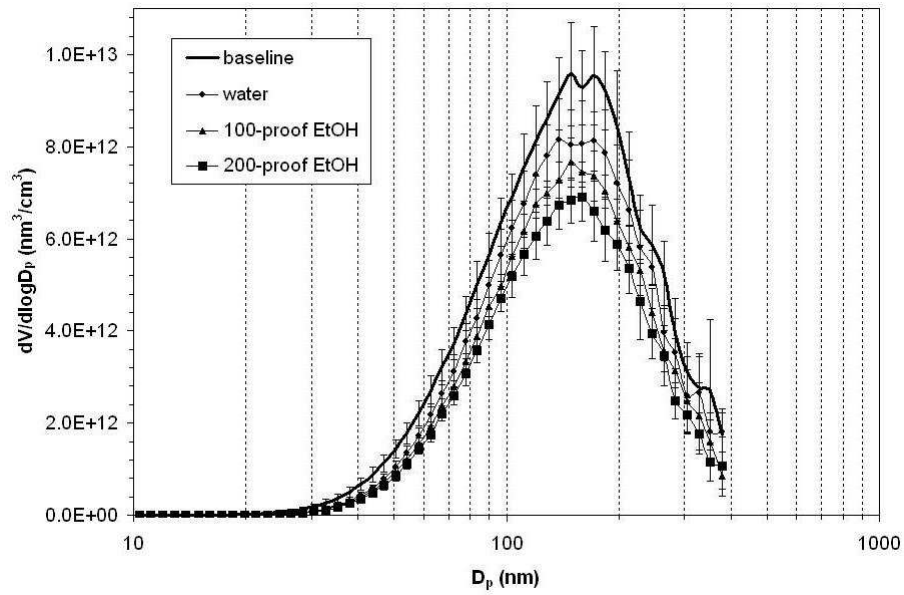


Figure 4.35: Volume-weighted particle size distributions; 25% flowrate.

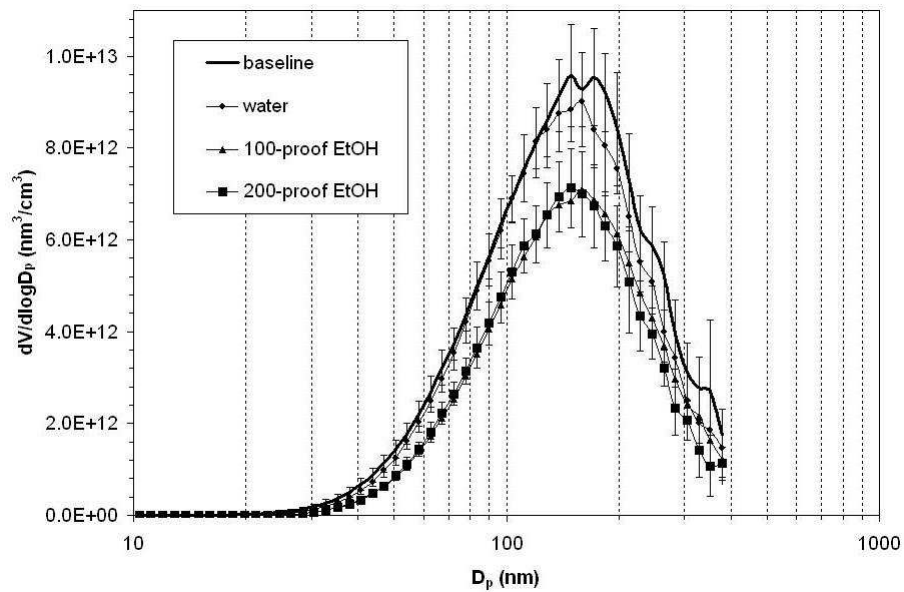


Figure 4.36: Volume-weighted particle size distributions; 40% flowrate.

The same trend can be observed in both plots: Compared to baseline, all fumigants resulted in decreased peak particle volume concentrations, with 200-proof ethanol

producing the best results—followed by 100-proof ethanol and water. However, from the second plot it is clear that the higher flowrate of 40% did not result in any significant further reduction in peak particle volume concentrations.

#### 4.4.2.2 Total Particle Volume Concentrations

The following bar plot in Figure 4.37 shows the total particle volume concentrations:

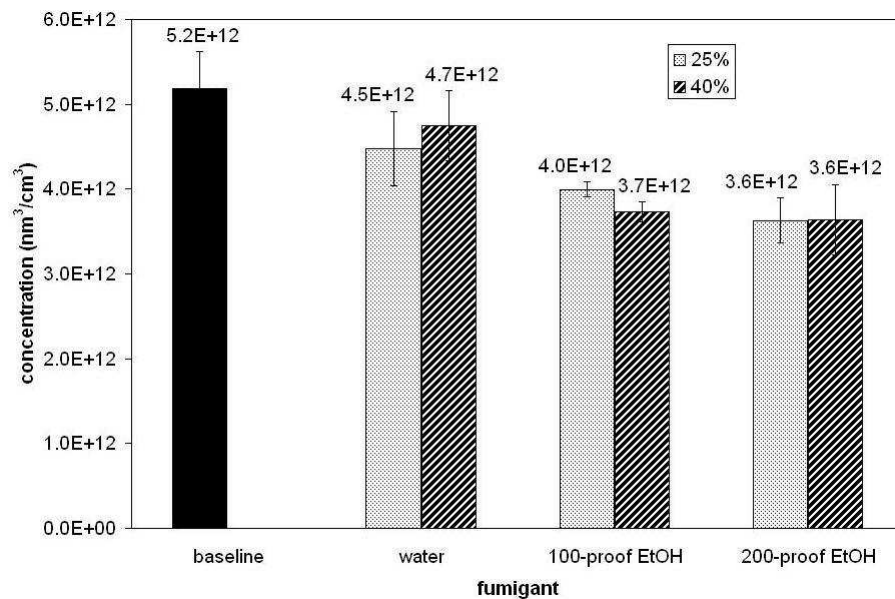


Figure 4.37: Total particle volume concentrations.

In agreement with the size distributions discussed above, the smallest concentrations of particle volume were obtained with 200-proof ethanol. Being an oxygenate, ethanol has the ability to inhibit the formation of soot precursors during combustion; the extra oxygen also helps oxidize the soot that has been formed. Further, the longer ignition delay brought about by the ethanol also tends to enhance the mixing of diesel fuel with air; this improved *air utilization* favors a more complete combustion, with less soot formation. As an additional factor, the fumigation of alcohol reduced the amount of diesel fuel burned.

#### 4.4.2.3 Number-Weighted Particle Size Distributions

The effect of water, 100-proof, and 200-proof ethanol on the number-weighted particle size distributions is shown below in Figures 4.38 and 4.39, for 25% and 40% flowrates, respectively.

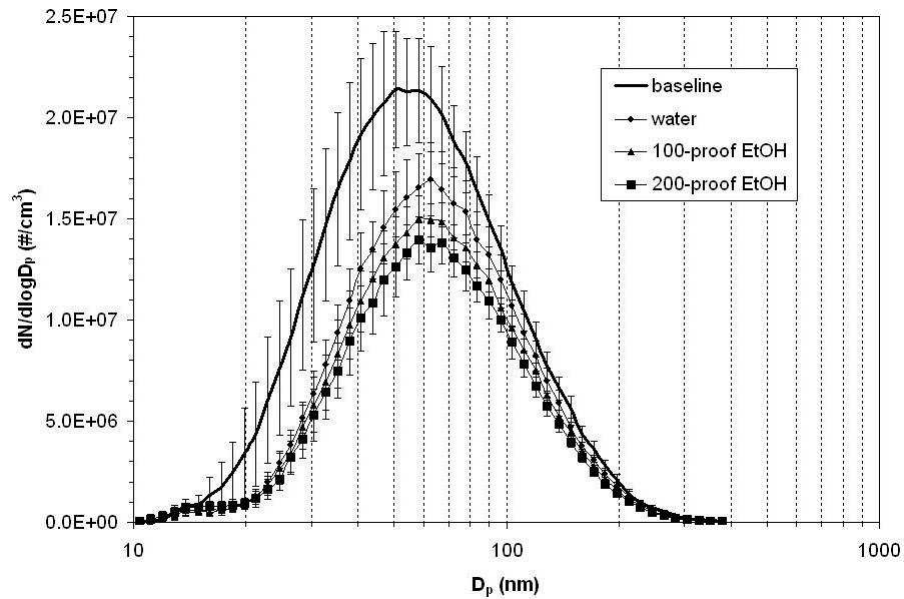


Figure 4.38: Number-weighted particle size distributions; 25% flowrate.

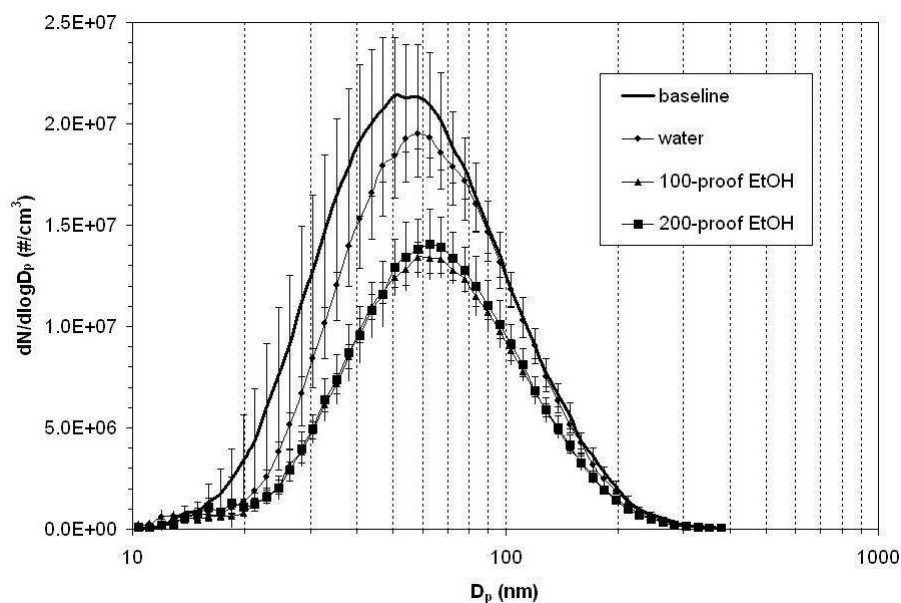


Figure 4.39: Number-weighted particle size distributions; 40% flowrate.

The trends exhibited in the above number-weighted size distributions are similar to the volume-weighted ones: Compared to baseline, all fumigants resulted in decreased peak particle number concentrations, with 200-proof ethanol producing the largest peak reductions—then followed by 100-proof ethanol and water. Also, similarly to what was observed in the volume-based case, the higher flowrate of 40% did not seem result in any significant further reduction in peak particle volume concentrations—except for water, which exhibited a poorer performance at 40% flowrate. Interesting to note is the slight shift towards *larger* particle diameters with fumigation.

#### 4.4.2.4 Total Particle Number Concentrations

The following bar plot in Figure 4.40 shows the total particle number concentrations:

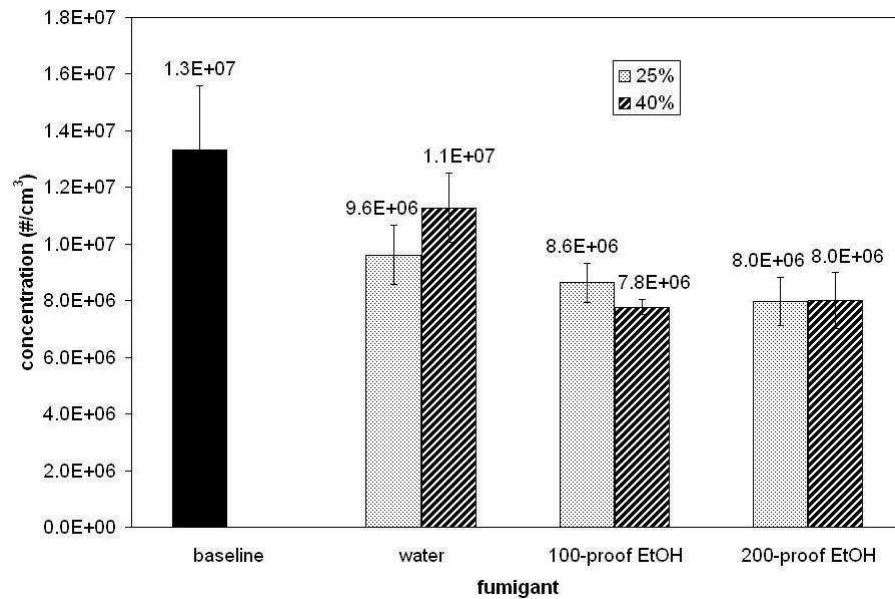


Figure 4.40: Total particle number concentrations.

Once more, smaller levels in total particle number concentrations were observed in all cases, when compared to the baseline level. Ethanol fumigation—in either proof—resulted in larger reductions than water injection. It is unclear whether a higher flow of fumigant would be beneficial: Water yielded smaller reductions at 40% flowrate, whereas 100-proof ethanol seemed to be more effective at higher flowrates. In the case of 200-proof ethanol, the difference in flowrate did not seem to play a significant role in decreasing particle number concentrations.

#### 4.4.3 Effect on NO<sub>x</sub> Emissions

The bar plot in Figure 4.41 below shows the total NO<sub>x</sub> emissions.

It is worth noting the fact that water resulted in significantly smaller concentrations of NO<sub>x</sub> than either proof of ethanol. As it has been previously stated, water injection is expected to lower exhaust NO<sub>x</sub> concentrations, primarily because of a combination of dilution effect (displacement of intake air oxygen) and a thermal effect (cooling). Ethanol is also capable to displace intake air oxygen and also cool the

intake charge, thus lowering  $\text{NO}_x$  (which is true in the present case). In some instances, however, the sudden premixed combustion of ethanol may also cause a raise in peak in-cylinder temperatures, consequently *increasing* the formation of  $\text{NO}_x$ . The injection of water in a higher flowrate (40%) caused a further reduction in  $\text{NO}_x$ , thus stressing the significance of its dilution and thermal effects on  $\text{NO}_x$  formation.

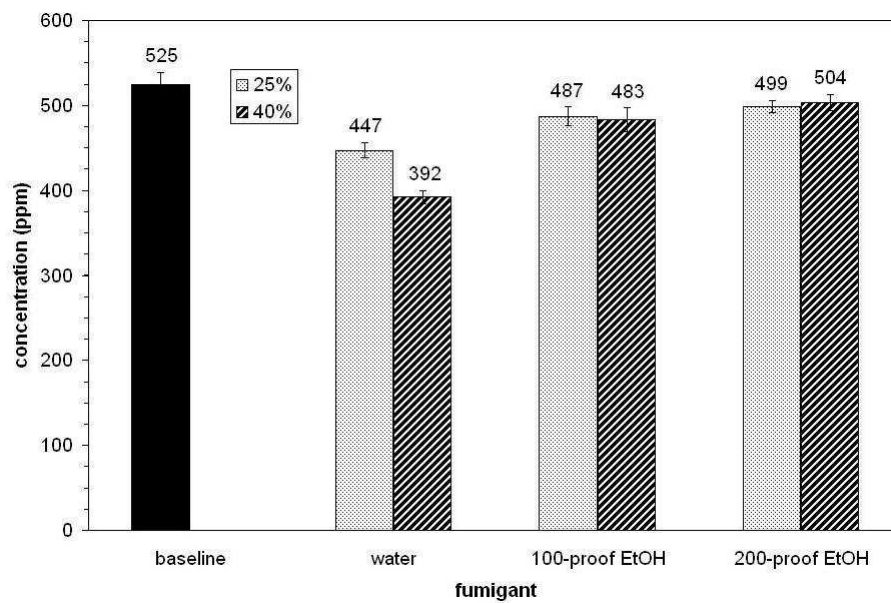


Figure 4.41: Exhaust  $\text{NO}_x$  concentrations.

#### 4.4.4 Effect on $\text{NO}_2/\text{NO}_x$ Ratios

The bar plot in Figure 4.42 below shows the fraction of  $\text{NO}_2$  present in the total exhaust  $\text{NO}_x$  concentrations.

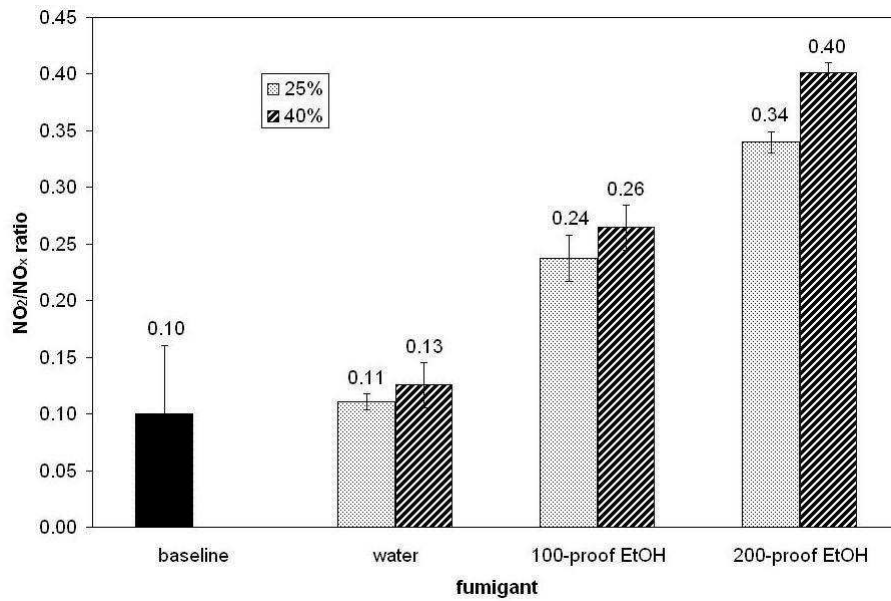


Figure 4.42: Exhaust  $\text{NO}_2/\text{NO}_x$  Ratios.

The following reaction responsible for in-cylinder  $\text{NO}_2$  formation in diesel engines was previously presented in Section 2.2.2:



The dissociation of either water or ethanol during combustion is likely to result in the formation of  $\text{HO}_2$  radicals, which in turn react with  $\text{NO}$  to form  $\text{NO}_2$ . This increase in  $\text{HO}_2$  radicals due to water or ethanol dissociation may provide an explanation for the increased levels of  $\text{NO}_2$  observed with both ethanol fumigation and water injection.

#### 4.4.5 Effect on Unburned Hydrocarbons Emissions

The effect of water injection and ethanol fumigation on the exhaust emissions of HC is shown in the bar plot in Figure ?? below.



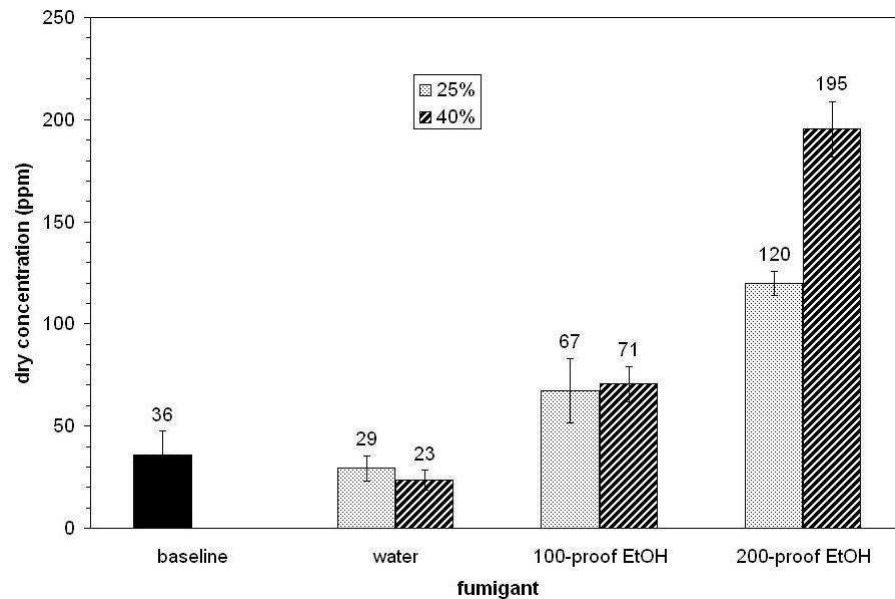


Figure 4.43: Concentrations of unburned hydrocarbons (dry).

As it would be expected, the emissions of HC increased significantly with the addition of ethanol—200-proof ethanol representing the worst case. Such high concentration levels are primarily due to unburned ethanol, originating from the quenching of the premixed air-ethanol charge at the cylinder walls, in a mechanism similar to the formation of HC in spark-ignition engines. The loss of fresh charge during the valve overlapping periods is another possible reason for the high HC emissions. Water injection, on the other hand, resulted in slightly lower levels of unburned HC emissions when compared to baseline. No explanation can be found for this result. Some authors [44, 134] have reported slight *increases* in HC emissions with water injection.

#### 4.4.6 Effect on Intake Manifold Temperature

The effect of water injection and ethanol fumigation on the average intake manifold temperature is shown in the bar plot in Figure 4.44 below.

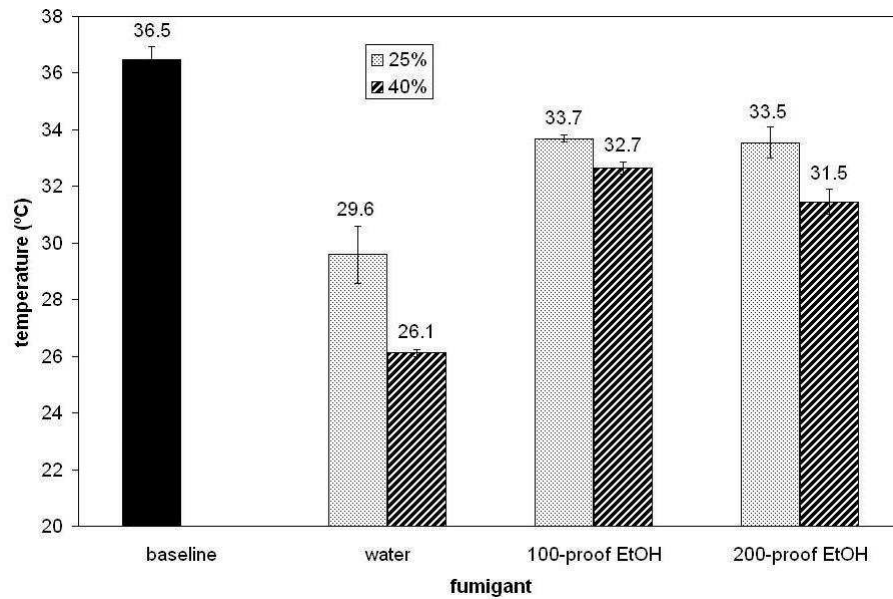


Figure 4.44: Intake manifold temperatures.

Similarly to what was observed in Part I, the injection of water resulted in the coolest intake air temperatures. This is not surprising because ethanol has a lower latent heat of vaporization than water. In any case, the intake air temperatures were lowered with either water injection or ethanol fumigation.

## 4.5 Sources of Inconsistencies in the Results

### 4.5.1 Poor Cylinder-to-Cylinder Distribution

The present study addressed the effect of water injection and ethanol fumigation on the performance, and particularly on the emissions of a 4-cylinder diesel engine. The intention was to use a very simple and retrofittable fumigation system, consisting of a single air atomizing nozzle to introduce the fumigants into the intake manifold. Because of its simplicity it was already expected that this method would cause some degree of inconsistency in the experimental results. Problems related to poor distribution of fumigant among the cylinders were expected to some extent. Indeed,

quite inconsistent results were observed particularly when the atomizing nozzle was mounted downstream of the aftercooler. This arrangement probably resulted in poor cylinder-to-cylinder distribution of fumigant, producing results that were often inconsistent. The problem of fumigant maldistribution is well known and it has been reported in the studies by several authors, such as Chen et al. [28], Shropshire and Bashford [121], Baranescu [19], and Jiang et al. [70]. In order to enhance the evaporation and mixing of the fumigants it was decided that the best choice would be to mount the nozzle upstream of the aftercooler, and that was the configuration used in Part III.

#### 4.5.2 Engine Speed Instabilities

Even the fumigation using the upstream nozzle configuration was not immune to problems, as it was demonstrated by episodes of engine speed instability. These typically consisted of sudden drops in engine speed and were not uncommon, particularly at the low engine load of 40 N-m. A typical example of a sudden drop in speed occurred in Part III, with the engine running at 80 N-m and 25% 200-proof ethanol fumigation. The plot in Figure below shows the engine speed over a 53-second period:

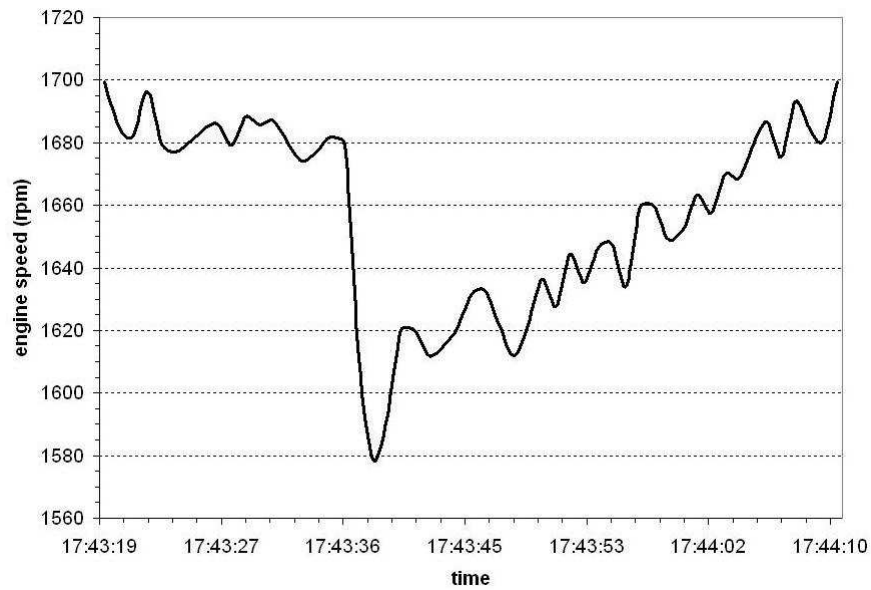


Figure 4.45: Sudden drop in engine speed; 80 N-m, 25% 200-proof ethanol; 53 s.

Another example of a sudden speed drop over a 2-minute period is shown in Figure 4.46 below:

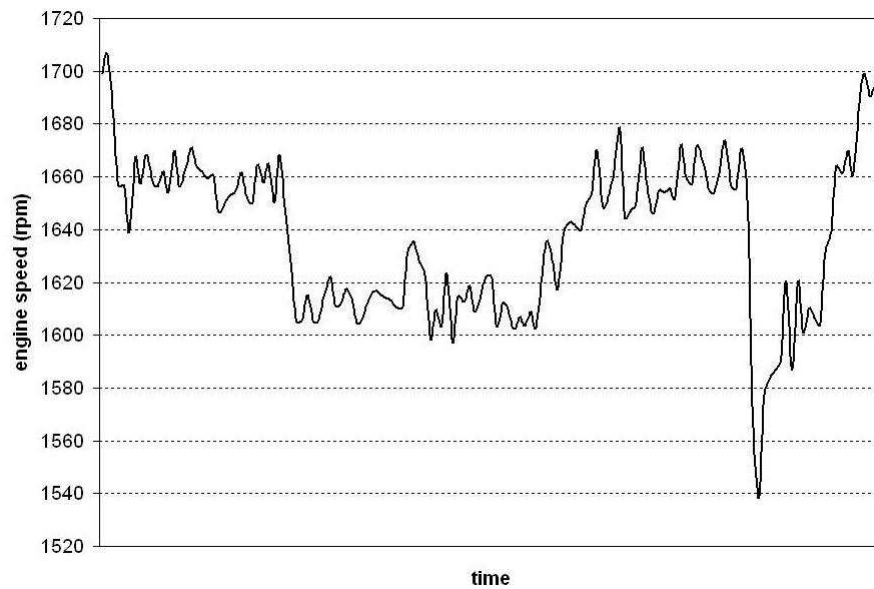


Figure 4.46: Sudden drop in engine speed; 40 N-m, 40% 200-proof ethanol; 2 min.

The following plots in Figures 4.47, 4.48, and 4.49 show the engine speed over

15-minute periods. The sharp drops in speed are evident.

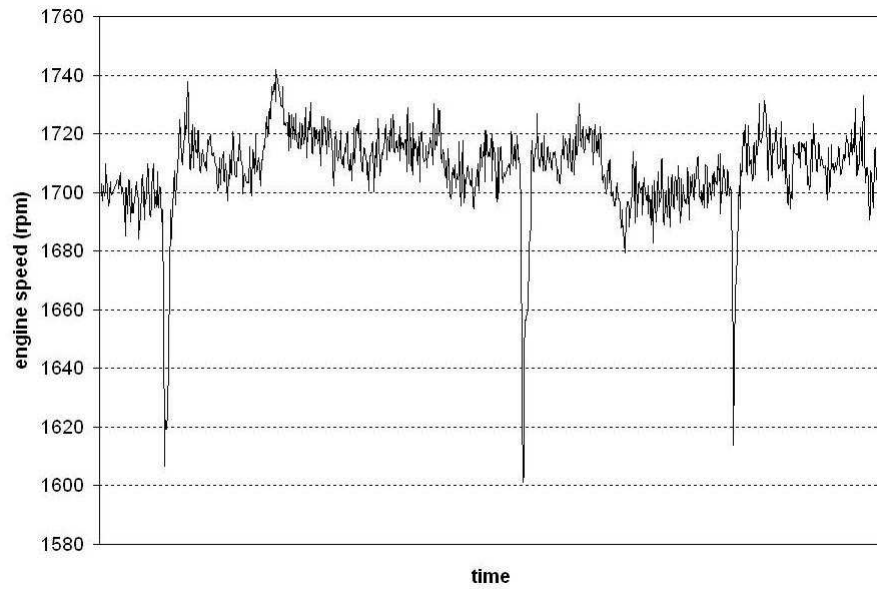


Figure 4.47: Sudden drops in engine speed; 40 N-m, 25% 200-proof ethanol; 15 min.

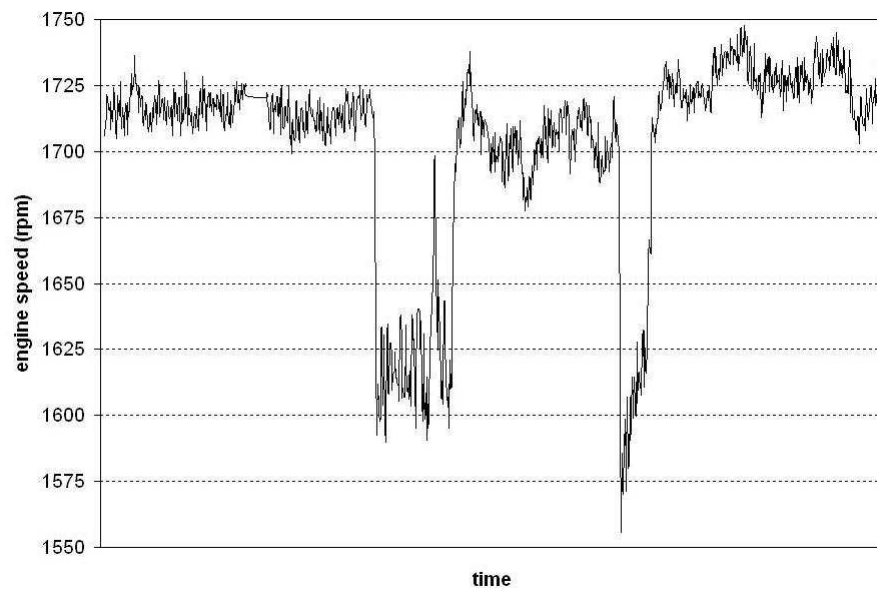


Figure 4.48: Sudden drops in engine speed; 40 N-m, 25% 200-proof ethanol; 15 min.

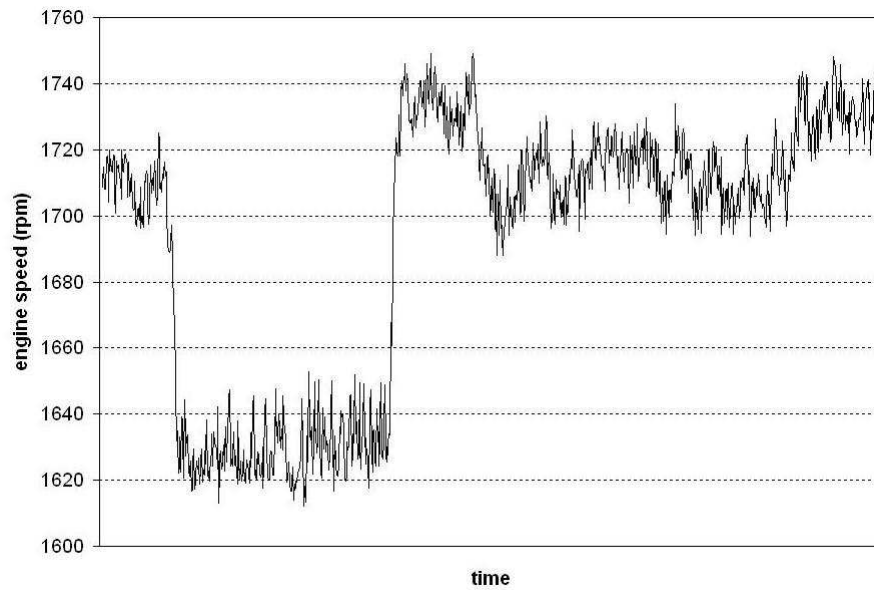


Figure 4.49: Sudden drops in engine speed; 40 N-m, 40% water; 15 min.

As it can be noticed, the maldistribution of fumigant among the cylinders was the probable cause for the instabilities in engine speed shown in the plots above. Also, inconsistent flow and accumulation of liquid in the intake manifold may also have contributed to the inconsistencies in the results.

# Chapter 5

## Conclusion and Recommendations

### 5.1 Summary of Effects of Fumigation on Engine Performance and Emissions

The overall effect of water injection and ethanol fumigation on the engine performance and exhaust emissions with upstream fumigation at 80 N-m (Part III) can be summarized as follows:

**Brake Thermal Efficiency** As it was previously shown in Figure 4.34, the brake thermal efficiency tended to *decrease* slightly with the fumigation of ethanol at 80 N-m. At this load level, the introduction of ethanol probably increased the ignition delay to such an extent that the combustion process was shifted further into the expansion stroke, thus decreasing engine output.

**Particle Volume Emissions** There were reductions in the total particle volume concentrations with either water, 100-, or 200-proof ethanol. Absolute (200-proof) gave the best results, probably because of its higher oxygen content and also because of the better air utilization brought about by the longer ignition delay. The offset of diesel fuel also contributed to the lower particle volume concentrations.

**Particle Number Emissions** In a similar trend, any fumigant resulted in decreases in total particle number concentrations. Ethanol yielded better results than water, but proof did not seem to cause any significant difference.

**NO<sub>x</sub> Emissions** In the present study, reductions in NO<sub>x</sub> emissions were observed at all times. Water tended to result in more pronounced reductions than ethanol.

**NO<sub>2</sub>/NO<sub>x</sub> Ratios** The introduction of either water or ethanol resulted in increased formation of NO<sub>2</sub>, when compared to baseline diesel operation. This was probably due to the dissociation of water or ethanol at the high combustion temperatures, resulting in the formation of radicals that favor the formation of NO<sub>2</sub>. The cooler regions around the flame—particularly at lower loads—also favor the formation of NO<sub>2</sub>.

**HC Emissions** The exhaust HC emissions of were significantly increased with the fumigation of ethanol. Absolute ethanol resulted in even higher levels of HC emissions. The injection of water caused a slight reduction in hydrocarbons emissions.

### 5.1.1 Overall Conclusions

The general final conclusions of the present work can be summarized as follows:

- The upstream nozzle location gave better results than the downstream configuration
- In general, both water and ethanol were able to decrease PM and NO<sub>x</sub> emissions when compared to baseline levels
- Ethanol has shown to be more effective at reducing PM emissions, whereas water performed better at reducing NO<sub>x</sub> emissions
- Ethanol proof did not cause any significant effect on the ability to decrease PM or NO<sub>x</sub> emissions



- In general, the higher fumigant flowrate (40%) did not perform better than the 25% flowrate

## 5.2 Suggestions for Future Work

To overcome—or at least minimize—the problems associated with the use of a simple fumigation system it would become necessary to incorporate strategies that aim at improving the distribution of fumigant among the cylinders. An even fumigant distribution is of paramount importance when stable engine operation and consistent results are desired. This could be accomplished with the utilization of more sophisticated approaches, such as the use of multiple atomizing nozzles or even the use of electronically-controlled multi-point injectors. Such methods were successfully employed in the studies by Shropshire and Goering [122], Shropshire and Bashford [121], Savage et al. [116], Hayes et al. [57], among others.

With ethanol fumigation the combustion process is extremely complex, combining the characteristics of the premixed burning of the homogeneous alcohol-air charge with the—already complex—diesel combustion process. The injection of water also affects diesel combustion by altering the ignition delay and the rates at which the burning reaction proceed. Therefore, to investigate the effect of ethanol fumigation and water injection on the in-cylinder rates of pressure rise and rates of heat release would provide a valuable insight into how the combustion process is affected by fumigation. This would be particularly interesting at high ethanol substitution levels, approaching the engine knocking threshold. Lastly, the measurement of unregulated exhaust emissions—such as aldehydes—would also be worthwhile doing, especially in the case of ethanol fumigation, when aldehydes emissions are greatly increased.

## References

- [1] *Model 3782 Water-based Condensation Particle Counter Operation and Service Manual*. TSI Inc., Shoreview (Minn.), Revision B, Apr. 2005.
- [2] *Model 3936 Scanning Mobility Particle Sizer<sup>TM</sup> (SMPS<sup>TM</sup>) Spectrometer Operation and Service Manual*. TSI Inc., Shoreview (Minn.), Revision M, Apr. 2008.
- [3] *Series 3080 Electrostatic Classifiers Operation and Service Manual*. TSI Inc., Shoreview (Minn.), Revision H, Apr. 2008.
- [4] *Standard Specification for Diesel Fuel Oils*. ASTM Standard D 975 - 09b, ASTM International, West Conshohocken (Pa.), 2009.
- [5] ABD-ALLA, GH. Using exhaust gas recirculation in internal combustion engines: a review. *Energy Conversion and Management*, May 2002, vol. 43, no. 8, p. 1027–1042.
- [6] ABDUL-KHALEK, I., KITTELSON, DB., and BREAR, F. The Influence of Dilution Conditions on Diesel Exhaust Particle Size Distribution Measurements. *SAE Technical Paper Series*, 1999, no. 1999-01-1142.
- [7] ———. Nanoparticle Growth During Dilution and Cooling of Diesel Exhaust: Experimental Investigation and Theoretical Assessment. *SAE Technical Paper Series*, 2000, no. 2000-01-0515.

- [8] ABTHOFF, J., SCHUSTER, H., LANGER, H., and LOOSE, G. The Regenerable Trap Oxidizer—An Emission Control Technique for Diesel Engines. *SAE Technical Paper Series*, 1985, no. 850015.
- [9] ABU-QUDAIS, M., HADDAD, O., and QUDAISAT, M. The effect of alcohol fumigation on diesel engine performance and emissions. *Energy Conversion & Management*, Mar. 2000, vol. 41, no. 4, p. 389–399.
- [10] ADELMAN, H. Alcohols in Diesel Engines—A Review. *SAE Technical Paper Series*, 1981, no. 790956.
- [11] AEROSOL DYNAMICS INC. *Continuous, laminar flow water-based particle condensation device and method*. SV. HERING and MR. STOLZENBURG. *U.S. Patent*, 6,712,881 B2. 2004-03-30.
- [12] AGARWAL, AK. and DAS, LM. Biodiesel Development and Characterization for Use as a Fuel in Compression Ignition Engines. *ASME Journal of Engineering for Gas Turbines and Power*, Apr. 2001, vol. 123, no. 2, p. 440–447.
- [13] AGARWAL, D., KUMAR, L., and AGARWAL, AK. Performance evaluation of a vegetable oil fuelled compression ignition engine. *Renewable Energy*, June 2008, vol. 33, no. 6, p. 1147–1156.
- [14] ALI, Y. and HANNA, MA. Alternative diesel fuels from vegetable oils. *Bioresource Technology*, 1994, vol. 50, no. 2, p. 153–163.
- [15] ALIN, L. *Försök med etanol i diesel. "Diesohol"*. KFB - Rapport 1997:50, Kommunikationsforskningsberedningen (KFB), Stockholm, 1997.
- [16] ALPERSTEIN, M., SWIM, WB., and SCHWEITZER, PH. Fumigation Kills Smoke—Improves Diesel Performance. *SAE Transactions*, 1958, vol. 66.
- [17] AMANN, CA. and SIEGLA, DC. Diesel Particulates—What They Are and Why. *Aerosol Science and Technology*, Dec. 1981, vol. 1, no. 1, p. 73–101.

- [18] AMES, BN. A Bacterial System for Detecting Mutagens and Carcinogens. In SUTTON, HE. and HARRIS, MI. (eds.). *Mutagenic Effects of Environmental Contaminants*. New York: Academic Press, 1972, p. 57–66.
- [19] BARANESCU, RA. Fumigation of Alcohols in a Multicylinder Diesel Engine—Evaluation of Potential. *SAE Technical Paper Series*, 1986, no. 860308.
- [20] BARNES, KD., KITTELSON, DB., and MURPHY, TE. Effect of Alcohols as Supplemental Fuel for Turbocharged Diesel Engines. *SAE Technical Paper Series*, 1975, no. 750469.
- [21] BENVENUTTI, LH., MARQUES, CST., and BERTRAN, CA. Chemiluminescent emission data for kinetic modeling of ethanol combustion. *Combustion Science and Technology*, 2005, vol. 177, no. 1, p. 1–26.
- [22] BERG, R. and EGEBÄCK, KE. *Blandbränsle etanol/diesel. Slutrapport och emissionsbilaga.* KFB - Rapport 1997:35, Kommunikationsforskningsberedningen (KFB), Stockholm, 1997.
- [23] BOSCH, D., DÖRGES, U., GOERGENS, G., HUNKERT, S., and LIANG, JR. The New Diesel Engine in the New Beetle. *SAE Technical Paper Series*, 1998, no. 891981.
- [24] BRO, K. and PEDERSEN, PS. Alternative diesel fuels: an investigation of methanol, ethanol, methane and ammonia in a DI diesel engine with pilot ignition. *SAE Technical Paper Series*, 1977, no. 770794.
- [25] BROUKHIYAN, EMH. and LESTZ, SS. Ethanol Fumigation of a Light Duty Automotive Diesel Engine. *SAE Technical Paper Series*, 1981, no. 811209.
- [26] BRUSCA, S. and LANZAFAME, R. Evaluation of the Effects of Water Injection in a Single Cylinder CFR Cetane Engine. *SAE Technical Paper Series*, 2001, no. 2001-01-2012.

- [27] BURTSCHER, H. Physical characterization of particulate emissions from diesel engines: a review. *Journal of Aerosol Science*, July 2005, vol. 36, no. 7, p. 896–932.
- [28] CHEN, J., GUSSERT, D., GAO, X., GUPTA, C., and FOSTER, D. Ethanol Fumigation of a Turbocharged Diesel Engine. *SAE Technical Paper Series*, 1981, no. 810680.
- [29] CHENG, AS., DIBBLE, RW., and BUCHHOLZ, BA. The Effect of Oxygenates on Diesel Engine Particulate Matter. *SAE Technical Paper Series*, 2002, no. 2002-01-2002.
- [30] DEC, JE. A Conceptual Model of DI Diesel Combustion Based on Laser-Sheet Imaging. *SAE Technical Paper Series*, 1997, no. 970873.
- [31] DELLINGER, B., PRYOR, WA., CUETO, R., SQUADRITO, GL., HEGDE, V., and DEUTSCH, WA. Role of free radicals in the toxicity of airborne fine particulate matter. *Chemical Research in Toxicology*, 2001, vol. 14, no. 10, p. 1371–1377.
- [32] DEMIRBAS, A. Progress and recent trends in biodiesel fuels. *Energy Conversion and Management*, Jan. 2009, vol. 50, no. 1, p. 14–34.
- [33] ———. Biofuels securing the planet's future energy needs. *Energy Conversion and Management*, Sept. 2009, vol. 50, no. 9, p. 2239–2249.
- [34] ECKLUND, EE., BECHTOLD, RL., TIMBARIO, TJ., and MCCALLUM, PW. State-of-the-Art Report on the Use of Alcohols in Diesel Engines. *SAE Technical Paper Series*, 1984, no. 840118.
- [35] EGEBÄCK, KE. *Forskning och fältförsök med en blandning av etanol i dieselolja*. KFB - Rapport 1999:20, Kommunikationsforskningsberedningen (KFB), Stockholm, 1999.

- [36] EKHOLM, K., KARLSSON, M., TUNESTÅL, P., JOHANSSON, R., JOHANSSON, B., and STRANDH, P. Ethanol-Diesel Fumigation in a Multi-Cylinder Engine. *SAE Technical Paper Series*, 2008, no. 2008-01-0033.
- [37] ENGA, BE., BUCHMAN, MF., and LICHTENSTEIN, IE. Catalytic Control of Diesel Particulates. *SAE Technical Paper Series*, 1982, no. 820184.
- [38] FLYNN, PF., DURRETT, RP., HUNTER, GL., zur LOYE, AO., AKINYEMI, OC., DEC, JE., and WESTBROOK, CK. Diesel Combustion: An Integrated View Combining Laser Diagnostics, Chemical Kinetics, and Empirical Validation. *SAE Technical Paper Series*, 1999, no. 1999-01-0509.
- [39] GATOWSKI, JA., BALLEES, EN., CHUN, KM., NELSON, FE., EKCHIAN, JA., and HEYWOOD, JB. Heat Release Analysis of Engine Pressure Data. *SAE Technical Paper Series*, 1984, no. 841359.
- [40] GERDES, KR. and SUPPES, GJ. Miscibility of Ethanol in Diesel Fuels. *Industrial & Engineering Chemistry Research*, 2001, vol. 40, no. 3, p. 949–956.
- [41] GOERING, CE. and WOOD, DR. Overfueling a diesel engine with carbureted ethanol. *Transactions of the ASAE*, 1981, no. 81-1048.
- [42] GOLDEMBERG, J. and MACEDO, IC. The Brazilian Alcohol Program—an overview. *Energy for Sustainable Development*, May 1994, vol. 1, no. 1, p. 17–22.
- [43] GRAY, KA., ZHAO, L., and EMPTAGE, M. Bioethanol. *Current Opinion in Chemical Biology*, Apr. 2006, vol. 10, no. 2, p. 141–146.
- [44] GREEVES, G., KHAN, IM., and ONION, G. Effects of water introduction on diesel engine combustion and emissions. *Symposium (International) on Combustion*, 1977, vol. 16, no. 1, p. 321–336.

- [45] GREEVES, G., KHAN, IM., WANG, CHT., and FENNE, I. Origins of Hydrocarbon Emissions from Diesel Engines. *SAE Technical Paper Series*, 1977, no. 770259.
- [46] GRIFFITH, DR., SAVAGE, LD., and GOERING, CE. Evaluation of an Ethanol-Fumigated Diesel Tractor. *ASAE Meeting Paper*, 1988, no. 88-1558.
- [47] HALLGREN, BE. and HEYWOOD, JB. Effects of Oxygenated Fuels on DI Diesel Combustion and Emissions. *SAE Technical Paper Series*, 2001, no. 2001-01-0648.
- [48] HANSEN, AC., ZHANG, Q., and LYNE, PWL. Ethanol-diesel fuel blends—a review. *Bioresource Technology*, Feb. 2005, vol. 96, no. 3, p. 277–285.
- [49] HARDENBERG, HO. and SCHAEFER, AJ. The Use of Ethanol as a Fuel for Compression Ignition Engines. *SAE Technical Paper Series*, 1981, no. 811211.
- [50] HARRINGTON, JA. and SHISHU, RC. A Single-Cylinder Engine Study of the Effects of Fuel Type, Fuel Stoichiometry, and Hydrogen-to-Carbon Ratio and CO, NO, and HC Exhaust Emissions. *SAE Technical Paper Series*, 1973, no. 730476.
- [51] HARRIS, SJ. and MARICQ, MM. Signature size distributions for diesel and gasoline engine exhaust particulate matter. *Journal of Aerosol Science*, June 2001, vol. 32, no. 6, p. 749–764.
- [52] HAUPT, D., NORD, K., EGEBÄCK, KE., and AHLVIK, P. Hydrocarbons and Aldehydes from a Diesel Engine Running on Ethanol and Equipped with EGR, Catalyst, and DPF. *SAE Technical Paper Series*, 2004, no. 2004-01-1882.
- [53] HAVEMANN, HA., RAO, MRK., and NARASIMHAN, TL. Leistungssteigerung durch das „Vergaser-Diesel-Verfahren“ mit Alkohol. *Mtz Jahrgang*, 1958, vol. 19, no. 2, p. 50–55.

- [54] HAVEMANN, HA., RAO, MRK., NATARAJAN, A., and NARASIMHAN, TL. Alcohol in Diesel Engines. *Automobile Engineer*, 1954, vol. 44, no. 6, p. 256–262.
- [55] ———. Alcohol with Normal Diesel Fuels—Part II. *Gas and Oil Power*, 1955, vol. 50, p. 45–50.
- [56] HAWKER, PN. Diesel emission control technology. *Platinum Metal Review*, 1995, vol. 39, no. 1, p. 2–8.
- [57] HAYES, TK., SAVAGE, LD., WHITE, RA., and SORENSON, SC. The Effect of Fumigating Different Ethanol Proofs on a Turbocharged Diesel Engine. *SAE Technical Paper Series*, 1988, no. 880497.
- [58] HAYNES, BS. and WAGNER, HGg. Soot formation. *Progress in Energy and Combustion Science*, 1981, vol. 7, no. 4, p. 229–273.
- [59] HEISEY, JB. and LESTZ, SS. Aqueous Alcohol Fumigation of a Single-Cylinder DI Diesel Engine. *SAE Technical Paper Series*, 1981, no. 811208.
- [60] HEITLAND, H., RINNE, G., WILLMANN, M., VANHAELST, R., and WISLOCKI, K. IC Engines for 100 Miles/Gallon Cars. *SAE Technical Paper Series*, 2001, no. 2001-01-0258.
- [61] HENEIN, N. Analysis of pollutant formation and control and fuel economy in diesel engines. *Progress in Energy and Combustion Science*, 1976, vol. 1, no. 4, p. 165–207.
- [62] HERING, SV. and STOLZENBURG, MR. A Method for Particle Size Amplification by Water Condensation in a Laminar, Thermally Diffusive Flow. *Aerosol Science and Technology*, Jan. 2005, vol. 39, no. 5, p. 428–436.
- [63] HERING, SV., STOLZENBURG, MR., QUANT, FR., OBERREIT, DR., and KEADY, PB. A Laminar-Flow, Water-Based Condensation Particle Counter (WCPC). *Aerosol Science and Technology*, July 2005, vol. 39, no. 7, p. 659–672.



- [64] HERZOG, P. HSDI diesel engine developments towards Euro IV . In *Future Engine and System Technologies*. London: Professional Engineering Publications, 1998.
- [65] HEYWOOD, JB. *Internal Combustion Engine Fundamentals*. New York: McGraw-Hill, 1988. 930 p. ISBN 0-07-028637-X.
- [66] HILDEN, DL., ECKSTROM, JC., and WOLF, LR. The Emissions Performance of Oxygenated Diesel Fuels in a Prototype DI Diesel Engine. *SAE Technical Paper Series*, 2001, no. 2001-01-0650.
- [67] HILLIARD, JC. and WHEELER, RW. Nitrogen Dioxide in Engine Exhaust. *SAE Technical Paper Series*, 1979, no. 790691.
- [68] HOLMER, E., BERG, PS., and BERTILSSON, BI. The Utilization of Alternative Fuels in a Diesel Engine Using Different Methods. *SAE Technical Paper Series*, 1980, no. 800544.
- [69] HOUSER, KR., LESTZ, SS., DUKOVICH, M., and YASBIN, RE. Methanol Fumigation of a Light Duty Automotive Diesel Engine. *SAE Technical Paper Series*, 1980, no. 801379.
- [70] JACKSON, MM., CORKWELL, KC., and DEGROOTE, CC. Study of Diesel and Ethanol Blends Stability. *SAE Technical Paper Series*, 2003, no. 2003-01-3191.
- [71] JELDEN, H. VW Lupo, the world's first 3-liter car. *SAE Technical Paper Series*, 2000, no. 2000-01-C044.
- [72] JIANG, Q., OTTIKUTTI, P., van GERPEN, J., and van METER, D. The Effect of Alcohol Fumigation on Diesel Flame Temperature and Emissions. *SAE Technical Paper Series*, 1990, no. 900386.

- [73] JONES, JH., KINGSBURY, WL., LYON, HH., MUTTY, PR., and THURSTON, KW. Development of a 5.7 Litre V8 Automotive Diesel Engine. *SAE Technical Paper Series*, 1978, no. 780412.
- [74] KEGL, B. and PEHAN, S. Reduction of Diesel Engine Emissions by Water Injection. *SAE Technical Paper Series*, 2001, no. 2001-01-3259.
- [75] KITTELSON, DB. Engines and nanoparticles: a review. *Journal of Aerosol Science*, June 1998, vol. 29, no. 5/6, p. 575–588.
- [76] KITTELSON, DB., WATTS, W., and JOHNSON, J. *Diesel Aerosol Sampling Methodology*. CRC E-43 Final Report, University of Minnesota, Minneapolis (Minn.), 2002.
- [77] KNUTSON, EO. and WHITBY, KT. Aerosol classification by electrical mobility: apparatus, theory, and applications. *Journal of Aerosol Science*, Nov. 1975, vol. 6, no. 6, p. 443–451.
- [78] KREMER, FG. and FACHETTI, A. Alcohol as Automotive Fuel – Brazilian Experience. *SAE Technical Paper Series*, 2000, no. 2000-01-1965.
- [79] KRESO, AM., JOHNSON, JH., GRATZ, LD., BAGLEY, ST., and LEDDY, DG. A Study of the Effects of Exhaust Gas Recirculation on Heavy-Duty Diesel Engine Emissions. *SAE Technical Paper Series*, 1998, no. 981422.
- [80] KRIEGER, RB. and BORMAN, GL. The Computation of Apparent Heat Release for Internal Combustion Engines. *ASME Paper*, 1966, no. 66-WA/DGP-4.
- [81] LADOMMATOS, N., ABDELHALIM, SM., ZHAO, H., and HU, Z. The Dilution, Chemical, and Thermal Effects of Exhaust Gas Recirculation on Diesel Engine Emissions - Part 1: Effect of Reducing Inlet Charge Oxygen. *SAE Technical Paper Series*, 1996, no. 961165.

- [82] ———. The Dilution, Chemical, and Thermal Effects of Exhaust Gas Recirculation on Diesel Engine Emissions - Part 2: Effects of Carbon Dioxide. *SAE Technical Paper Series*, 1996, no. 961167.
- [83] ———. The Dilution, Chemical, and Thermal Effects of Exhaust Gas Recirculation on Diesel Engine Emissions - Part 3: Effects of Water Vapour. *SAE Technical Paper Series*, 1997, no. 971659.
- [84] ———. The Dilution, Chemical, and Thermal Effects of Exhaust Gas Recirculation on Diesel Engine Emissions - Part 4: Effects of Carbon Dioxide and Water Vapour. *SAE Technical Paper Series*, 1997, no. 971660.
- [85] ———. The effects of carbon dioxide in exhaust gas recirculation on diesel engine emissions. *Proceedings of the Institution of Mechanical Engineers, Part D: Journal of Automobile Engineering*, 1998, vol. 212, no. 1, p. 25–42.
- [86] LAVOIE, GA., HEYWOOD, JB., and KECK, JC. Experimental and Theoretical Investigation of Nitric Oxide Formation in Internal Combustion Engines. *Combustion Science and Technology*, 1970, vol. 1, p. 313–326.
- [87] LI, N., SIOUTAS, C., CHO, A., SCHMITZ, D., MISRA, C., SEMPFF, J., WANG, MY., OBERLEY, T., FROINES, J., and NEL, A. Ultrafine particulate pollutants induce oxidative stress and mitochondrial damage. *Environmental Health Perspectives*, 2003, vol. 111, no. 4, p. 455–460.
- [88] LIOTTA, FJ. and MONTALVO, DM. The Effect of Oxygenated Fuels on Emissions from a Modern Heavy-Duty Diesel Engine. *SAE Technical Paper Series*, 1993, no. 932734.
- [89] LITZINGER, T., STONER, M., HESS, H., and BOEHMAN, A. Effects of oxygenated blending compounds on emissions from a turbo-charged direct injection diesel engine. *International Journal of Engine Research*, 2000, vol. 1, no. 1, p. 57–70.

- [90] LIU, BYH. and PUI, DYH. Equilibrium bipolar charge distribution of aerosols. *Journal of Colloid and Interface Science*, Nov. 1974, vol. 49, no. 2, p. 305–312.
- [91] LUCKE, CE. and WOODWARD, SM. The Use of Alcohol and Gasoline in Farm Engines. *U.S. Department of Agriculture Farmers' Bulletins*, 1907, no. 277, p. 1–40.
- [92] MARICQ, MM. Chemical characterization of particulate emissions from diesel engines: A review. *Journal of Aerosol Science*, Nov. 2007, vol. 38, no. 11, p. 1079–1118.
- [93] MARICQ, MM., CHASE, RE., PODSIADLIK, DH., SIEGL, WO., and KAISER, EW. The Effect of Dimethoxy Methane Additive on Diesel Vehicle Particulate Emissions. *SAE Technical Paper Series*, 1998, no. 982572.
- [94] MARRIOTT, CD., WILES, MA., GWIDT, JM., and PARRISH, SE. Development of a Naturally Aspirated Spark Ignition Direct-Injection Flex-Fuel Engine. *SAE Technical Paper Series*, 2008, no. 2008-01-0319.
- [95] MATHIS, U., RISTIMÄKI, J., MOHR, M., KESKINEN, J., NTZIACHRISTOS, L., SAMARAS, Z., and MIKKANEN, P. Sampling Conditions for the Measurement of Nucleation Mode Particles in the Exhaust of a Diesel Vehicle. *Aerosol Science and Technology*, 2004, vol. 38, no. 12, p. 1149–1160.
- [96] ALTERNATE FUELS COMMITTEE OF THE ENGINE MANUFACTURERS ASSOCIATION. A Technical Assessment of Alcohol Fuels. *SAE Technical Paper Series*, 1982, no. 820261.
- [97] MCCORMICK, RL. and PARISH, R. *Technical Barriers to the Use of Ethanol in Diesel Fuel*. Milestone Report NREL/MP-540-32674, National Renewable Energy Laboratory, Golden (Colo.), Nov. 2001.

- [98] MEIRING, P., HANSEN, AC., VOSLOO, AP., and LYNE, PWL. High Concentration Ethanol-Diesel Blends for Compression-Ignition Engines. *SAE Technical Paper Series*, 1983, no. 831360.
- [99] MELLOR, AM., MELLO, JP., DUFFY, KP., EASLEY, WL., and FAULKNER, JC. Skeletal Mechanism for NO<sub>x</sub> Chemistry in Diesel Engines. *SAE Technical Paper Series*, 1998, no. 981450.
- [100] MERRYMAN, EL. and LEVY, A. Nitrogen Oxide Formation in Flames: The Roles of NO<sub>2</sub> and Fuel Nitrogen. In *Proceedings of Fifteenth International Symposium on Combustion*. 1975, p. 1073.
- [101] MIYAMOTO, N., OGAWA, H., NURUN, NM., OBATA, K., and ARIMA, T. Smokeless, Low NO<sub>x</sub>, High Thermal Efficiency, and Low Noise Diesel Combustion with Oxygenated Agents as Main Fuel. *SAE Technical Paper Series*, 1998, no. 980506.
- [102] MOREIRA, JR. and GOLDEMBERG, J. The alcohol program. *Energy Policy*, Apr. 1999, vol. 27, no. 4, p. 229–245.
- [103] MUELLER, CJ., PICKETT, LM., SIEBERS, DL., PITZ, WJ., WESTBROOK, CK., and MARTIN, GC. Effects of Oxygenates on Soot Processes in DI Diesel Engines: Experiments and Numerical Simulations. *SAE Technical Paper Series*, 2003, no. 2003-01-1791.
- [104] MURPHY, MJ., TAYLOR, JD., and MCCORMICK, RL. *Compendium of Experimental Cetane Number Data*. Subcontractor Report NREL/SR-540-36805, National Renewable Energy Laboratory, Golden (Colo.), Sept. 2004.
- [105] NABI, N., MINAMI, M., OGAWA, H., and MIYAMOTO, N. Ultra Low Emission and High Performance Diesel Combustion with Highly Oxygenated Fuel. *SAE Technical Paper Series*, 2000, no. 2000-01-0231.

- [106] NAKATA, K., UTSUMI, S., OTA, A., KAWATAKE, K., KAWAI, T., and TSUNOOKA, T. The Effect of Ethanol Fuel on a Spark Ignition Engine. *SAE Technical Paper Series*, 2006, no. 2006-01-3380.
- [107] PANTAR, AV. and CORKWELL, KC. E Diesel: A Viable Alternative Fuel. *SAE Technical Paper Series*, 2004, no. 2004-28-0074.
- [108] PARK, K., CAO, F., KITTELSON, DB., and MCMURRY, PH. Relationship between Particle Mass and Mobility for Diesel Exhaust Particles. *Environmental Science and Technology*, 2003, vol. 37, no. 3, p. 577–583.
- [109] PISCHINGER, FF. The Diesel Engine for Cars—Is There a Future? *ASME Journal of Engineering for Gas Turbine and Power*, July 1998, vol. 120, no. 3, p. 641–647.
- [110] RAKOPOULOS, CD., HOUNTALAS, DT., ZANNIS, TC., and LEVENDIS, YA. Operational and Environmental Evaluation of Diesel Engines Burning Oxygen-Enriched Intake Air or Oxygen-Enriched Fuel: A Review. *SAE Technical Paper Series*, 2004, no. 2004-01-2924.
- [111] REN, Y., HUANG, Z., MIAO, H., DI, Y., JIANG, D., ZENG, K., LIU, B., and WANG, X. Combustion and emissions of a DI diesel engine fuelled with diesel-oxygenate blends. *Fuel*, Sept. 2008, vol. 87, no. 12, p. 2691–2697.
- [112] RICARDO, HR. Combustion in Diesel Engines. In *Proceedings of the 1929–1930 Session*, vol. XXIV. London: The Institution of Automobile Engineers, Mar. 1930, p. 645–665.
- [113] ROBERTS, CE., NAEGELI, D., and CHADWELL, C. The Effect of Water on Soot Formation Chemistry. *SAE Technical Paper Series*, 2005, no. 2005-01-3850.

- [114] RUSSELL, MF. The dependence of diesel combustion on injection rate. In *Future Engine and System Technologies*. London: Professional Engineering Publications, 1998.
- [115] SAKURAI, H., TOBIAS, HJ., PARK, K., ZARLING, D., DOCHERTY, KS., KITTELSON, DB., MCMURRY, PH., and ZIEMANN, PJ. On-line measurements of diesel nanoparticle composition and volatility . *Atmospheric Environment*, Mar. 2003, vol. 37, no. 9-10 p. 1199–1210.
- [116] SAVAGE, LD., WHITE, RA., COLE, S., and PRITCHETT, G. Extended Performance of Alcohol Fumigation in Diesel Engines through Different Multi-point Alcohol Injection Timing Cycles. *SAE Technical Paper Series*, 1986, no. 861580.
- [117] SCHAEFER, AJ. and HARDENBERG, HO. Ignition Improvers for Ethanol Fuels. *SAE Technical Paper Series*, 1981, no. 810249.
- [118] SHAH, SR., MAIBOOM, A., and TAUZIA, JF., X. HÉTET. Experimental Study of Inlet Manifold Water Injection on a Common Rail HSDI Automobile Diesel Engine, Compared to EGR with Respect to PM and NOx Emissions and Specific Consumption. *SAE Technical Paper Series*, 2009, no. 2009-01-1439.
- [119] SHAHID, EM. and JAMAL, Y. A review of biodiesel as vehicular fuel. *Renewable and Sustainable Energy Reviews*, Dec. 2008, vol. 12, no. 9, p. 2484–2494.
- [120] SHIRVANI, H., GOERING, CE., and SORENSON, SC. Performance of Alcohol in Diesel Engines. *SAE Technical Paper Series*, 1981, no. 810681.
- [121] SHROPSHIRE, GJ. and BASHFORD, LL. A Comparison of Ethanol Fumigation Systems for a Diesel Engine. *Agricultural Engineering*, May 1984, vol. 65, no. 5, p. 17–23.

- [122] SHROPSHIRE, GJ. and GOERING, CE. Ethanol Injection into a Diesel Engine. *Transactions of the ASAE*, 1982, vol. 25, no. 3, p. 570–575.
- [123] SIMONSEN, H. and CHOMIAK, J. Testing and Evaluation of Ignition Improvers for Ethanol in a DI Diesel Engine. *SAE Technical Paper Series*, 1995, no. 952512.
- [124] SISON, K., LADOMMATOS, N., SONG, H., and ZHAO, H. Soot generation of diesel fuels with substantial amounts of oxygen-bearing compounds added. *Fuel*, Feb. 2007, vol. 86, no. 3, p. 345–352.
- [125] STONE, R. *Introduction to Internal Combustion Engines*. 3rd ed. Warrendale (Pa.): Society of Automotive Engineers, 1999. 660 p. ISBN 0-76-800495-0.
- [126] STONER, M. and LITZINGER, T. Effects of Structure and Boiling Point of Oxygenated Blending Compounds in Reducing Diesel Emissions. *SAE Technical Paper Series*, 1999, no. 1999-01-1475.
- [127] STOUT, BA., PEART, RM., BUCHELE, WF., and FINCH, E. Brazil Promotes PROALCOOL for Petroleum Independence. *Agricultural Engineering*, Apr. 1978, vol. 59, no. 4, p. 30–33.
- [128] STRAIT, J., BOEDICKER, JJ., and JOHANSEN, KC. Diesel Oil and Ethanol Mixtures for Diesel-Powered Farm Tractors. *SAE Technical Paper Series*, 1979, no. 790958.
- [129] SULLIVAN, NW. and BASHFORD, LL. Pre-turbocharger alcohol fumigation in a diesel tractor. *Transactions of the ASAE*, 1981, no. 81-3581.
- [130] SURAWSKI, NC., MILJEVIC, B., ROBERTS, BA., MODINI, RL., R., S., BROWN, RJ., BOTTLE, SE., and RISTOVSKI, ZD. Particle Emissions, Volatility, and Toxicity from an Ethanol Fumigated Compression Ignition Engine. *Environmental Science and Technology*, 2010, vol. 44, no. 1, p. 229–235.



- [131] TAKAHASHI, F. and GLASSMAN, I. Sooting correlations for premixed flames. *Combustion Science and Technology*, May 1984, vol. 37, no. 1-2, p. 1–19.
- [132] TAYLOR, CF. *The Internal-Combustion Engine in Theory and Practice*, vol. 2. revised ed. Cambridge (Mass.): MIT Press, 1985. 795 p. ISBN 0-26-270027-1.
- [133] TURNER, JWG., PEARSON, R.J., HOLLAND, B., and PECK, R. Alcohol-Based Fuels in High Performance Engines. *SAE Technical Paper Series*, 2007, no. 2007-01-0056.
- [134] UDAYAKUMAR, R., SUNDARAM, S., and SRIRAM, R. Reduction of NOx Emissions by Water Injection into the Inlet Manifold of a DI Diesel Engine. *SAE Technical Paper Series*, 2003, no. 2003-01-0264.
- [135] VARDE, KS. and MANOHARAN, NK. Characterization of Exhaust Emissions in a SI Engine Using E85 and Cooled EGR. *SAE Technical Paper Series*, 2009, no. 2009-01-1952.
- [136] WALKER, J. Low sulfur fuel stimulates particulate trap sales. *Diesel Progress*, May–June 1998, p. 78–79.
- [137] WILSON, RP., MUIR, EB., and PELLICCIOTTI, FA. Emissions Study of a Single-Cylinder Diesel Engine. *SAE Technical Paper Series*, 1974, no. 740123.
- [138] WRAGE, KE. and GOERING, CE. Technical Feasibility of Diesohol. *Transactions of the ASAE*, 1980, vol. 23, no. 6, p. 1338–1343.
- [139] YEH, LI., RICKEARD, DJ., DUFF, JLC., BATEMAN, JR., SCHLOSBERG, RH., and CAERS, RF. Oxygenates: An Evaluation of their Effects on Diesel Emissions. *SAE Technical Paper Series*, 2001, no. 2001-01-2019.
- [140] YILMAZ, N., DONALDSON, AB., and JOHNS, A. Some Perspectives on Alcohol Utilization in a Compression Ignition Engine. *SAE Technical Paper Series*, 2005, no. 2005-01-3135.

- 
- [141] YU, RC. and SHAHED, SM. Effects of Injection Timing and Exhaust Gas Recirculation on Emissions from a D.I. Diesel Engine. *SAE Technical Paper Series*, 1981, no. 811234.
- [142] YÜKSEL, F. and YÜKSEL, B. The use of ethanol-gasoline blend as a fuel in an SI engine. *Renewable Energy*, June 2004, vol. 29, no. 7, p. 1181–1191.
- [143] ZEL'DOVICH, YaB. The Oxidation of Nitrogen in Combustion and Explosions. *Acta Physicochemica U.R.S.S.*, 1946, vol. XXI, no. 4, p. 577–628.



## Appendix A

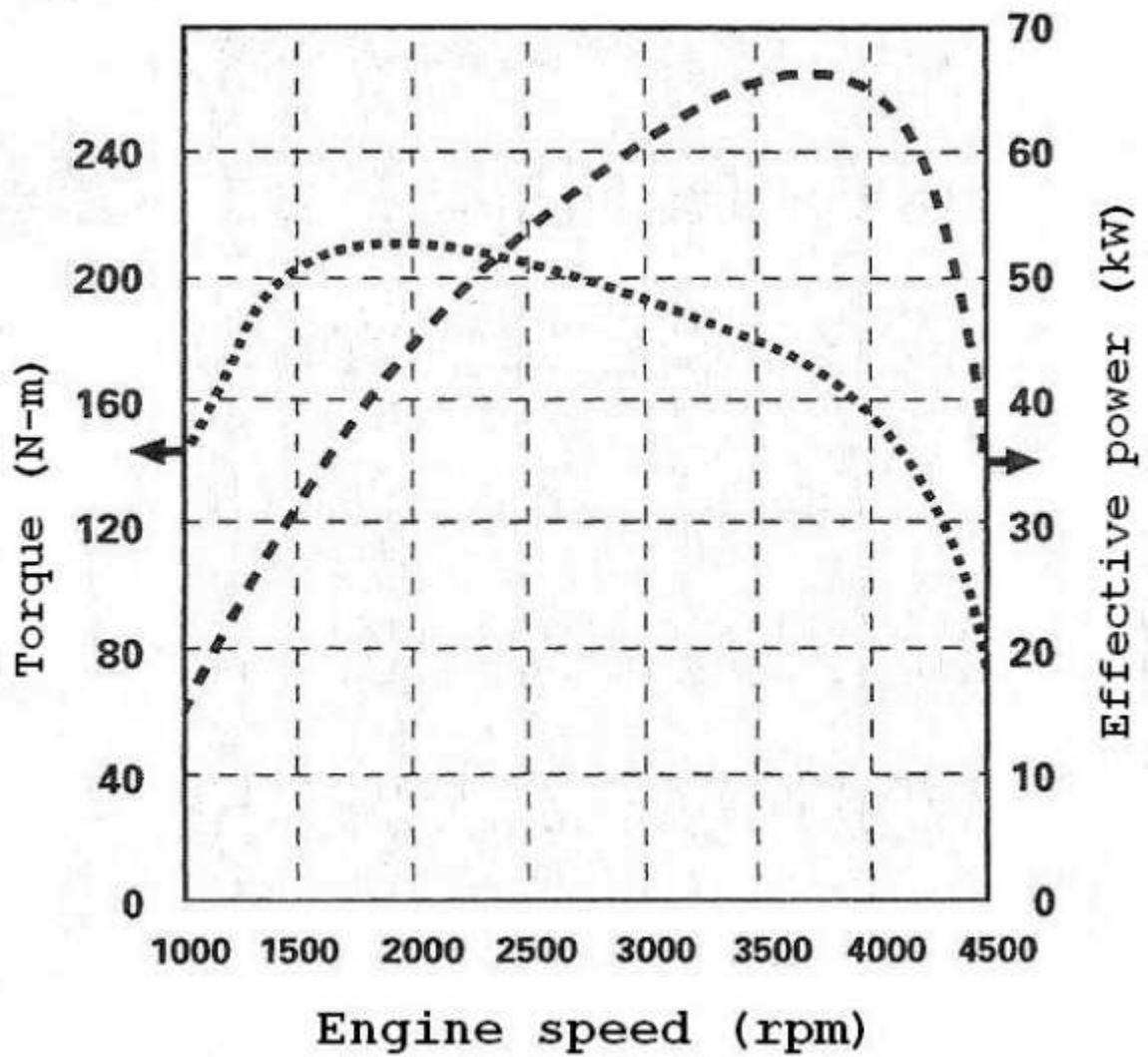


Figure A.1: Performance curves of the Volkswagen 1.9L TDI engine [23]

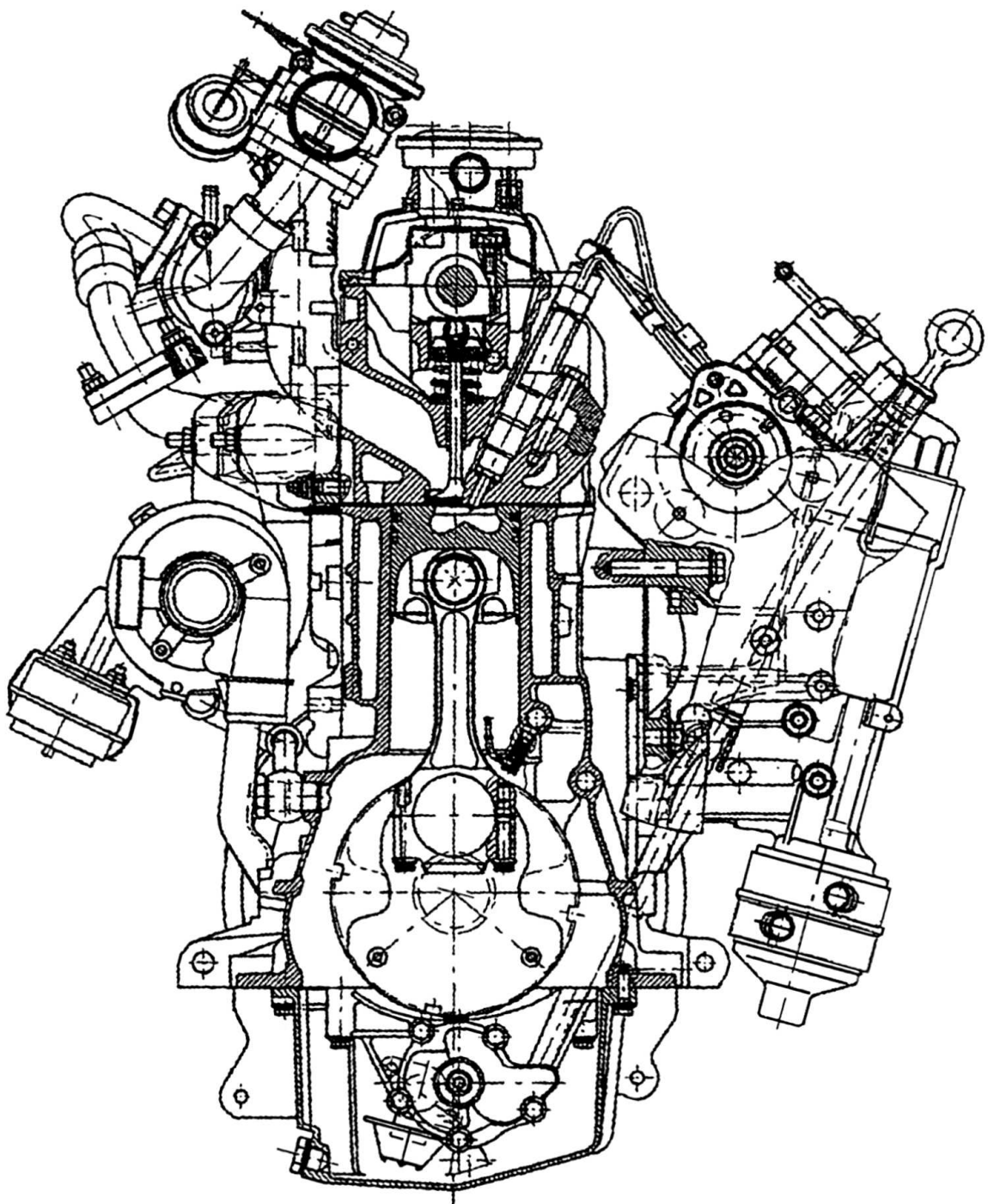


Figure A.2: Sectional view of the Volkswagen 1.9L TDI engine [23]

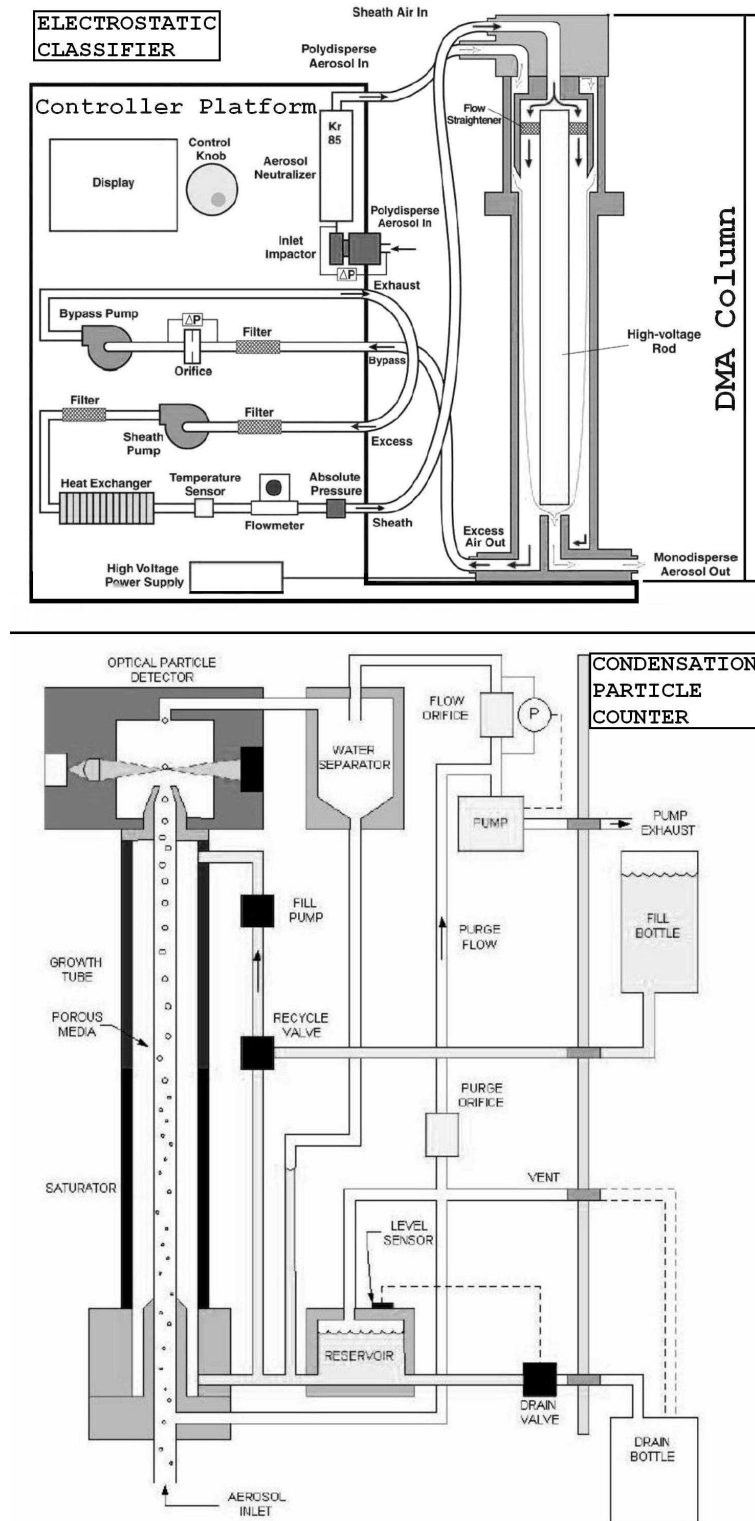


Figure A.3: The instruments which comprise the SMPS: the electrostatic classifier (top) [3] and the water-based condensation particle counter (bottom) [1]

|   | BASELINE |          | 25% 100-PROOF |          | 40% 100-PROOF |          | 25% WATER |          | 40% WATER |          |
|---|----------|----------|---------------|----------|---------------|----------|-----------|----------|-----------|----------|
|   | AVERAGE  | STDEV    | AVERAGE       | STDEV    | AVERAGE       | STDEV    | AVERAGE   | STDEV    | AVERAGE   | STDEV    |
| <b>40 N-m downstream</b>  |          |          |               |          |               |          |           |          |           |          |
| Mean exhaust temperature (°C)   | 269      | 0.8      | 256           | 0.6      | 254           | 0.5      | 251       | 0.5      | 251       | 1.2      |
| Engine speed (rpm)  | 1683     | 13       | 1733          | 11       | 1691          | 22       | 1707      | 13       | 1698      | 12       |
| NOx concentration (ppm)   | 207      | 2.3      | 95            | 1.2      | 90            | 0.8      | 132       | 1.1      | 120       | 13.3     |
| # of SMPS scans   | 4        |          | 4             |          | 4             |          | 4         |          | 2         |          |
| average overall dilution ratio  | 386      |          | 378           |          | 377           |          | 445       |          | 447       |          |
| Total particle number concentration (#/cm <sup>3</sup> )                | 1.15E+08 | 6.86E+06 | 1.45E+08      | 4.76E+06 | 1.64E+08      | 6.82E+06 | 1.73E+08  | 1.60E+07 | 2.10E+08  | 2.20E+06 |
| Total particle volume concentration (nm <sup>3</sup> /cm <sup>3</sup> ) | 8.30E+12 | 3.16E+11 | 7.77E+12      | 1.18E+11 | 6.91E+12      | 3.77E+11 | 9.42E+12  | 7.24E+11 | 9.99E+12  | 3.48E+11 |
| Inlet manifold temperature (°C)   | 48       | 0.4      | 31            | 0.3      | 27            | 0.4      | 27        | 0.2      | 27        | 0.6      |
| Variation in NOx relative to baseline (%)                               | -        | -        | -53.9         | 0.8      | -56.6         | 0.8      | -36.0     | 0.5      | -41.9     | 1.8      |
| Variation in total particle number (%)                                  | -        | -        | 26.0          | 1.8      | 42.3          | 2.9      | 49.7      | 4.2      | 81.5      | 5.2      |
| Variation in total particle volume (%)                                  | -        | -        | -6.5          | 0.3      | -16.8         | 0.8      | 13.5      | 0.8      | 20.3      | 0.9      |
| <b>40 N-m upstream</b>  |          |          |               |          |               |          |           |          |           |          |
| Mean exhaust temperature (°C)   | 269      | 0.8      | 256           | 0.3      | 257           | 0.3      | 253       | 0.6      | 253       | 0.4      |
| Engine speed (rpm)  | 1683     | 13       | 1689          | 11       | 1694          | 13       | 1701      | 20       | 1712      | 12       |
| NOx concentration (ppm)   | 207      | 2.3      | 102           | 1.0      | 94            | 0.7      | 130       | 1.2      | 122       | 1.1      |
| # of SMPS scans   | 4        |          | 4             |          | 4             |          | 4         |          | 4         |          |
| average overall dilution ratio  | 386      |          | 358           |          | 329           |          | 366       |          | 366       |          |
| Total particle number concentration (#/cm <sup>3</sup> )                | 1.15E+08 | 6.86E+06 | 1.08E+08      | 3.21E+07 | 1.21E+08      | 6.92E+06 | 9.06E+07  | 8.61E+06 | 9.62E+07  | 4.54E+06 |
| Total particle volume concentration (nm <sup>3</sup> /cm <sup>3</sup> ) | 8.30E+12 | 3.16E+11 | 5.50E+12      | 1.12E+12 | 5.50E+12      | 2.75E+11 | 5.23E+12  | 3.02E+11 | 5.44E+12  | 1.21E+11 |
| Inlet manifold temperature (°C)   | 48       | 0.4      | 39            | 0.3      | 38            | 0.1      | 34        | 0.3      | 36        | 0.2      |
| Variation in NOx relative to baseline (%)                               | -        | -        | -50.4         | 0.7      | -54.4         | 0.8      | -37.3     | 0.5      | -41.0     | 0.6      |
| Variation in total particle number (%)                                  | -        | -        | -6.4          | 1.0      | 5.1           | 0.4      | -21.5     | 1.7      | -16.7     | 1.2      |
| Variation in total particle volume (%)                                  | -        | -        | -33.8         | 3.1      | -33.7         | 1.6      | -37.0     | 1.8      | -34.4     | 1.6      |

Figure A.4: Data for Part I

|   | BASELINE |          | 25% 100-PROOF |          | 40% 100-PROOF |          | 25% WATER |          | 40% WATER |          |
|---|----------|----------|---------------|----------|---------------|----------|-----------|----------|-----------|----------|
|   | AVERAGE  | STDEV    | AVERAGE       | STDEV    | AVERAGE       | STDEV    | AVERAGE   | STDEV    | AVERAGE   | STDEV    |
| <b>80 N-m downstream</b>  |          |          |               |          |               |          |           |          |           |          |
| Mean exhaust temperature (°C)   | 382      | 1.1      | 371           | 0.5      | 413           | 1.8      | 363       | 1.1      | 364       | 0.7      |
| Engine speed (rpm)  | 1670     | 11       | 1727          | 10       | 1735          | 9        | 1704      | 15       | 1681      | 8        |
| NOx concentration (ppm)   | 437      | 3.3      | 321           | 3.8      | 341           | 3.6      | 304       | 2.8      | 277       | 2.0      |
| # of SMPS scans   | 4        |          | 4             |          | 4             |          | 4         |          | 4         |          |
| average overall dilution ratio  | 488      |          | 510           |          | 545           |          | 511       |          | 508       |          |
| Total particle number concentration (#/cm <sup>3</sup> )                | 1.82E+07 | 5.82E+05 | 3.34E+07      | 1.46E+06 | 3.06E+07      | 5.37E+06 | 4.31E+07  | 3.31E+05 | 5.23E+07  | 9.40E+05 |
| Total particle volume concentration (nm <sup>3</sup> /cm <sup>3</sup> ) | 9.24E+12 | 4.80E+11 | 8.78E+12      | 3.10E+11 | 3.59E+12      | 8.94E+11 | 1.10E+13  | 2.59E+11 | 1.14E+13  | 1.03E+12 |
| Inlet manifold temperature (°C)   | 44       | 0.2      | 24            | 0.1      | 24            | 0.1      | 25        | 0.2      | 24        | 0.1      |
| Variation in NOx relative to baseline (%)                               | -        | -        | -26.6         | 0.3      | -21.9         | 0.2      | -30.3     | 0.3      | -36.5     | 0.3      |
| Variation in total particle number (%)                                  | -        | -        | 83.7          | 3.7      | 68.4          | 7.9      | 137.1     | 4.6      | 188.1     | 6.7      |
| Variation in total particle volume (%)                                  | -        | -        | -5.0          | 0.3      | -61.1         | 5.8      | 18.5      | 1.1      | 23.2      | 1.8      |
| <b>80 N-m upstream</b>  |          |          |               |          |               |          |           |          |           |          |
| Mean exhaust temperature (°C)   | 382      | 1.1      | 381           | 0.8      | 381           | 1.1      | 370       | 1.1      | 366       | 1.3      |
| Engine speed (rpm)  | 1670     | 11       | 1687          | 11       | 1680          | 16       | 1692      | 12       | 1704      | 11       |
| NOx concentration (ppm)   | 437      | 3.3      | 321           | 2.3      | 291           | 5.4      | 298       | 4.7      | 237       | 7.5      |
| # of SMPS scans   | 4        |          | 4             |          | 4             |          | 4         |          | 4         |          |
| average overall dilution ratio  | 488      |          | 442           |          | 445           |          | 448       |          | 456       |          |
| Total particle number concentration (#/cm <sup>3</sup> )                | 1.82E+07 | 5.82E+05 | 1.64E+07      | 3.02E+05 | 1.99E+07      | 4.03E+05 | 2.37E+07  | 2.29E+06 | 3.68E+07  | 5.38E+05 |
| Total particle volume concentration (nm <sup>3</sup> /cm <sup>3</sup> ) | 9.24E+12 | 4.80E+11 | 7.49E+12      | 3.95E+11 | 7.43E+12      | 1.17E+12 | 8.95E+12  | 7.84E+11 | 9.10E+12  | 6.52E+11 |
| Inlet manifold temperature (°C)   | 44       | 0.2      | 39            | 0.2      | 36            | 0.1      | 34        | 0.2      | 33        | 0.1      |
| Variation in NOx relative to baseline (%)                               | -        | -        | -26.6         | 0.2      | -33.4         | 0.4      | -31.7     | 0.3      | -45.8     | 0.7      |
| Variation in total particle number (%)                                  | -        | -        | -9.8          | 0.4      | 9.6           | 0.4      | 30.5      | 2.0      | 102.4     | 3.6      |
| Variation in total particle volume (%)                                  | -        | -        | -18.9         | 1.2      | -19.6         | 1.8      | -3.2      | 0.2      | -1.6      | 0.1      |

Figure A.5: Data for Part I (cont.)



|   | BASELINE |          | 25% 100-PROOF |          | 40% 100-PROOF |          | 25% WATER |          | 40% WATER |          |
|---|----------|----------|---------------|----------|---------------|----------|-----------|----------|-----------|----------|
|   | AVERAGE  | STDEV    | AVERAGE       | STDEV    | AVERAGE       | STDEV    | AVERAGE   | STDEV    | AVERAGE   | STDEV    |
| <b>120 N-m downstream</b>   |          |          |               |          |               |          |           |          |           |          |
| Mean exhaust temperature (°C)   | 465      | 1.8      | 456           | 0.9      | 462           | 1.3      | 444       | 1.4      | 442       | 1.0      |
| Engine speed (rpm)  | 1713     | 19       | 1732          | 11       | 1716          | 14       | 1711      | 14       | 1716      | 12       |
| NOx concentration (ppm)   | 623      | 8.9      | 452           | 3.9      | 391           | 3.8      | 402       | 3.5      | 344       | 2.2      |
| # of SMPS scans   | 4        |          | 4             |          | 4             |          | 4         |          | 4         |          |
| average overall dilution ratio  | 544      |          | 566           |          | 580           |          | 532       |          | 552       |          |
| Total particle number concentration (#/cm <sup>3</sup> )                | 3.04E+07 | 2.94E+06 | 2.25E+07      | 1.42E+06 | 3.30E+07      | 5.63E+06 | 2.95E+07  | 2.19E+06 | 3.50E+07  | 8.43E+05 |
| Total particle volume concentration (nm <sup>3</sup> /cm <sup>3</sup> ) | 1.55E+13 | 4.13E+11 | 1.58E+13      | 1.04E+12 | 2.97E+13      | 9.59E+12 | 2.00E+13  | 2.96E+12 | 2.43E+13  | 1.63E+12 |
| Inlet manifold temperature (°C)   | 53       | 0.2      | 28            | 0.1      | 26            | 0.1      | 30        | 0.1      | 30        | 0.1      |
| Variation in NOx relative to baseline (%)                               | -        | -        | -27.4         | 0.5      | -44.7         | 0.8      | -35.5     | 0.6      | -44.7     | 0.8      |
| Variation in total particle number (%)                                  | -        | -        | -26.0         | 3.0      | 8.7           | 1.2      | -3.1      | 0.4      | 15.3      | 1.6      |
| Variation in total particle volume (%)                                  | -        | -        | 1.9           | 0.1      | 91.9          | 19.7     | 29.1      | 2.6      | 57.1      | 2.9      |
| <b>120 N-m upstream</b>   |          |          |               |          |               |          |           |          |           |          |
| Mean exhaust temperature (°C)   | 465      | 1.8      | 467           | 1.2      | 474           | 1.2      | 447       | 1.3      | 439       | 1.7      |
| Engine speed (rpm)  | 1713     | 19       | 1687          | 11       | 1682          | 12       | 1699      | 20       | 1707      | 23       |
| NOx concentration (ppm)   | 623      | 8.9      | 466           | 3.1      | 438           | 4.4      | 404       | 10.8     | 340       | 15.5     |
| # of SMPS scans   | 4        |          | 4             |          | 4             |          | 4         |          | 4         |          |
| average overall dilution ratio  | 544      |          | 482           |          | 486           |          | 449       |          | 486       |          |
| Total particle number concentration (#/cm <sup>3</sup> )                | 3.04E+07 | 2.94E+06 | 2.93E+07      | 2.55E+06 | 2.93E+07      | 7.31E+05 | 2.22E+07  | 8.98E+05 | 2.51E+07  | 1.39E+06 |
| Total particle volume concentration (nm <sup>3</sup> /cm <sup>3</sup> ) | 1.55E+13 | 4.13E+11 | 1.73E+13      | 1.33E+12 | 2.23E+13      | 9.11E+11 | 1.53E+13  | 2.06E+12 | 1.50E+13  | 1.36E+12 |
| Inlet manifold temperature (°C)   | 53       | 0.2      | 44            | 0.3      | 42            | 0.6      | 40        | 0.2      | 40        | 0.1      |
| Variation in NOx relative to baseline (%)                               | -        | -        | -21.9         | 0.4      | -45.4         | 0.8      | -35.1     | 0.7      | -45.4     | 1.1      |
| Variation in total particle number (%)                                  | -        | -        | -3.5          | 0.4      | -3.7          | 0.4      | -26.9     | 3.0      | -17.4     | 2.0      |
| Variation in total particle volume (%)                                  | -        | -        | 11.7          | 0.6      | 44.1          | 1.7      | -1.4      | 0.1      | -3.2      | 0.2      |

Figure A.6: Data for Part I (cont.)

| 40 N-m(baseline)  | BEFORE   |          | AFTER    |          |
|---|----------|----------|----------|----------|
|   | AVERAGE  | STDEV    | AVERAGE  | STDEV    |
| Mean exhaust temperature (°C)   | 254      | 0.4      | 244      | 0.3      |
| NOx concentration (ppm)   | 192      | 1.5      | 288      | 2.5      |
| # of SMPS scans   | 4        |          | 5        |          |
| average overall dilution ratio  | 620      |          | 769      |          |
| Total particle number concentration (#/cm <sup>3</sup> )                | 8.25E+07 | 5.43E+05 | 3.16E+07 | 2.31E+06 |
| Total particle volume concentration (nm <sup>3</sup> /cm <sup>3</sup> ) | 6.59E+12 | 1.87E+11 | 5.68E+12 | 1.87E+11 |

| 80 N-m(baseline)  | BEFORE   |          | AFTER    |          |
|---|----------|----------|----------|----------|
|   | AVERAGE  | STDEV    | AVERAGE  | STDEV    |
| Mean exhaust temperature (°C)   | 374      | 0.6      | 355      | 0.7      |
| NOx concentration (ppm)   | 421      | 2.5      | 488      | 4.7      |
| # of SMPS scans   | 4        |          | 4        |          |
| average overall dilution ratio  | 680      |          | 818      |          |
| Total particle number concentration (#/cm <sup>3</sup> )                | 2.28E+07 | 4.94E+05 | 1.14E+07 | 3.07E+05 |
| Total particle volume concentration (nm <sup>3</sup> /cm <sup>3</sup> ) | 9.41E+12 | 5.67E+11 | 5.51E+12 | 1.28E+11 |

| 120 N-m(baseline)   | BEFORE   |          | AFTER    |          |
|---|----------|----------|----------|----------|
|   | AVERAGE  | STDEV    | AVERAGE  | STDEV    |
| Mean exhaust temperature (°C)   | 445      | 9.7      | 413      | 0.8      |
| NOx concentration (ppm)   | 528      | 76.1     | 850      | 15.9     |
| # of SMPS scans   | 4        |          | 5        |          |
| average overall dilution ratio  | 595      |          | 811      |          |
| Total particle number concentration (#/cm <sup>3</sup> )                | 3.48E+07 | 3.47E+06 | 6.89E+06 | 4.11E+05 |
| Total particle volume concentration (nm <sup>3</sup> /cm <sup>3</sup> ) | 1.62E+13 | 7.08E+11 | 4.89E+12 | 2.05E+11 |

Figure A.7: Data for Part II

|  | BASELINE |          | 25% 100-PROOF |          | 40% 100-PROOF |          | 25% WATER |          | 40% WATER |          | 25% 200-PROOF |          | 40% 200-PROOF |          |
|--|----------|----------|---------------|----------|---------------|----------|-----------|----------|-----------|----------|---------------|----------|---------------|----------|
|  | AVERAGE  | STDEV    | AVERAGE       | STDEV    | AVERAGE       | STDEV    | AVERAGE   | STDEV    | AVERAGE   | STDEV    | AVERAGE       | STDEV    | AVERAGE       | STDEV    |
| Mean exhaust temperature (°C)                                | 358      | 3        | 357           | 2        | 357           | 2        | 354       | 2        | 349       | 2        | 362           | 2        | 364           | 2        |
| Engine speed (rpm)   | 1715     | 51       | 1718          | 15       | 1701          | 21       | 1697      | 19       | 1704      | 16       | 1705          | 29       | 1712          | 26       |
| HC_Chartlene [ppm]   | 36       | 12       | 67            | 16       | 71            | 9        | 29        | 6        | 23        | 5        | 120           | 6        | 195           | 13       |
| NOx concentration (ppm)                                      | 525      | 14       | 487           | 11       | 483           | 14       | 447       | 9        | 392       | 8        | 499           | 7        | 504           | 10       |
| NO concentration (ppm)                                       | 473      | 33       | 371           | 18       | 355           | 19       | 398       | 10       | 343       | 9        | 329           | 6        | 301           | 7        |
| average overall dilution ratio                               | 548      |          | 549           |          | 538           |          | 541       |          | 543       |          | 556           |          | 573           |          |
| NO/NOx ratio   | 0.90     | 0.06     | 0.76          | 0.02     | 0.73          | 0.02     | 0.89      | 0.01     | 0.87      | 0.02     | 0.66          | 0.01     | 0.60          | 0.01     |
| Inlet manifold temperature (°C)                              | 36       | 0.5      | 34            | 0.1      | 33            | 0.2      | 30        | 1.0      | 26        | 0.1      | 34            | 0.5      | 31            | 0.5      |
| # of SMPs scans  | 10       |          | 10            |          | 10            |          | 10        |          | 10        |          | 10            |          | 10            |          |
| Total part. number conc. (#/cm <sup>3</sup> )                | 1.33E+07 | 2.25E+06 | 8.63E+06      | 6.87E+05 | 7.78E+06      | 2.79E+06 | 9.61E+06  | 1.05E+06 | 1.13E+07  | 1.24E+06 | 7.97E+06      | 8.48E+05 | 8.00E+06      | 9.92E+05 |
| Total part. volume conc. (mm <sup>3</sup> /cm <sup>3</sup> ) | 5.19E+12 | 4.29E+11 | 4.00E+12      | 8.53E+10 | 3.73E+12      | 1.19E+11 | 4.48E+12  | 4.35E+11 | 4.75E+12  | 4.15E+11 | 3.63E+12      | 2.62E+11 | 3.64E+12      | 4.17E+11 |
| Variation in total part. number (%)                          | -        | -        | -35.2         | 7.1      | -41.6         | 8.3      | -27.9     | 5.6      | -15.3     | 3.0      | -40.2         | 8.2      | -40.0         | 8.2      |
| Variation in total part. volume (%)                          | -        | -        | -23.0         | 2.2      | -28.1         | 2.7      | -13.8     | 1.4      | -8.5      | 0.9      | -30.1         | 3.0      | -29.9         | 3.2      |
| Variation in NOx (%)   | -        | -        | -7.3          | 0.2      | -8.0          | 0.3      | -14.8     | 0.5      | -25.3     | 0.8      | -5.1          | 0.2      | -4.1          | 0.1      |
| Variation in HC (%)  | -        | -        | 86.3          | 32.6     | 95.6          | 33.9     | -18.9     | 7.3      | -34.9     | 13.6     | 232.2         | 78.3     | 441.7         | 148.1    |

Figure A.8: Data for Part III